SEDIMENTOLOGICAL STUDIES ON TIPAM ROCKS OF KOLASIB DISTRICT, MIZORAM

C. ZORAMTHARA

DEPARTMENT OF GEOLOGY

MIZORAM UNIVERSITY

SEDIMENTOLOGICAL STUDIES ON TIPAM ROCKS OF KOLASIB DISTRICT, MIZORAM

By

C. ZORAMTHARA

Ph. D Regd. No. MZU/Ph.D/436 of 15.05.2012

Thesis submitted in fulfilment for the award of the
Degree of Doctor of Philosophy
in Geology

MIZORAM UNIVERSITY

AIZAWL

DEPARTMENT OF GEOLOGY

MIZORAM UNIVERSITY

AIZAWL-796004

CERTIFICATE

Certify that Mr. C. Zoramthara has carried out research under our supervision and guidance in the Department of Geology, Mizoram University. The results of the research work by Mr. C. Zoramthara have been presented in this thesis entitled 'Sedimentological studies on Tipam rocks of Kolasib District, Mizoram' and the same has been submitted to Mizoram University, Aizawl, Mizoram for the degree of Doctor of Philosophy.

Mr. C. Zoramthara has fulfilled all the requirements under the Ph.D. regulations of the Mizoram University. To the best of my knowledge, this thesis as a whole or any part thereof has not been submitted to this University or any other institution for any degree.

(Dr. JIMMY LALNUNMAWIA)
Supervisor
Department of Geology
Mizoram University

DECLARATION

I, C. Zoramthara, hereby declare that the subject matter of this thesis is the record of work done by me, that the contents of this thesis did not form basis of the award of any previous degree to me or to the best of my knowledge to anybody else, and that the thesis has not been submitted by me for any research degree in any other University/Institute.

This is being submitted to Mizoram University for the degree of the Doctor of Philosophy in Geology.

Date   :   (C. ZORAMTHARA)

Place   : Aizawl   Research Scholar

(Dr. Jimmy Lalnunmawia)

Head of Department   **(Supervisor)**

esteemed laboratory. Thanks, are also due to all the Scientist and Research Scholar of Geochemistry Division, NGRI for their support throughout the analytical work.

Special thank goes to Mrs. Cory Lalbiakzuali and Mr. Lalramdina, Research scholars for helping me out in the preparation of map. I am also thankful to my colleague Dr. P.C. Rohmingliana and Dr. R. Lalawmpuii for their spirited help during interpretation of the work.

I would like to dedicate this thesis to my former Supervisor, Dr. Victor Zochhuana Ralte, Associate Professor in the Department of Geology who has passed away in 2015.

Last, but not least, I would like to express my deep sense of gratitude to my family, my wife Shirley and my children Martha and Jarrell, for their love, patience, and understanding—as they allowed me to concentrate on my work during the entire course of this study. Acknowledgement also goes to CK Family, my mom and dad and my brothers and sisters for their prayers and support.

Above all, I thank the almighty God for giving me opportunity, strength and wisdom he bestowed upon me.

Date: (C. ZORAMTHARA)

Research Scholar
Department of Geology
Mizoram University

CONTENTS

CHAPTER 1

INTRODUCTION

CHAPTER 2

REGIONAL GEOLOGY AND GEOLOGY OF THE STUDY AREA

CHAPTER 3

REVIEW OF LITERATURE

CHAPTER 4

METHODOLOGY

CHAPTER 5

GRAIN SIZE ANALYSIS

CHAPTER 6

PETROGRAPHY

CHAPTER 7

HEAVY MINERAL ANALYSIS

CHAPTER 8

GEOCHEMISTRY

CHAPTER 9

SUMMARY AND CONCLUSION

REFERRENCES

CHAPTER- 1

INTRODUCTION

1.1. RATIONALE OF THE STUDY

Mizoram, which is located in the southeastern corner of Northeast India represents one of the thickest sedimentary basins across the globe and preserves nearly 8000 m thick or more. It occupied an important place in Indian geology in terms of its tectonic evolution and as a good resource for oil and gas. Geologically, the whole of Mizoram is covered by a huge pile of sedimentary succession belonging to the Tertiary Group of rocks and has been divided into three Groups namely, the Barail, the Surma and the Tipam Groups in ascending order of their age respectively. Many workers are of the strong opinion that, this part of the area is the southern extension of Surma basin.

Even though Mizoram is covered by a thick succession of sedimentary rock, only a few workers have worked in terms of Sedimentology, which is the study of formation of sedimentary rock and their processes that occurred during the time of their formation. Sediments which are produced by disintegration of preexisting rocks or by precipitation of solution are consolidated into sedimentary rock by a process known as diagenesis which is very important as it imprint the nature of changes that occurred during the time of consolidation of sediments into sedimentary rocks.

The study area exposes a good succession of sedimentary rock belonging to Tipam Group and the Tipam sandstone in particular predominates the entire area with admixtures of bands of shale and siltstone. Although a number of published

literatures are available regarding Tipam sandstone in other regions of North East India, there is no detailed investigation and published literature made so far from the study area. The various methods and techniques of sedimentary analyses such as grain size analysis, petrography, heavy minerals study and geochemistry are useful to depict provenance, mode of formation, depositional environment, maturity of sediments, tectonic settings and nature of weathering. So, the present research also attempt to carry out sedimentological studies on the exposed Tipam sandstone of the study area in order to find out and understand the nature of source rock, tectonic settings and weathering history.

1.2. LOCATION OF THE STUDY AREA

The state of Mizoram lies in the eastern most corner of India bordering Myanmar in the east and south, Bangladesh and the state of Tripura in the west, Manipur and Cachar district of Assam in the north. The geographical area of the state is about 21,081 square kilometers lying between the coordinates of $21^o56'$N to $24^o31'$N latitudes and $92^o16'$E to $93^o26'$E longitudes with maximum aerial dimension of 285 km from north to south, and from east to west of 115 km (Rintluanga, 1994). The state is connected with Assam through National Highway No. 54 and is also well connected by air with Kolkota, Guwahati and Imphal via Lengpui Airport.

The study area is located within Kolasib District of Mizoram, particularly to the north western part of the State. It is covered within the Survey of India Toposheet No 83 D/11 & 83 D/12 and falls within the coordinates of latitudes N 24° 10' 74.0" to N 24° 20' 74.9" and longitudes E 92° 34' 92.4" to E 92° 35' 48.9". The location map of the study area is shown in figure 1.1.

2
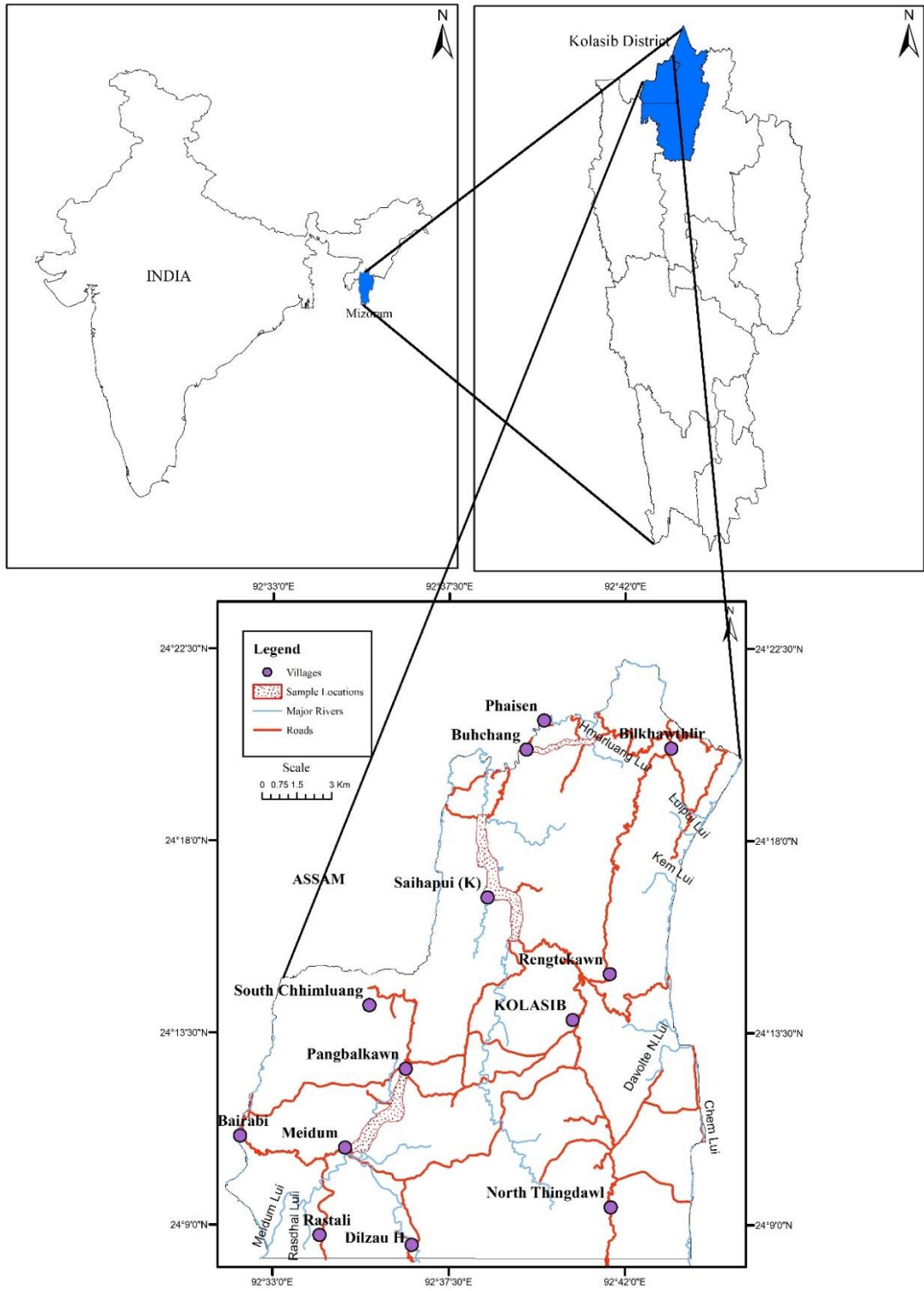
Figure 1.1 : Location Map of the Study Area

3

1.3. FLORA AND FAUNA

The State of Mizoram is well known within the country for its natural beauty and the rich and diversified floral and faunal assemblages. The Sub-tropical trees, plants, bushes, grasses and a variety of bamboos, in particulars, are some of the most common flora found in this part of the region in India. Herbaceous plants, fern and allies, orchids and other epiphytes also make a long list of plants endemic to this area. The forest of Mizoram is still a house for some of the wild animals like leopard, tiger, sambhar, deer, bear, wild pig, mountain goat, flying squirrel, monkey, snakes and other reptiles. However, there is unfortunate risk of the entire floral and faunal population within the State. The rich populations of zoo-botanical species are dwindling at an alarming rate due to lack of awareness in proper management of forest and wild practices of pouching in certain remote villages. The extensive practice of Jhum Cultivation, or in other words Shifting Cultivation in rural areas largely contributes to the destruction of forest in lieu of cultivation that involves clearing of forest and firing as the preliminary preparation for cropping. If not taken seriously on these matter and related issues, the entire State will become barren within next few decades.

1.4. CLIMATE

Mizoram has a moderate humid climate characterized by short winters and long summers with heavy rainfall. The temperature usually varies from minimum of 4-6°C to maximum of 18-23°C during winter, 21°C to 38°C during summer and 18°C to 25°C during autumn season. The State is under direct influence of southwest monsoon and experiences heavy rainfall with an annual average rainfall of about 2500

mm. The months of July and August are considered to be the wettest months while the months of December and January form the driest months of the year (Rintluanga, 1994).

1.5. GEOMORPHOLOGY

Mizoram has a hostile terrain characterized by its highly undulated, gentle to very steep and rugged topography. Almost all the hill ranges and valleys are more or less narrowly trending in the N-S to NNE-SSW directions. The average elevation in Mizoram is about 900 meters above Mean Sea Level and elevation ranges from 40 meters at Bairabi (north western Mizoram) to 2157 meters above Mean Sea Level at Phawngpui (Blue Mountain) along the Myanmar border. The general elevation increases from west to east towards Myanmar. The ridges are generally characterized by hard, compact and resistant older rock whereas the valleys and the synclinal trough are composed of younger and softer formations (Ganguly, 1983).

"The common drainage patterns include dendritic, rectangular and parallel drainage patterns which characterized the streams and rivers of Mizoram. There are five major rivers that drained the entire state such as Tlawng (Dhaleswari), Tuirial (Sonai) Tuivawl, Chhimtuipui (Koladyne) and Karnafuli. The above first three rivers flow in the north ward direction starting from the central part of the state whereas the latter two rivers are the two important southerly flowing rivers (Rintluanga, 1994)".

1.6. SCOPE OF THE STUDY

Sedimentology is one of the most important and interesting subjects in Geology. Special interest is usually given in sedimentary terrain due to its potentiality in oil and gas reserves as well as for the possible associated economic deposits like

limestone, coal, radioactive minerals, etc. Therefore, it is very much required and necessary to carry out detail geological research in the selected study area of Kolasib District in Mizoram to document and find out the geological history of the Tipam Sandstones exposed in the area. There are various approaches of studies which are helpful and successfully employed in sedimentological research. Petrographic studies of sandstones have been widely used by sedimentologist during the past few decades to decipher the provenance and tectonic setting of source areas (Pettijohn *et. al.,* 1972; Dickinson and Suczek, 1979; Dickinson, 1982, 1985, 1988; Dickinson *et. al.,* 1983; Potter, 1986). The statistics on particle size is a function of availability of different size of sedimentary particles and also the process operating on the particles during the time of transportation and deposition. Grain size analysis is useful tool to depict graphical size distribution. Heavy mineral analysis helps in understanding the nature of source rocks or provenance and stratigraphic correlation, particularly in un-fossiliferous sedimentary successions, evaluation of diagenetic history of source rocks, and perhaps, may serve an important tool for classifying the sedimentary rocks (Chenkual *et. al.*, 2010). The sedimentary geochemistry serves the purpose of delineating the actual type of the sedimentary rock using geochemical classification. The technique is also successfully utilized in deciphering different tectonic set up and provenance.

Regardless of a having a good and well exposed sedimentary succession of Tipam Group of rocks in the study area around Kolasib District, geological information is of limited extent, and hence inadequate to envisage the geological set up as a whole. Keeping the whole aspects of deficiency and inadequacy of geological records, sedimentological investigation with special emphasis on petrography, textural

6

analysis, heavy mineral analysis and geochemistry is proposed to be done to have an insight information and knowledge on the depositional history, tectonic setting and provenance of the study area.

1.7. OBJECTIVES

1. To decipher the nature of weathering, provenance and tectonic setting of the Tipam sediments using geochemical data.

2. To understand the palaeoenvironment of deposition and provenance employing textural and petrographical analysis.

CHAPTER 2

REGIONAL GEOLOGY AND GEOLOGY OF THE STUDY AREA

2.1 REGIONAL GEOLOGY

The Indo-Burma Ranges which demonstrate the collision between the Indian plate and Eurasian plate along the eastern part of the Indian sub-continent by its oblique collision with the Asian landmass and constitute "The Patkoi-Naga-Manipur-Chin Hills-Arakan Yoma region forming westerly convex arcuate belt trending in NW-SE at its southern extreme and ENE-WSW trending at the Northern end and represent the Outer Arc Ridge in an arc ridge setup". Around 200 km wide and 1400 km long Central Myanmar Basin of Paleogene-Neogene age occur on the east of Eastern Boundary Thrust (EBT). To the further east lies the Shan-Sagaing fault of N-S trending. Two molasse basin i.e. Tipam and Surma basins developed by the close of Oligocene on the foreland side of the Indo-Myanmar region. To the northern extreme of Upper Assam were developed the Tipam molasse sequence and the fold belt of the sub-flysch molasse Surma basin developed in an open basin, south of the Meghalaya plateau (Nandy, 2017).

To the west of the Indo-Myanmar mobile belt lies the Bengal basin which include most of West Bengal, Bangladesh and the northern part of Bay of Bengal. The Bengal Basin anchor the Tertiary sediments with recent alluviam deposits by the sediment influx of Ganga- Bahmaputra meghna delta.

"The Neogene Surma basin is surrounded by post-Barail unconformity, subsequently faulted (Kaladan fault) to the east; the E-W Dauki fault and NE-SW Disang thrust to the north and northeast; the NE-SW Sylhet fault (Nandy, 1986)", and Barisal-Chandpur high concealed below the alluvium of Bangladesh (Sengupta,1966) to the west and north west. The surma group with the recent sediments occurs as westerly convex N-S fold belt for a strike length of about 550 km, with a maximum width of 200 km. The basin covers lower part of Assam, Tripura, Mizoram, western part of Manipur, Sylhet and Chittagong districts of Bangladesh and Arakan coastal zone of Myanmar.

2.2 GEOLOGY OF THE STUDY AREA

Mizoram, which is believed to be a part of the southern extension of Surma Valley by many workers, began its evolution subsequent to the regional upliftment of Barail succession and thus, was related with the plate behaviour in the subduction zone west of Arakan - Yoma, after the widening of the Indian Ocean (Evans, 1964). Sarkar and Nandy (1976) have the impression that there are huge variations in the lithology, mineralogy, primary-sedimentary structures and degree of compaction between sedimentary succession of Mizoram and that of the typical Surma. The whole succession of Mizoram accommodates rhythmic alternation of arenaceous and argillaceous rocks of Palaeogene and Neogene age. Rocks of the area includes silty-sandstone, sandstone, siltstone, shale, mudstone, silt and their admixture of varying proportions along with a few pockets of shell-limestone, calcareous sandstone and intraformational conglomerates. "Almost all the rocks are thrown into a series of approximately N-S trending, longitudinally plunging anticlines and synclines. The

general strike direction of the rock formation is N-S with dip amount varying from 20°- 50° either towards east or west (Ganju, 1975 and Ganguly, 1983)". Significantly, the western flanks of the State along with the neighbouring areas i.e Tripura and Cachar district of Assam, are characterised by younger rock formations folded into narrow, box-like anticlines in alternation with wide and flat synclines, while the eastern part of the state shows dominance older rock formations folded into tight, linear anticlines and synclines (Ganguly, 1983). In the region, about 15 major long and arcuate anticlines and corresponding synclines are observed (Nandy *et.* al., 1983).

The Tertiary rocks of Mizoram have been organised into the Barail, the Surma and the Tipam Groups in the ascending order. Karunakaran (1974) and Ganju (1975) worked out the stratigraphic succession minor divergence which is given in Table 2.1 along with the geological map given in fig. 2.1. The presence of Barail group in Mizoram is still rather controversial even as of now and has given rise to more speculations. Many workers from Geological Survey of India like Nandy (1972, 1982) and Nandy *et. al.*, (1983) predict that the rocks in the eastern part of Mizoram are of Barail Group. In contradiction, workers from ONGC like Ganju (1975), Ganguly (1975) and Shrivastava *et. al.* (1979) believe the absence of Barails in Mizoram.

The Barail Group (Table 2.1) which consists mostly of pale-gray, fine to very fine-grained, carbonaceous sandstone, with minor siltstone and silty shale, is believed to have been deposited during a major regression that resulted in the exposure of most of the Indian platform part of the Bengal Basin. The rocks are represented to have been mainly tide dominated shelf environment deposits (Alam, 1991). The Barail

rock in general comprises dominantly pale-gray to brown, very fine to fine grained sandstone with minor siltstone and silty shale interbeds.

Surma group of the study area has been divided into two on the ground of abundance of sandstone and shale as Bhuban Subgroup (Lower, Middle and Upper Bhuban Formation) and Boka Bil Formation (Evans, 1932). Repeated transgression and regression have resulted in the formation of the lower to middle Miocene Surma Group. The Surma Group of Mizoram happens to attain a thickness of more than 4 km and consisting mainly of dark gray shale, siltstone, fine to coarse-grained sandstone, and occasional intraformational conglomerate. The Middle Bokabil Member is represented by sandier units within the dominantly argillaceous Bokabil Formation, whereas the Middle Bhuban Member is a more argillaceous distribution of the dominant arenaceous Bhuban Formation. These descriptions of the broad subdivisions of the Bhuban and Bokabil Formations are difficult to correlate with the lithology of the Surma Group penetrated in the subsurface as well as exposed succession of the EFB, where majority of the Bhuban Formation is dominantly argillaceous. The upper part of the Bokabil Formation is pelitic, and is traditionally known as the 'Upper Marine Shale' (Holtrop and Keizer, 1970).

The upper Mio–Pliocene Tipam Group unconformably rests over the Boka Bil Formation and is further divided into the Tipam Sandstone and Girujan Clay Formations. Yellowish brown to reddish brown color, coarse-grained, cross-bedded to ripple-laminated sandstone with plenty of fossil woods and minor siltstone and mudstone signifies Tipam sandstone.

Table 2.1:Stratigraphic Succession of Mizoram (Modified after Karunakaran, 1974 and Ganju, 1975)

Age	Group	Formation	Unit	Generalized Lithology
Recent	Alluvium			Silt, clay and gravel

_____Unconformity_____

Age	Group	Formation	Unit	Generalized Lithology
Early Pliocene to Late Miocene	TIPAM (+900m)			Friable sandstone with occasional clay bands

_____Conformable and transitional contact _____

Age	Group	Formation	Unit	Generalized Lithology
Miocene	S	Bokabil (+950m)		Shale, siltstone and sandstone

_____Conformable and transitional contact _____

Age	Group	Formation	Unit	Generalized Lithology
	U		Upper Bhuban (+1100m)	Arenaceous predominating with sandstone,shale and siltstone
		B		

___Conformable and transitional contact _____

Age	Group	Formation	Unit	Generalized Lithology
to	H	Middle Bhuban (+3000m)		Argillaceous predominating with shale, siltstone-shale alternations and sandstone
	R	U		

___Conformable and transitional contact _____

Age	Group	Formation	Unit	Generalized Lithology
		B		
Upper Oligocene	M	A	Lower Bhuban (+900m)	Arenaceous predominating with sandstone and silty-shale
		N		
	A (+5950m)			

_____Unconformity obliterated by faults _____

Age	Group	Formation	Unit	Generalized Lithology
Oligocene	BARAIL (+3000m)			Shale, siltstone and sandstone

_____ Lower contact not seen_____
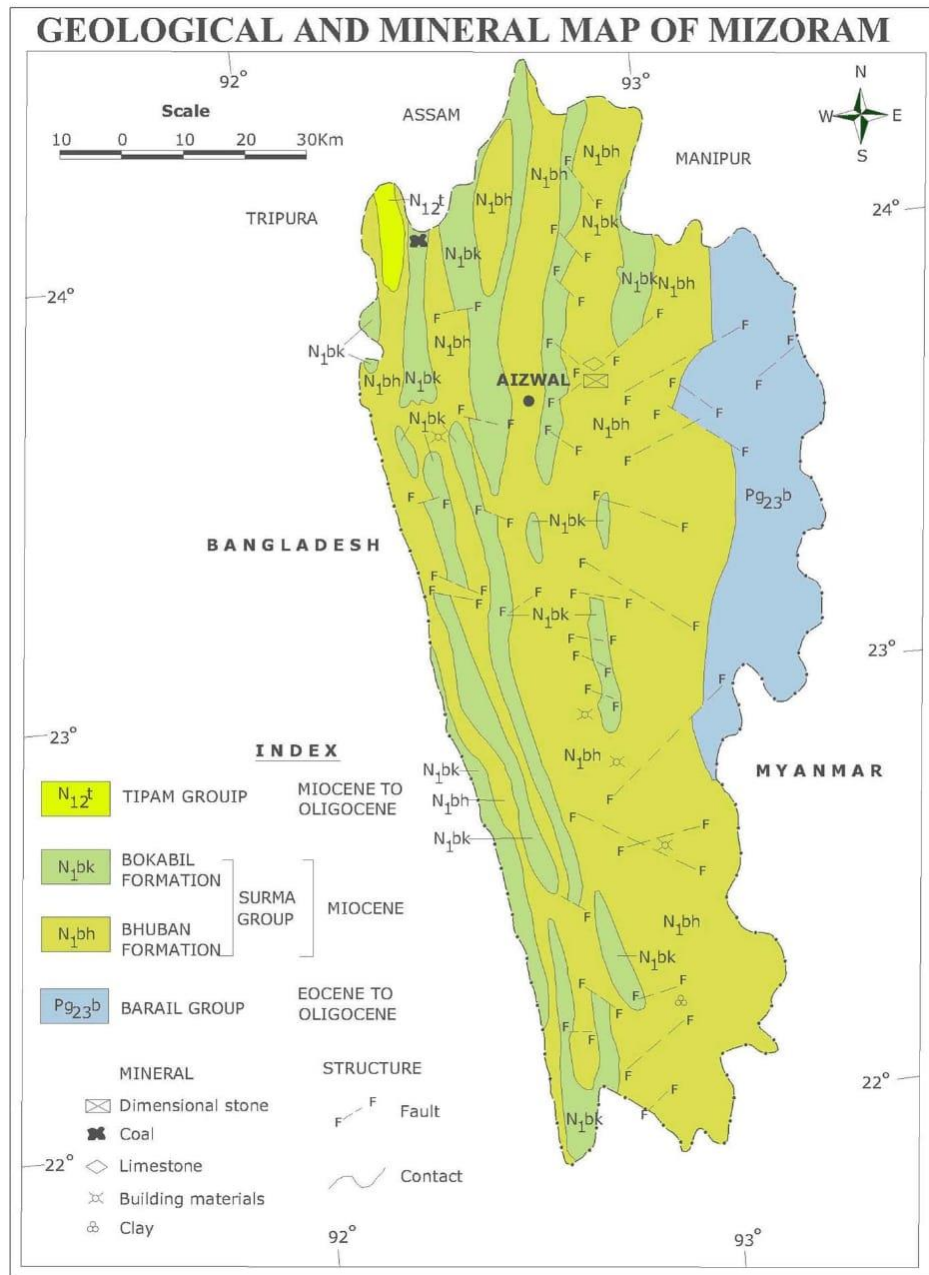
Figure 2.1: Geological Map of Mizoram according to Geological Survey of India

A thick succession of Tertiary rocks in the Kolasib district of Mizoram is represented by the Middle and Upper Bhuban Formation, the Boka bil Formation of Surma Group of rocks and also the Tipam sandstone formation. However, the present study is confined to the Tipam sandstones, on the road cut sections near Buhchang, Saihapui and Meidum-Pangbalkawn villages. The sandstones in this area are illustrated by its soft and friable nature. The sandstones of the study area are associated with alternating bands of shale/mud with varying thickness from one place to another. Wave ripples, parallel beddings, cross-beddings, wavy, flaser, lenticular beddings and sole marks like flute caste and load caste are the common Primary sedimentary structures readily observed in the sandstones of the study area. Other than the primary sedimentary structures are mud clasts of varied shapes and sizes, and leaching of iron ores are also some of the common secondary sedimentary features found in the sandstones. Quartz, feldspars and micas are the major minerals constituting the bulk mineralogy that can be identified megascopically. The detail lithological characteristics are represented in the litho-column in figure 2.2 (A-D) and geological map of the study are is also represented in figure 2.3

Figure 2.2 (A): Litho-column of Meidum to Pangbalkawn section of the study area.

clay	silt	sand	gravel	description	index

Sand-shale alternation with high shale proportion.

Brown sandstone with cross bedding, red shale due to Fe-leaching

MP-22

Brown sandstone with thin beds of shale

Shale with thin lens of sand

Sand-shale alternation with sand dominant, heterolithic bedding

N24⁰11.190
E92⁰36.600
Elv- 116

MP-21

Brown sandstone with large scale cross bedding, mud clast, faulting observed

Brown sandstone with thin shale bed, large scale cross bedding, wavy beding, Fe-leaching, Sandstone bed 5 inch to 1 feet

MP-20

Shale with lenticular bedding

N195⁰/36⁰

Brown sandstone with thick lenses of clay.

Shale with thin lenses of sand, flaser bedding

Sand-shale alternation with thick lenses of clay, flaser bedding.

MP-19

Shale with thick lenses of sand

N24⁰11.027
E92⁰35.489
Elv- 102m

Index:
- Brown Sand
- Shale
- Sand lens
- Clay Lens
- *MP* Sample
- Mud Clast
- Cross bedded sand
- Lenticular bedding

Figure 2.2 (B): Litho-column of Meidum to Pangbalkawn section of the study area.

Figure 2.2 (C): Litho-column of Saihapui section of the study area.
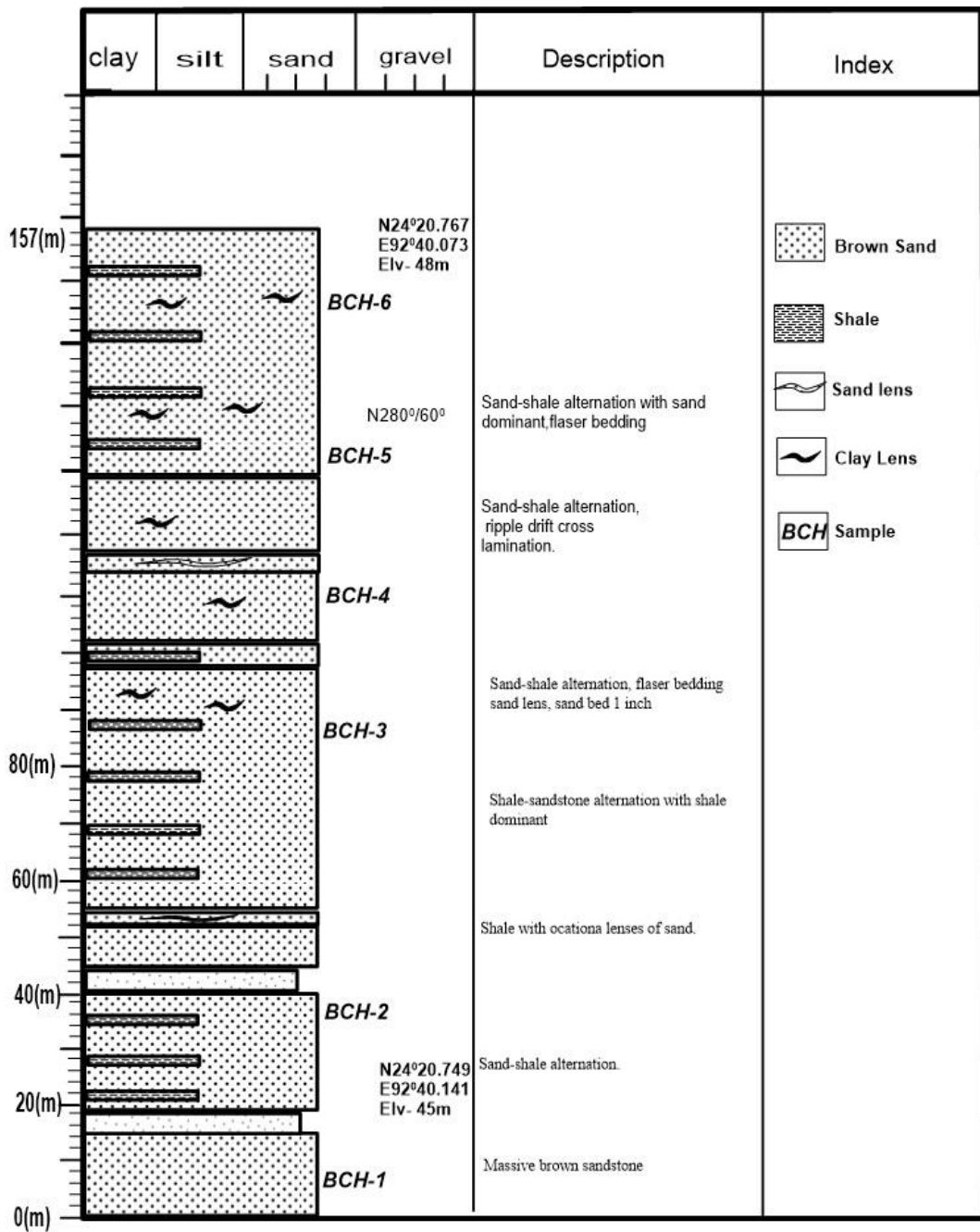
Figure 2.2 (D): Litho-column of Buhchang section of the study area.
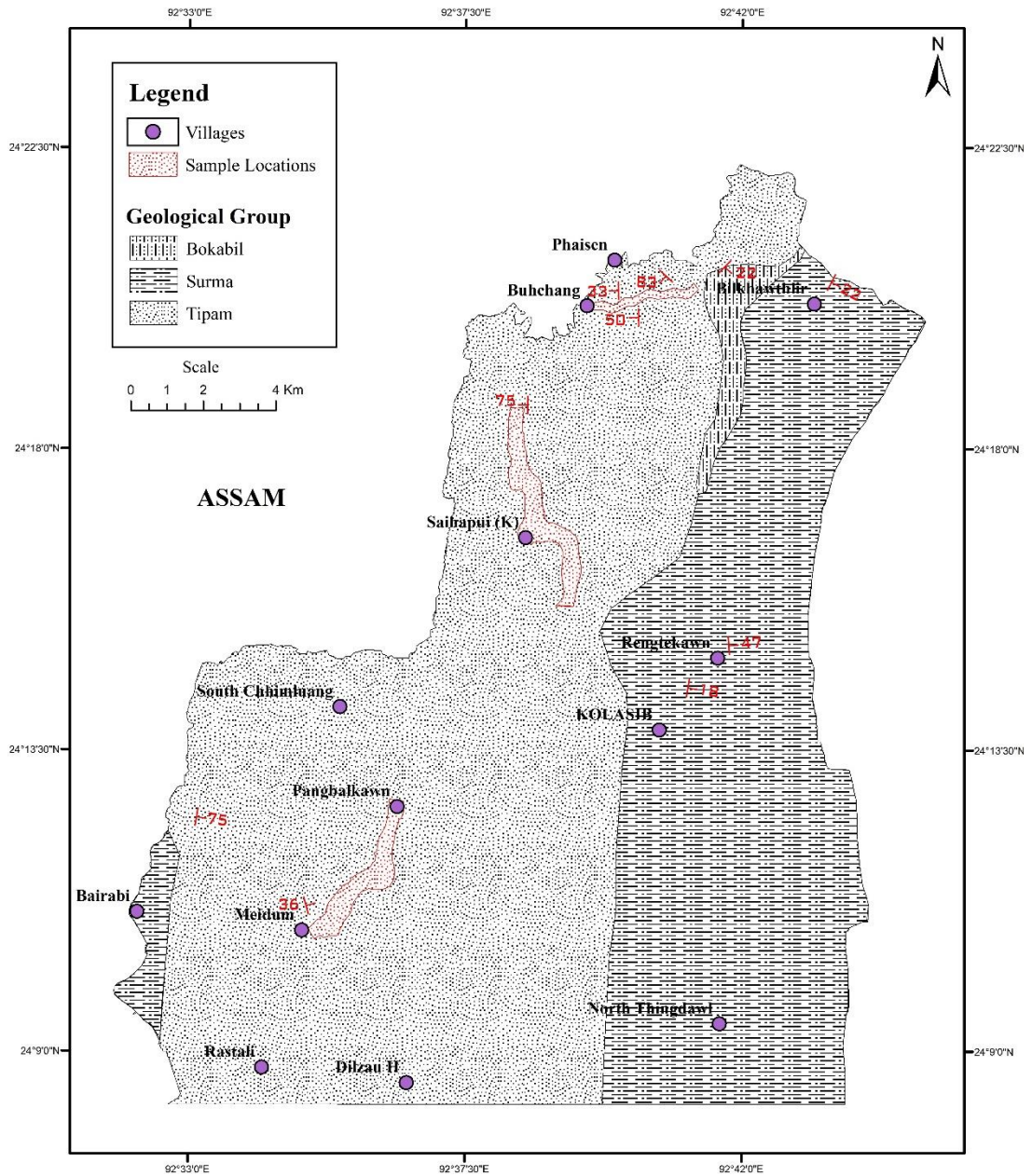
Figure 2.3: Geological map of the study area

Figure 2.4 Sandstone and Shale alternation of Tipam sandstones

Figure 2.5 Rhythmic alternation of Tipam sandstone and shale
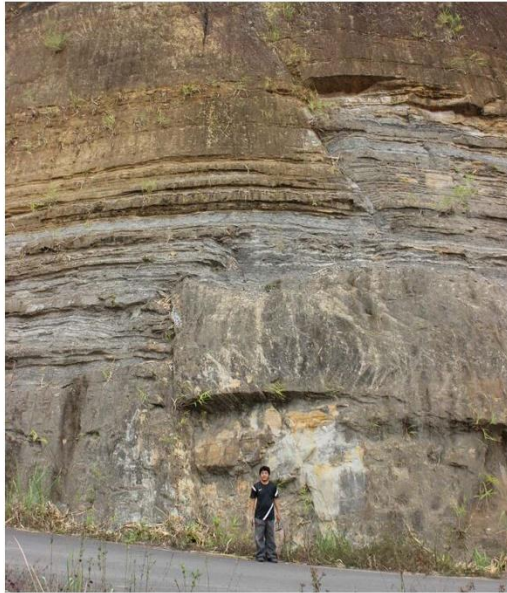
Figure 2.6 Faulting in Tipam sandstones

Figure 2.7 Folding in Tipam sandstones

Figure 2.8 Shale and Sandstone alternation of the study area

Figure 2.9 Interference wave ripples in Tipam sandstone

Figure 2.10 Large Scale cross bedding in Tipam sandstone

Figure 2.11 Liesegang in Tipam sandstone

Figure 2.12 Load casts in Tipam sandstone
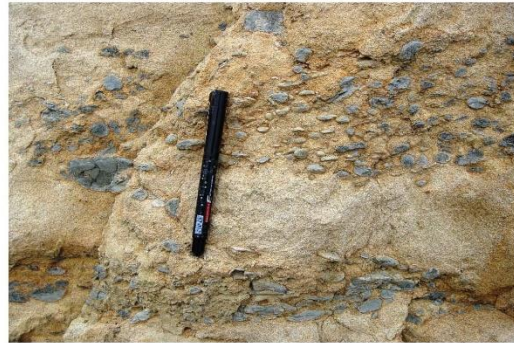
Figure 2.13 Clasts of Mud within Tipam sandstone

Figure 2.14 Cross bedding within the sand lens

Figure 2.15 Cross bedding in Tipam sandstone

CHAPTER 3

REVIEW OF LITERATURE

In spite of having a good and well exposed Tipam group of rocks in the study area, however, geological studies, particularly the sedimentological aspects carried out in the Tipams are still very meager, and are not at par with the other Group of rocks like the Surmas. Many workers have carried out sedimentological studies in the Tertiary succession of the adjoining areas like Surma-Tipam groups of Upper Assam valley, South of Brahmaputra (Dutta *et. al.*, 1980), Upper Tertiary Tipam sandstone of the Kameng foothills of Arunachal Himalayas (Hazarika, 1984). In 1992, Geologists from ONGC such as Lal M, Singh S K, Sundarajan V, Shah L, Das, D and Saha, T carried out heavy mineral analysis on the Bhuban Formation, Bokabil Formation of Surma Group and the Tipam Group from Rengte and the adjoining Teidukhan anticlines. They have identified and reported the different heavy mineral suites for each Group of rocks mentioned above. The Surma group of rocks consist of tourmaline, epidote, rutile, chloritoid, garnet, staurolite and hornblende; the suite in Boka bil Formation is tourmaline, chloritoid, staurolite, rutile, zircon and garnet whereas the mineral suite of Tipam Group of rocks is characterized by epidote, staurolite, kyanite, tourmaline, hornblende, chloritoid, rutile, garnet, enstatite, zircon, chlorite and zoisite. The application of Cerium anomaly as indicator of eustatic sea-level changes is shales of anoxic facies was studied by Wilde *et. al.,* (1995) from the middle Ordovician through the lower Silurian of Scotland and concluded that positive anomaly of Ce would indicate a lowering of sea level as the apparent depth on the redox curve would reflect more oxic conditions. Negative Ce anomaly with time would

indicate a rise in sea level as the apparent depth reflects more anoxic conditions. Heavy mineral suite in the Tura sandstone, East Garo Hills, Meghalaya was studied by Das P. K. and Duarah B. P, (1996). Plank and Langmuir (1998) have studied the chemical composition of subducting sediment and found out that GLOSS is dominated by terrigenous material (76 wt% terrigenous, 7 wt% calcium carbonate, 10 wt% opal, 7 wt% mineral-bound H_2O^+ and therefore similar to Upper Continental Crust (UCC) in composition with exception in the enrichment of Ba, Mn and the middle and heavy REE.

Paleontological studies of Tipam sandstone was carried out by Tiwari and Mehrotra, (2000) and inferred a prevalence of warm and humid climate during the time of deposition of Tipam sandstones. Sedimentation and subsidence of Miocene sediments during Continent-Continent collision of Bengal Basin, Bangladesh was studied by Uddin *et. al.,* (2003) and have found out that subsidence of Sylhet trough had not taken place by the end of Miocene. The post-Miocene subsidence is due to southward thrusting of the Shillong plateau along Dauki fault. Hossain *et. al.,* (2006) have analyzed major and trace elements from Sylhet Basin of Bangladesh and found out that the average composition of sandstones and mudrocks of Sylhet sediments tends to have higher SiO_2 content as compared to average Upper Continental Crust (UCC) and strongly depleted in CaO, Na_2O and Sr, depleted to lesser degree in Nb, Rb, Ba, K_2O, MgO and Al_2O_3 especially in Tipam and Dupitila sandstones. Roy *et. al.,* in 2006 have studied provenance of exposed Tipam sandstone of Sylhet, Bangladesh and suggest the source of Tipam sandstone as pre-existing sedimentary rock, igneous and metamorphic rock with quartzose recycled orogen and mixed provenance under semi-humid to humid climatic conditions. Provenance, tectonic

setting and weathering on Surma group of Bengal basin was studied by Rahman *et. al.,* (2007) employing Geochemistry and concluded that the sandstones of Surma group of Bengal basin were derived from felsic rock sources. Uddin *et. al.*, (2007) have studied the provenance of Cenozoic sediments of Assam and Bengal foreland basin using heavy minerals and concluded that the Miocene and younger rocks of Assam and Bengal basin were derived from orogenic terrain. Uddin *et. al.*, (2008) have also studied the Cenozoic sediments of Bengal basin, Bangladesh and inferred that the Barail sediments may have been derived from proto-Himalayas and/or Indo Burma ranges, Miocene and Pliocene sediments of mostly metamorphic source. Paleogene record of Himalayan erosion of Bengal Basin, Bangladesh was also workout by Najman *et. al.,* (2008). They dated the Barail Formation at Eocene to early Miocene (38 Ma to <21 Ma). Provenance study shows that the Barail Formation represents the first input of Himalayan-derived sediments to the Bengal Basin. In 2009, Sahoo *et. al.,* have studied the processes, mechanism and depositional environment of early Miocene sediments of upper Assam Basin and deduce that the sediments are deposited in prograding environment where the supply of sediments in the basin exceeds the accommodation space available and a wide spread deposition of fluvial Tipam sediments occur with cyclic deposition of fining upward sequence. Islam, (2010) has studied petrography of subsurface Neogene sandstones of Bengal basin of Bangladesh and infer that the sands were derived from quatzose recycled orogen such as fold thrust province or a collision suture zone with a source of sediments from eastern Himalayas or Indo-Burma Ranges.

In 2010, L. Chengkual, T. Kataki, and J.N. Sarma have also identified the heavy mineral assemblages present in the Tertiary rocks of the Teidukhan anticline,

Kolasib district and worked out the provenance of the rock. They have concluded that the source of the sediment was complex in nature comprising of igneous rock and pegmatite to high rank metamorphic rocks and reworked sediment supply. Lalmuankimi *et. al*., (2010) have studied the fossiliferous calcareous sandstone of Upper Bhuban Formation of Mizoram and found out that the succession has yield a benthic and planktic foraminifera which depict the Miocene age of the formation. The geochemical study of Upper bhuban sandstone of Muthi, Mizoram disclose that the average CIA value was higher than the Upper continental crust indicating high intensity of chemical weathering in the source area with tectonic settings of active continental margin (Lalmuankimi *et. al.,* 2011). Singh *et. al.,* (2011) have studied the Paleoecology of the Upper Bhuban and Tipam sediments of Mizoram, India and concluded that the Upper Bhuban formation were deposited under tropical-subtropical and humid climatic conditions while the Tipam group of rocks was deposited under tropical humid to subtropical climatic conditions in fresh water environment. Borgohain Pradip, (2011) has studied textural variation of Tipam Reservoir of Digboi Oilfield of Upper Assam and have concluded that the sediments of Tipam of Upper Assam were mainly deposited in a fluvial environment under river tractive current. The grain-size distribution of Tipam sandstone in the section of Tipong Pani river of Assam was again studied by Borgohain Pradip, (2012). The study reveals that the sediments of Tipam sandstone of Tipong Pani river section was deposited in a fluvial environment. Again, Borgohain Pradip in 2012 also studied the grain size distribution and prepared the vertical litho-section of exposed Tipam sandstone along Dilli river, Assam. Based on his findings, he had concluded that the Tipam sandstones were deposited under fluvatile environment. Borgohain Pradip, (2012) has studied the heavy

27

mineral suits of sub-surface Tipam sandstone of upper Assam and concluded that the sediments of Tipam sandstone were derived from varied source with short transportation under fluvial environment. Ralte, (2012) have also worked out the provenance of the Tipam sandstone from the Kolasib district of Mizoram using heavy mineral analysis and have suggests a complex provenance comprising of high-grade metamorphic source as well as igneous and sedimentary sources with a relatively short transportation for these sediments. Okeyode and Jibiri in 2012 have analyzed the sediments from Ogun river, South Western Nigeria and suggest that sediments deposited under fluvial environment generally indicate immature to mature poorly sorted to moderately well sorted sediments. Chutia *et. al.,* in 2013 have analyzed the geochemical composition and source area weathering of Tipam sandstones from a few oil fields of Upper Assam Basin, India. Based on their studies, the chemical index of alteration of Tipam sandstones indicate moderate weathering in the source area and was dominated by rocks of tonalitic and granodioritic composition and K-metasomatism played a significant role. Sarma J. N. and Chutia Ananya, (2013) have studied petrography of sub-surface Tipam sandstone of upper Assam and infer that the Tipam sandstone were mostly derived from middle and upper rank metamorphic sources with tectonic setup of transitional recycled orogen. Again, Sarma J. N. and Chutia Ananya, (2013) have also studied the petrography and heavy mineral suite of Tipam sandstone on the Tipam hill of Sita Kunda area, upper Assam, India. Their studies indicate that the source of Tipam sandstone comprises low, middle as well as upper rank metamorphic source with mixed and quartzose recycled origin. Chandra *et. al,* in 2013 have Studied the petrified wood forest of Mizoram and disclose the existence of semi evergreen to deciduous forest in Mizoram during Neogene which

shows a warm and humid climate was prevailing in the region during the time of deposition of Tipam sediments.

Lalnunmawia *et. al.,* (2014) have classified and studied the provenance of exposed Bhuban formation of Durtlang road section, Aizawl, Mizoram. Accordingly, they classified the sandstone into litharenite and sublitharenite of igneous and metamorphic source mainly from Himalayan ranges and the Indo-Burmese collision zone. Rajkonwar *et. al.,* (2014) have Studied ichnofacies of Bhuban formation (Surma Group) of Mizoram and concluded that the rocks of middle Bhuban were deposited under high energy conditions and sandy shifting substrate in foreshore zone. Rai *et. al.,* (2014) have also studied the nannofossil biostratigraphy of Bhuban formation, Mizoram and concluded the age to be of Burdigalian to late Messinian. Lalnuntluanga *et. al.,* in 2014 have studied magnetostratigraphy of Miocene Bhuban Formation of Surma Basin in Mizoram, India. Their studies from four sections infer the youngest bed to be 8.699 Ma and the oldest bed to be 16.726 Ma. Amireh, (2014) have studied grain size of the Lower Cambrian to Lower Cretaceous clastic sequence of Jordan and coined a new grain size parameter called the mean sorting index where mean grain size and sorting parameters were employed. From his study, he concluded that the average of mean-sorting index for a group of sand size particles can be employed successfully to discriminate between fluvial channel sand deposits, the fluvial flood plain/ overbank/ bar top sand deposits and the shallow marine sand deposits. Lui, (20015) has analyzed the grain size of well-sorted sediment using autocorrelation techniques and concluded that it offers a more accurate estimation of the grain size distribution and the associated inherent parameters of the mixed size sediments. Bharali *et. al.,* (2017) have studied provenance, tectonic setting and paleoclimatic condition

prevailing during the time of deposition of Upper Bhuban formation using grain size analysis, petrographic studies and heavy mineral analysis and concluded that the sandstone belongs to litharenite and wacke which were deposited in an active continental margin to recycled orogen settings. Periasamy and Venkatashwarlu, (2017) have employed Petrographic and geochemical studies of Jurassic sandstones From the Jhuria Formation, Kachchh Basin, Gujarat, India to deduce the provenance and tectonic setting. From the petrographic studies, the sandstones were classified into arkose, sub-litharenite, wacke and quartz arenite. The tectonic discrimination diagram based on the elemental concentrations and elemental ratio plots Jhuria sandstones in continental rift and collision settings. Baiyegunhi *et. al.,* (2017) have studied the statistics and depositional pattern of the Ecca Group sandstones in the Eastern Cape Province, South Africa and found out that most of the sandstones are very fine to fine grained, moderately sorted to well sorted in nature indicating dominance of low energy environment. Vereshchagin *et. al*., (2018) employed the U-Pb ages of detrital zircons and the chemical composition of detrital garnet and tourmaline from Jurassic-Cretaceous siliciclastic rock of Northern Siberian Craton in which detrital zircon display two age populations, dominated by Late Paleozoic and Paleoprotozoic-Archean zircons while pyrope association depicts high-grade metamorphic rock of the Siberian Craton. Several sources of detrital materials are indicated by the chemical composition of garnet. Garzanti, E. and Ando, S. in 2019 have studied the error associated in sampling and studying heavy minerals and suggest not to use heavy minerals alone for studying provenance of a sandstone but to combine with petrographic analysis in thin section routinely. Hussain, M. F. and Bharali, B. in 2019 have studied the whole-rock geochemistry of Tertiary sediments of Mizoram Foreland

Basin. The CIA and CIW values of both Barail and Surma suggest their derivation from moderately weathered source rock. Form their studies, similarities in the geochemical characteristics of Tertiary sediments of Mizoram foreland basin with the Siwalik foreland sediments suggest source of sediments from Himalaya under active continental margin. Sincavage *et. al*., (2019) have studied the stratigraphic architect, facies distribution and downstream reservoir characteristics of the Ganges-Brahmaputra-Meghna Delta by coupling rate of mass extraction with input grain-size distribution, accommodation and sediment input from multiple transport pathway and observed a low rates of fining and sand-rich channel facies along the western margin of Sylhet basin.

CHAPTER 4

METHODOLOGY

4.1. INTRODUCTION

In sedimentological research, there are wide options of geological techniques to choose depending upon the target of research. The nature of work in the present research is, thus categorized accordingly into three broad categories, viz., Literature Survey, Geological Field Work and Laboratory Analysis.

4.2. LITERATURE SURVEY

Literature survey is an essential part of the current research. Relevant literatures with respect to the present work are collected from different sources. During literature survey, special interest is given to those papers and documents related to Tipam Group of rocks from the study area or any other region of North East India, through Journals, Memoir and/or Books, and internet. Since the study area is virgin in any geoscientific investigation, limitation of literature is encountered, and hence numerous literatures on sandstones that are found to be helpful in the current work are collected. The collected literatures are reviewed and carefully studied so that the current research could be fully benefitted in helping build up of better ideas and having wide spectrum of determination to make consolidated scientific conclusions during interpretation and discussion of the generated data and scientific observations made.

4.3. GEOLOGICAL FIELD WORK

Extensive geological field work was carried out during the present research which is an essential proxy in any field base and field related geological research. Recognition of rock type and sedimentary structures, mapping of various litho units, measurement of lithological attributes (rock type, color, texture, thickness of the bed, degree of induration, nature of weathering, primary and secondary sedimentary structures and attitude of beds- dip and strike), preparation of geological map and collection of exposed samples were the main task that was carried out during the entire fieldwork. Field outcrop of the sedimentary strata, different sedimentary structures and any other information that could be seen during field work are documented in the form of field photograph. Structurally, the area under study is a syncline. So, utmost care was taken while collecting the samples in order to avert repetition of bed. During field work, 47 fresh and un-weathered sandstone samples were collected for detailed systematic studies in the laboratory from the lithological succession having thickness of about 876 meters. The sandstone samples collected were carefully labelled and packed in a sample bag for further studies at the laboratory. After preliminary investigation at the laboratory, of the 47 samples collected, 20 samples were finally selected for grain size analysis, petrographic analysis, heavy mineral analysis and whole rock chemical analysis.

4.4. LABORATORY ANALYSIS

The present research requires different laboratory analyses in the form of various procedures and techniques. In doing so, the samples collected were refined into representative set of samples and the samples were variously prepared as per

requirement of the techniques employed. The laboratory works performed during the research were discussed in the following under different heads like grain size analysis, thin section and petrography, heavy mineral analysis and geochemical analysis. The analysis was done in the Department of Geology, Mizoram University and the National Geophysical Research Institute (NGRI) in Hyderabad.

4.4.1. GRAIN SIZE ANALYSIS

Size analysis of the studied sandstone samples were done following conventional sieving procedure of Krumbein and Pettijohn, (1938). As the Tipam sandstones are characterized by their soft, loose and friable nature; disintegration of grains for size analysis is done by simply soaking the samples in the water in the containers for about 2 to 3 days. The samples are then boiled with water along with a dilute hydrochloric acid (10%) to remove the authegenic clay, carbonate and ferruginous coatings on the grain. The samples were again treated with hydrogen peroxide to remove the organic compounds binding the grains. After thorough washing with distilled water, the samples are dried in the hot air oven for about 3 to 4 hours at the temperature of about 70º C. The cone-and-quartering method of sample is applied to weigh out 100 grams of the loose grains from the bulk sample. These loose grains are then placed on top of a stack of screens arrange from bottom to top in order of increasing sieve diameter. When the stack is shaken using sieve shaker, the particles divide into several fractions, depending on the number of sieves in the stack. The fraction lying on each sieve was collected separately and weighted (Sengupta, 2007). The frequency of weight retained in each pan was recorded and further used for studying the statistical parameters of grainsize distribution of Tipam sandstones. Test

sieves of ASTM standard with a mesh nos. of 20, 30, 40, 50, 70, 100, 140, 200, 270 and 325 are used for the present study.

4.4.2. THIN SECTION AND PETROGRAPHY

Thin section slides were prepared, analyzed, studied and photograph using Leica DDM2700P Petrological microscope and point counting was done using PERTOG Stepping stage at the Department of Geology, Mizoram University. A point counting technique after Gazzi-Dickinson method was followed with counting of four hundred (400) grains on 20 thin section slides. Primary detrital constituents such as quartz, feldspar and rock fragments were studied and recorded for classification of sandstones and for further interpretation such as provenance (Basu *et. al*., 1975 and Tortosa *et. al*., 1991), paleoclimate study Suttner *et. al*., 1981 and Weltje, 1994) and tectonic settings (Dickinson & Suczeck, 1979 and Dickinson *et. al*., 1983) of Tipam sandstone. The detrital grains commonly taken into consideration in the work include micas, particularly muscovite and biotite.

4.4.3. HEAVY MINERAL ANALYSIS

In the present study, heavy mineral separation has been carried out following the funnel separation method of Krumbein and Pettijohn, (1938) using Bromoform (Sp. Gr. 2.89). Bromoform are highly toxic and suspected carcinogens. They may absorb through the skin and are apparently cumulative for the body. Hence, they should be used in a fume hood in a well-ventilated room with gloves (Hauf and Airey, 1980). Sample size ranging from 70 to 80 mesh (ASTM) have been mixed thoroughly to get a better result of the heavies in different size grades.

The samples were thoroughly washed with Distilled water to remove the clay size particles. The samples were then thoroughly dried for separation. The separated heavy minerals were then washed with acetone to remove the bromoform. Heavy mineral thus separated were mounted on glass slides using Canada balsam for identification under the petrological microscope. The identification and photography of the separated heavy minerals of Tipam sandstone was done using Leica DDM2700 P Petrological microscope at the Department of Geology, Mizoram University. The percentage of each heavy minerals was calculated and recorded. The percentage of the heavies were calculated and Histogram and pie diagram were prepared for statistical representation. Out of the transparent, non-micaceous detrital minerals (omitting opaque, micaceous and authigenic minerals) the percentage of Zircon, Tourmaline and Rutile were recalculated to 100 to determine ZTR Maturity Index (Hubert, 1962).

4.4.4. GEOCHEMICAL ANALYSIS

Fresh sandstone samples of the study area were crushed and grind into powder with Agate mortar as fine as talcum powder for whole rock chemistry. Major oxides concentration was performed using Philips Model PW 2440 MagiX PRO wavelength dispersive X-ray Fluorescence spectrometry (WD-XRF) equipped with an automatic sample changer Model PW 2540 and software Super Q 3.0 at National Geophysical Research Institute, Hyderabad. Pressed Pellets were prepared from each of the powdered samples using boric acid in collapsible aluminum cups and pressed by hydraulic press at 20 tons. The pellets were analyzed at National Geophysical Research Institute, Hyderabad for determination of major oxides such as SiO_2, Al_2O_3, Fe_2O_3, MnO, MgO, CaO, Na_2O, K_2O, TiO_2, P_2O_5 of the studied Tipam sandstones.

For geochemical analysis of Trace element and REE, 0.05 g of grinded powder from each of the samples was weighted and put in a Savillex. To each of the samples, an acid mixture of 7(HF): 3(HNO_3) was added and the Savillex vessels were tightly closed and kept on a hot plate at ~ 150 ^{o}C for 48 hours. After the following 48 hours, the vessels were open and 1 to 2 drops of $HClO_4$ was added and evaporated for about one hour to near dryness. The remaining residue were dissolved by adding 10 ml of 1:1 HNO_3. After all the residue were dissolved, the samples were again kept in a hot plate for 30-40 minutes at 80 ^{o}C to dissolve all suspended particles and was transferred in 250 ml standard flask. 10 ml of 1:1 HNO_3 and Rhodium (Rh) solution was again added in the standard flask with Millipore water. Here, Rhodium (Rh) is used as an internal standard. Finally, 5 ml was taken out from 250 ml solution of the samples and was made 50 ml with Millipore water and the final solution was stored in Eppendorf tubes for High Resolution-ICPMS analysis at National Geophysical Research Institute, Hyderabad for determination of trace elements and REE such as Sc, V, Cr, Co, Ni, Cu, Zn, Ga, Rb, Sr, Y, Zr, Nb, Cs, Ba, La, Ce, Pr, Nd, Sm, Eu, Gd, Tb, Dy, Eo, Hr, Tm, Yb, Lu, Hf, Ta, Pb, Th and U. The HR-ICPMS was calibrated with standard GSR4.

CHAPTER 5

TEXTURAL ANALYSIS OF SANDSTONES

5.1 INTRODUCTION

The textural parameters of a sedimentary rock include shape, roundness, grain-size and particle arrangement (packing and fabric) (Friedman and Johnson, 1982). A careful study of the textural elements of sediments can give a vital clue to the environment of deposition (Friedman and Johnson, 1982). Analysis of grain parameters constitute one of the most important parameters for understanding the sedimentary processes and depositional environment of sedimentary rocks. As such, the present work is confined to this aspect only.

"Grain size analysis can be defined as the quantitative expression of the size frequency distribution of particles in granular, fragmental or powdered materials. It can also be expressed as the process by which the relative proportions of the particles of various sizes in the sediments can be determined" (Lakhar, 2010).

Size distribution in clastic sediments is one of the most important parameters for studying the nature of depositional media since it is related with the physical forces for transportation and deposition of sediments. Many workers like Krumbein, (1938), Inman, (1952), Folk and Ward, (1957), Passega, (1957), Shepard and Young, (1961), Visher, (1969) and Pettijohn, (1975) have attempted to established the relationship between the grain-size distribution of a particular sediments with different depositional environment. The distribution of grain size is considered to be

environment sensitive. Grain-size analysis despite has been widely used to interpret the depositional environment of clastic sediments, many other workers are of the opinion that this textural parameter alone is insufficient to conclude the depositional environment. However, analysis of the distribution of sediment particles can be use as supplementary information along with many other variables.

5.2 GRAPHIC REPRESENTATION OF GRAIN-SIZE DISTRIBUTION

The distribution of grain-size in sediments is a function of different particle sizes present in the parent material and the processes operating during transportation and deposition of the sediments. "Graphical presentation of the size distribution is necessary in order to interpret a given sedimentary accumulation (Friedman and Johnson, 1982)". Data can be presented graphically in the form of histogram, frequency curve and cumulative-frequency curve. Graphs are constructed so that the two coordinate axes are at right angle to each other where the abscissa represents the x-axis and ordinate represents the y-axis. Particle frequency which is the dependent variable is plotted in the ordinate or y-axis and particle size (in terms of Φ) is plotted in the abscissa (x-axis).

5.2.1 The Histogram

A histogram is a graphic representation of frequency-distribution data and is the simplest method of presenting grain size data graphically. It is simply a bar graph in which the weight percent of sediment in each size class is plotted as

Sample	0 Φ	0.5 Φ	1 Φ	1.5 Φ	2 Φ	2.5 Φ	3 Φ	3.5 Φ	4 Φ	4.5 Φ	5 Φ
MP 7	0	0	1.28	17.44	40.23	11.31	7.42	13.63	7.91	0.74	0
MP 9	0	0	2.3	24.35	44.28	9.63	4.29	8.76	5.19	0.43	0.21
MP 11	0	0.9	1.38	15.94	40.9	13.62	6.55	14.74	4.12	0.81	0.56
MP 16	0.03	0.99	1.35	16.68	40.2	14.15	6.44	13.51	3.91	1.24	1.13
MP 17	0	0	1.5	18.96	49.38	10.82	4.68	12.12	2.4	0.08	0.02
MP 19	0	0.66	4.68	43.2	27.81	7.4	4.24	8.46	2.69	0.06	0.4
MP 20	0	0.13	0.85	13.44	50.71	10.14	5.49	13.53	4.95	0.48	0.08
MP 21	0	0.2	0.41	11.69	51.26	9.73	3.96	11.03	7.43	3.31	0.21
MP 22	0	0.27	5.18	28.03	40.71	10.04	4.89	6.59	2.89	1.09	0.24
SP 1	0	0	1.71	29.25	44.97	8.03	3.39	8.8	3.31	0.32	0.1
SP 2	0	0.49	3.79	22.26	49.92	7.19	3.79	8.85	3.12	0.12	0.04
SP 3	0	0.62	2.1	39.53	34.2	6.18	4.17	9.19	2.53	0.33	0.19
SP 4	0	0.9	1.34	8.73	41.21	19.74	6.34	12.76	7.07	1.03	0.7
SP 6	0	0.4	1.95	6.99	48.53	19.63	5.54	9.27	5.28	1.6	0.64
BCH 1	0	0	0.34	7.49	34.74	26.38	6.83	14.23	7.75	1.4	0.38
BCH 2	0	0.35	2.55	4.62	38.47	24.12	7.64	11.12	9.68	1.19	0.24
BCH 3	0	0.96	3.57	10.01	41.84	16.35	8.1	8.11	8.17	2.02	0.84
BCH 4	0	0.69	4.55	39.73	25.14	7.1	3.71	9.54	5.58	1.75	1.38
BCH 5	0	0.8	1.55	8.83	45.57	20.96	6.3	8.14	6.1	1.1	0.44
BCH 6	0	0.54	2.2	8.11	46.27	21.41	6.1	7.89	5.55	0.89	0.51

Table 5.1: Frequency of weight retained (100 gm) in each pan for each sample of Tipam sandstones.

Sample	0 Φ	0.5 Φ	1 Φ	1.5 Φ	2 Φ	2.5 Φ	3 Φ	3.5 Φ	4 Φ	4.5 Φ	5 Φ
MP 7	0.00	0.00	1.28	18.72	58.95	70.26	77.68	91.31	99.22	99.96	99.96
MP 9	0.00	0.00	2.30	26.65	70.93	80.56	84.85	93.61	98.80	99.23	99.44
MP 11	0.00	0.90	2.28	18.22	59.12	72.74	79.29	94.03	98.15	98.96	99.52
MP 16	0.03	1.02	2.37	19.05	59.25	73.40	79.84	93.35	97.26	98.50	99.63
MP 17	0.00	0.00	1.50	20.46	69.84	80.66	85.34	97.46	99.86	99.94	99.96
MP 19	0.00	0.66	5.34	48.54	76.35	83.75	87.99	96.45	99.14	99.20	99.60
MP 20	0.00	0.13	0.98	14.42	65.13	75.27	80.76	94.29	99.24	99.72	99.80
MP 21	0.00	0.20	0.61	12.30	63.56	73.29	77.25	88.28	95.71	99.02	99.23
MP 22	0.00	0.27	5.45	33.48	74.19	84.23	89.12	95.71	98.60	99.69	99.93
SP 1	0.00	0.00	1.71	30.96	75.93	83.96	87.35	96.15	99.46	99.78	99.88
SP 2	0.00	0.49	4.28	26.54	76.46	83.65	87.44	96.29	99.41	99.53	99.57
SP 3	0.00	0.62	2.72	42.25	76.45	82.63	86.80	95.99	98.52	98.85	99.04
SP 4	0.00	0.90	2.24	10.97	52.18	71.92	78.26	91.02	98.09	99.12	99.82
SP 6	0.00	0.40	2.35	9.34	57.87	77.50	83.04	92.31	97.59	99.19	99.83
BCH 1	0.00	0.00	0.34	7.83	42.57	68.95	75.78	90.01	97.76	99.16	99.54
BCH 2	0.00	0.35	2.90	7.52	45.99	70.11	77.75	88.87	98.55	99.74	99.98
BCH 3	0.00	0.96	4.53	14.54	56.38	72.73	80.83	88.94	97.11	99.13	99.97
BCH 4	0.00	0.69	5.24	44.97	70.11	77.21	80.92	90.46	96.04	97.79	99.17
BCH 5	0.00	0.80	2.35	11.18	56.75	77.71	84.01	92.15	98.25	99.35	99.79
BCH 6	0.00	0.54	2.74	10.85	57.12	78.53	84.63	92.52	98.07	98.96	99.47

Table 5.2: Cumulative weight percentage of Tipam sandstones.

Sample No.	Mean (MZ)	Standard Deviation (Ƌ1)	Skewness (SK)	Graphic Kurtosis (KG)	√Ƌ-2	(KG*Ƌ2)/MZ
MP 7	2.08	0.77	2.65	1.22	1.29	0.35
MP 9	2.10	0.79	2.37	0.74	1.26	0.22
MP 11	2.14	0.65	1.12	0.83	1.54	0.16
MP 16	2.19	0.82	1.64	1.02	1.21	0.32
MP 17	2.07	0.62	1.13	0.43	1.61	0.08
MP 19	1.75	0.65	1.68	0.60	1.54	0.15
MP 20	2.33	0.65	1.91	0.67	1.55	0.12
MP 21	2.24	0.81	2.74	1.02	1.24	0.30
MP 22	1.84	0.60	1.16	0.54	1.66	0.11
SP 1	1.82	0.59	1.79	0.54	1.71	0.10
SP 2	1.92	0.70	1.13	0.51	1.42	0.13
SP 3	1.88	0.64	1.71	0.61	1.55	0.13
SP 4	2.30	0.76	1.20	0.81	1.31	0.20
SP 6	2.20	0.72	1.22	0.52	1.39	0.12
BCH 1	2.34	0.77	1.24	1.21	1.30	0.30
BCH 2	3.00	0.77	-2.24	0.49	1.29	0.10
BCH 3	2.86	1.01	-3.30	1.97	0.99	0.70
BCH 4	1.97	0.90	3.29	1.04	1.11	0.43
BCH 5	2.07	0.78	2.13	0.77	1.28	0.23
BCH 6	2.11	0.70	1.33	0.61	1.43	0.14

Table 5.3: Grain size parameters of Tipam sandstone.

Table 5.4 (A): Grain size discrimination functions with depositional conditions (Sahu, 1964) where $Y_1 = 15.6534 M_z + 65.7091 \sigma_1^- 2 - 2.0766 S_{ki} + 3.1135 K_g$ and $Y_{2=} 15.6534 M_{z+} 65.7091\ \sigma_1^{-2} + 18.1071\ S_{ki} + 18.5043\ K_g$

Sample	Y_1	RESULT	Y_2	RESULT
MP 7	-6.95	Aeolian Deposition	142.48	Shallow Agitated Marine
MP 9	-7.79	Aeolian Deposition	130.51	Shallow Agitated Marine
MP 11	-5.83	Aeolian Deposition	96.87	Shallow Agitated Marine
MP 16	-5.52	Aeolian Deposition	127.54	Shallow Agitated Marine
MP 17	-6.99	Aeolian Deposition	86.36	Shallow Agitated Marine
MP 19	-6.30	Aeolian Deposition	96.87	Shallow Agitated Marine
MP 20	-8.64	Aeolian Deposition	110.86	Shallow Agitated Marine
MP 21	-8.09	Aeolian Deposition	146.51	Shallow Agitated Marine
MP 22	-5.95	Aeolian Deposition	83.82	Shallow Agitated Marine
SP 1	-7.25	Aeolian Deposition	93.48	Shallow Agitated Marine
SP 2	-5.76	Aeolian Deposition	92.49	Shallow Agitated Marine
SP 3	-6.83	Aeolian Deposition	98.90	Shallow Agitated Marine
SP 4	-6.03	Aeolian Deposition	110.97	Shallow Agitated Marine
SP 6	-6.86	Aeolian Deposition	99.88	Shallow Agitated Marine
BCH 1	-4.98	Aeolian Deposition	120.23	Shallow Agitated Marine
BCH 2	-2.33	Beach Deposition	54.93	Beach Deposition
BCH 3	6.56	Aeolian Deposition	88.71	Shallow Agitated Marine
BCH 4	-7.60	Aeolian Deposition	162.72	Shallow Agitated Marine
BCH 5	-7.11	Aeolian Deposition	125.65	Shallow Agitated Marine
BCH 6	-6.56	Aeolian Deposition	100.52	Shallow Agitated Marine

Table 5.4 (B): Grain size discrimination functions with depositional conditions (Sahu, 1964) where $Y_3=0.2852$ Mz-8.7604-4.8932 $S_{ki}+0.0482$ K_g and $Y_4=0.7215$ Mz-0.4030 $\sigma_1^{-2}+6.7322$ $S_{ki}+5.2927$ K_g

Sample	Y_3	RESULT	Y_4	RESULT
MP 7	-17.57	Fluvial Deposition	25.57	Fluvial Deltaic
MP 9	-16.43	Fluvial Deposition	21.10	Fluvial Deltaic
MP 11	-8.52	Fluvial Deposition	13.34	Fluvial Deltaic
MP 16	-13.30	Fluvial Deposition	17.78	Fluvial Deltaic
MP 17	-8.33	Fluvial Deposition	11.22	Fluvial Deltaic
MP 19	-11.40	Fluvial Deposition	15.60	Fluvial Deltaic
MP 20	-12.32	Fluvial Deposition	17.90	Fluvial Deltaic
MP 21	-18.45	Fluvial Deposition	25.18	Fluvial Deltaic
MP 22	-8.34	Fluvial Deposition	11.89	Fluvial Deltaic
SP 1	-11.24	Fluvial Deposition	16.11	Fluvial Deltaic
SP 2	-9.30	Fluvial Deposition	11.50	Fluvial Deltaic
SP 3	-11.42	Fluvial Deposition	15.91	Fluvial Deltaic
SP 4	-10.29	Fluvial Deposition	13.77	Fluvial Deltaic
SP 6	-9.81	Fluvial Deposition	12.29	Fluvial Deltaic
BCH 1	-10.52	Fluvial Deposition	16.22	Fluvial Deltaic
BCH 2	6.58	Shallow Agitated Marine	-10.56	Turbidity Current
BCH 3	8.09	Shallow Agitated Marine	-10.16	Turbidity Current
BCH 4	-22.55	Fluvial Deposition	28.74	Fluvial Deltaic
BCH 5	-15.18	Fluvial Deposition	19.68	Fluvial Deltaic
BCH 6	-10.15	Fluvial Deposition	13.53	Fluvial Deltaic

a rectangle. It consists of bars arranged vertically along a horizontal scale representing various class limits. However, histogram cannot be used for determination of statistical parameters and the sieve interval selected while sieving analysis greatly affect their shapes. In order to know the general textural features of a sediments, histogram is very fruitful but is useless for detailed analysis (Friedman and Johnson, 1982).

In the present work, histogram for each sample is plotted as shown in the figure 5.2 (A) to 5.2 (E). All the histograms show a unimodal nature and with a sharp peak around 2Φ. Out of the total 20 samples, 15 % has a sharp peak at 1.5 Φ, 75 % at 2Φ, 7 % at 3.5Φ, and 2 % at 4Φ.

5.2.2 The Frequency Distribution Curves

"A frequency distributive curve is a plot of the frequency with which some variable occurs within arbitrarily defined subclass of a population. A frequency curve is prepared by plotting the proportion, in percent, of various grain sizes, the class limits of which are expressed in phi units" (Friedman and Johnson, 1982). By a rule, along the y-axis is plotted frequency and phi values along the x-axis. From the highest point of the frequency curves, modal values were obtained (Friedman and Johnson, 1982).

The frequency distribution curves of the sandstone samples of the study area are shown in figure 5.1 (A) to 5.1 (E). All the samples show unimodal pattern of curves in nature. 80 % of the samples have the primary mode lying at 2.5 Φ except for those sediment such as sample nos. MP-19, SP-3 and BCH-4, where the sharp peak lies between 1 Φ to 1.5 Φ.

Using 'one-function' approached from the frequency distribution curves, out of the twenty samples, 15 % show a strong negatively skewed, 70 % negatively skewed and 15 % show a normally distributed sediments with a sharp peak. Despite many exceptions, the frequency distributions of most river sands are characterized by positively skewed graph which may be the results in large part the presence of the fine-grained fraction. On the other hand, the one-function approach shows that the frequency distributions of beach sands tend to be symmetrical, negatively skewed, or slightly positively skewed (Friedman and Johnson, 1982). From the frequency distribution curves alone, it can be inferred than the sediments were deposited in an environment where marine processes are dominating over the river processes.
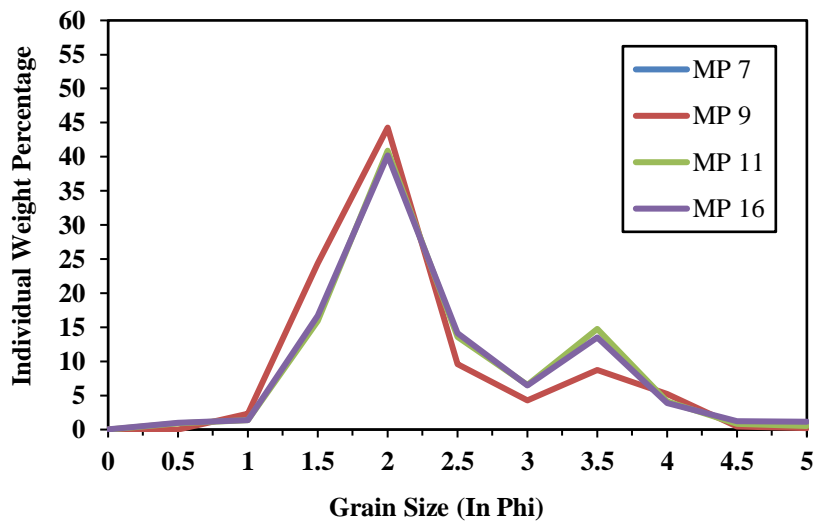
Fig. 5.1(A): Frequency Distribution Curve of MP 7, MP 9, MP 11 & MP 16
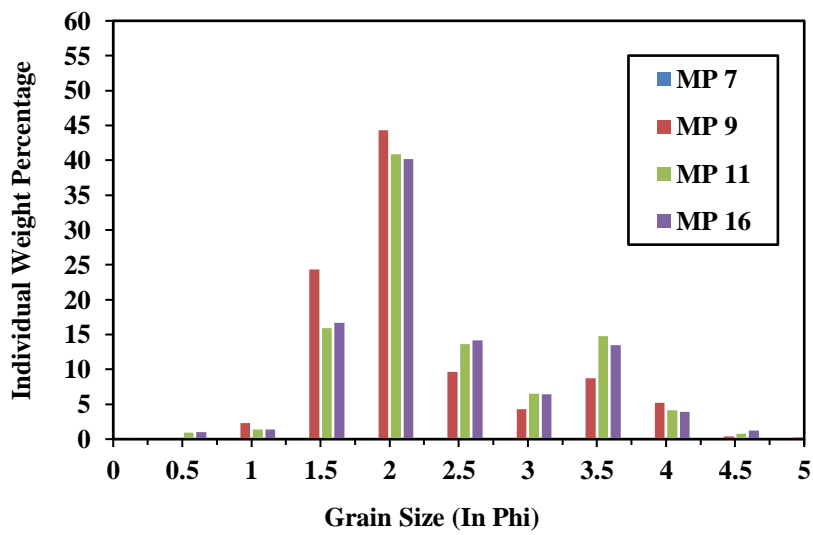
Fig. 5.2(A): Histogram of MP7, MP9, MP11 & MP16
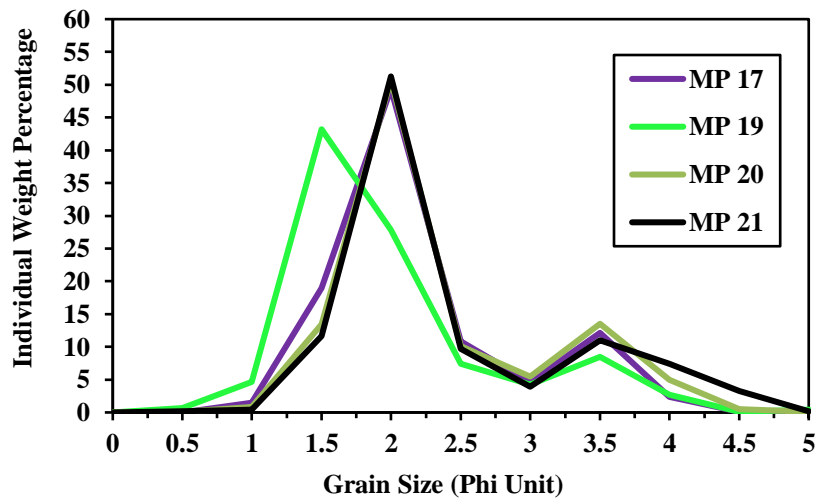
Fig. 5.1(B): Frequency Distribution Curve of MP 17, MP 19, MP 20 & MP 21
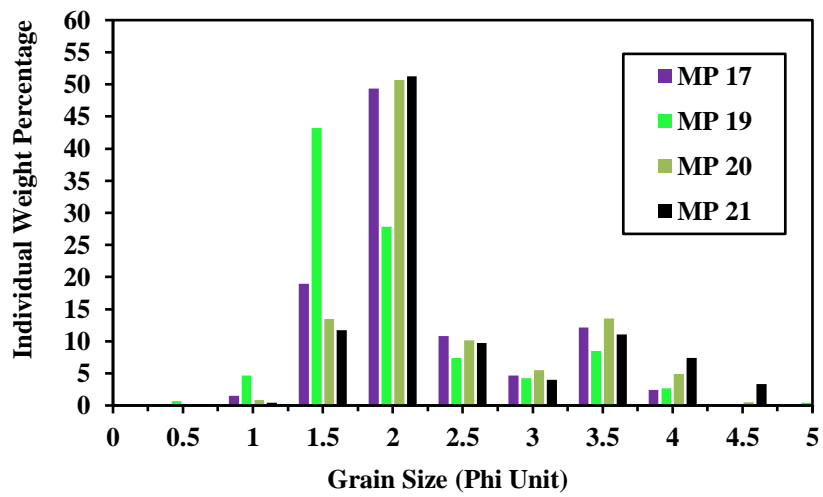
Fig. 5.2(B): Histogram of MP 17,MP 19, MP 20 & MP 21
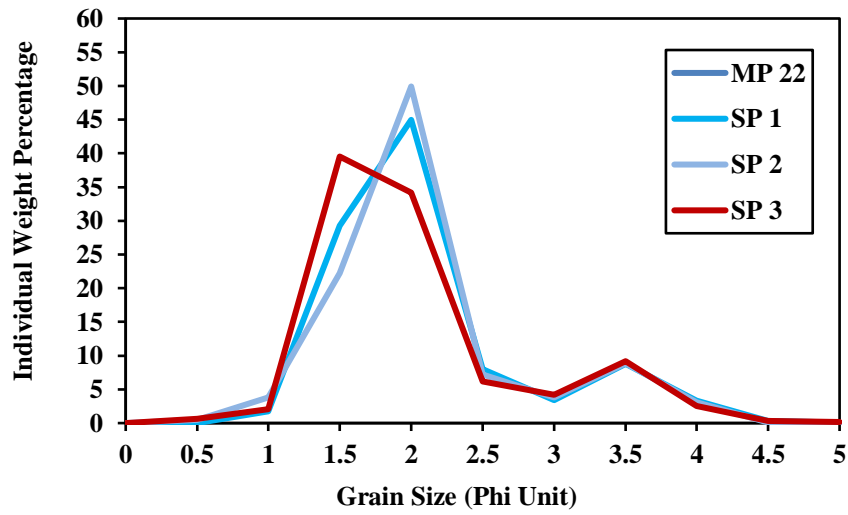
**Fig. 5.1(C): Frequency Distribution Curve of MP 22,
SP 1, SP 2 & SP 3**
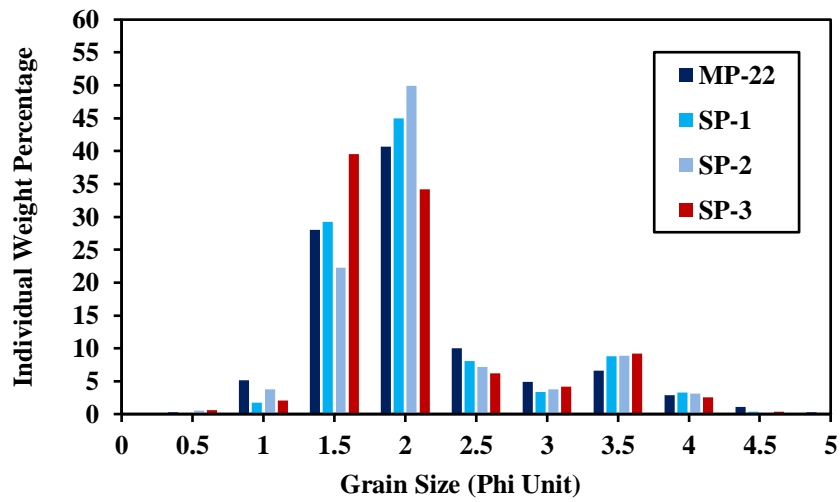
Fig. 5.2(C): Histogram of MP 22,SP 1, SP 2 & SP 3
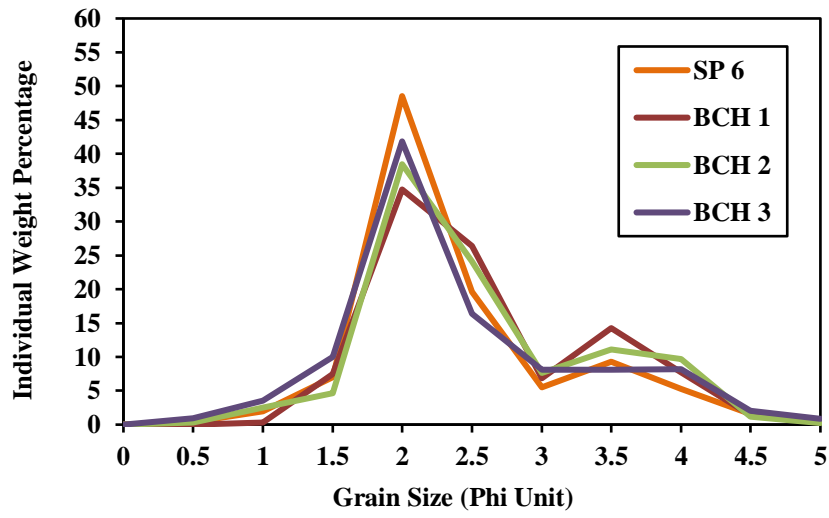
Fig. 5.1(D): Frequency Distribution Curve of MP 22, SP 1, SP 2 & SP 3
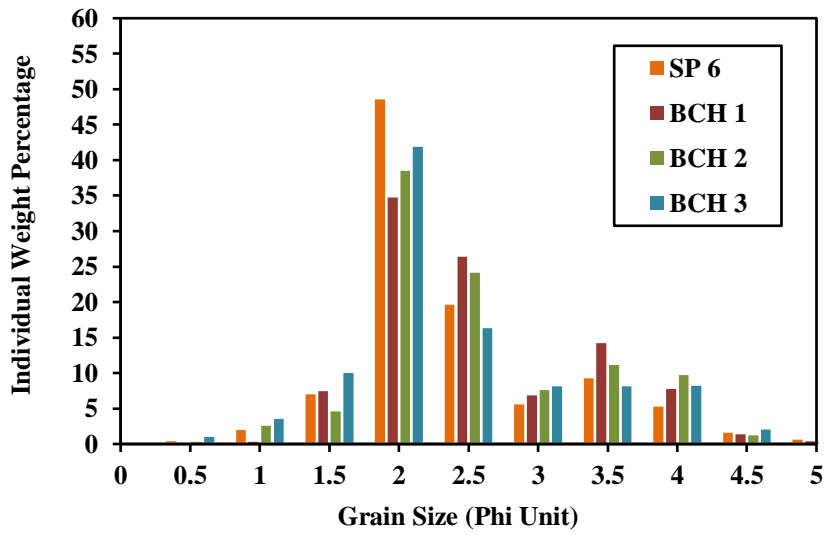
Fig. 5.2(D): Histogram of MP 22, SP 1, SP 2 & SP 3
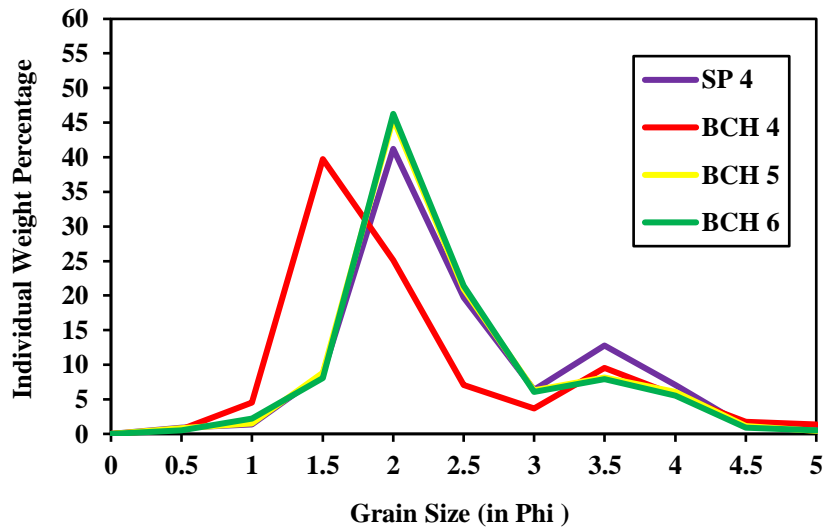
Fig. 5.1(E): Frequency Distribution Curve of SP 4, BCH 4, BCH 5 & BCH 6
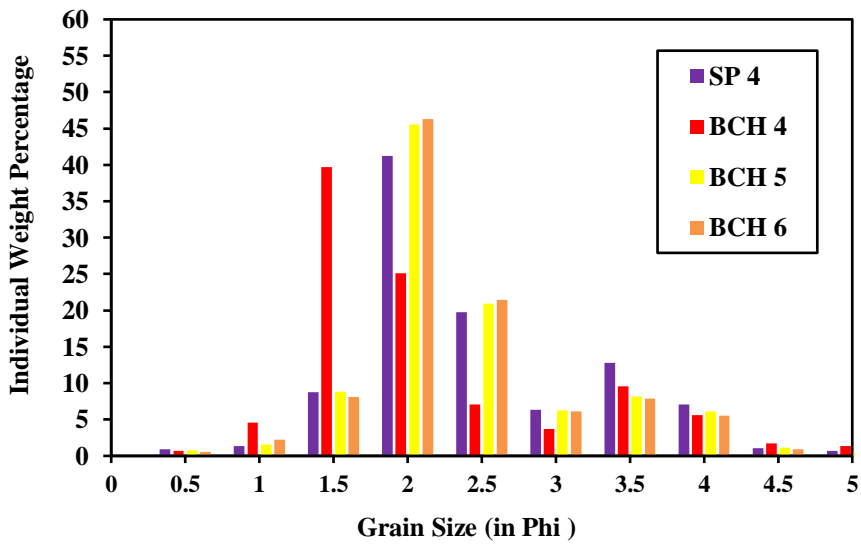
Fig. 5.2(E): Histogram of SP 4, BCH 4, BCH 5 & BCH 6

5.2.3 The Cumulative Frequency Curves

In the cumulative frequency curve, each point represents the sum of all the percentage of the previous (coarser) size classes and not just the frequency of each class which makes it different from the simple frequency curve. Various kinds of ordinate scales are used, the most common being arithmetic or probability.

Plots of the normal distributions using an arithmetic ordinate scale result in the S-shaped, or Ogive curves. "Log probability plots of cumulative curves are more useful than ogive curves with arithmetic scales because: (1) they test for normality of a distribution, (2) interpolation for statistical measures is more accurate, (3) the slope of line is a function of the standard deviation of the distribution (a steep slope means a low value for the standard deviation and a gentle slope means a high value), and (4) separate subpopulations, if present, are identifiable as individual straight-line segments (Visher, 1969)". Plotting in the log probability graphs of cumulative frequency curve distributions of the particle sizes come out as two or three or even more straight-line segments with different slopes separated by sharp break which reveal the mechanism of deposition of sediments. Three straight line segments in sand – the coarser end depict sediments deposited by rolling or sliding while the finer end segment represent deposition of particles carried in suspension. The largest segment at the center emphasize sediments moved by a jumping motion, saltation (Friedman and Johnson, 1982).

In the present work, the cumulative percentage obtained from the size analysis of the sandstone samples were plotted on log-probability ordinate scales. A close study of the log-probability curves of the sandstone samples of the study area

shows that, there are three to four sub populations produced mainly by four modes of transportation viz. rolling and sliding population, saltation population (1), saltation population (2) and suspension population (Figure 5.3). It can be observed here that, sorting is generally good in saltation population, whereas sorting is poor to fair in the suspended and rolling populations.
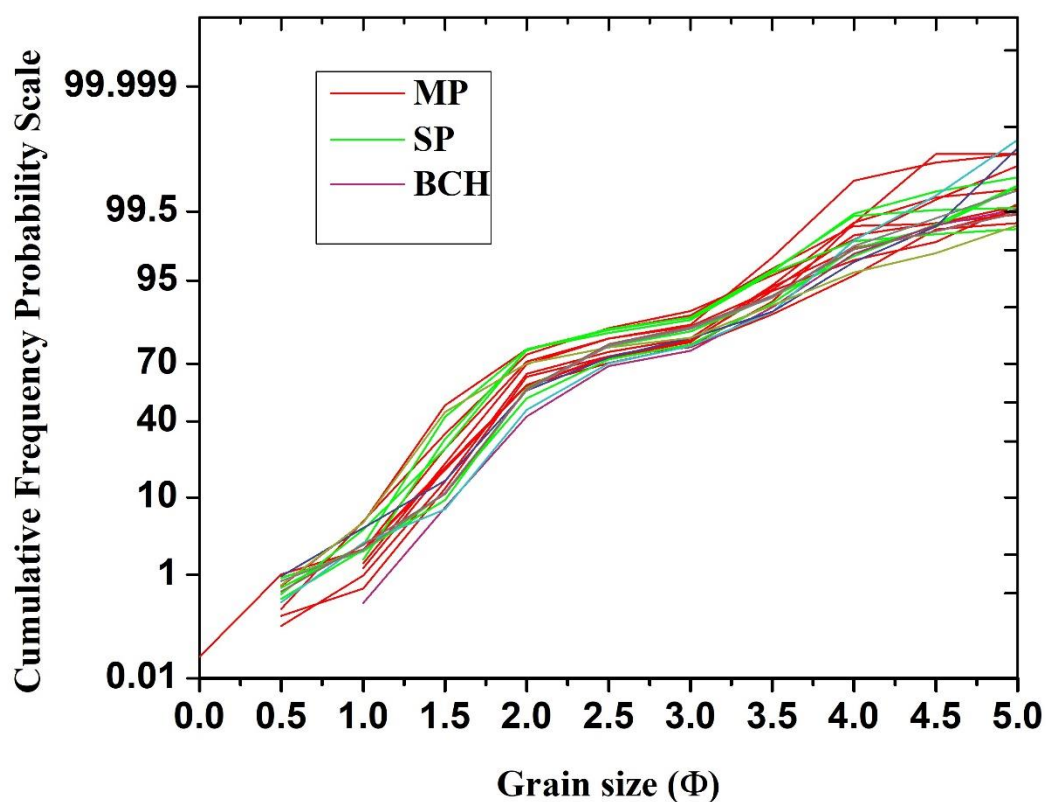
Figure 5.3: Arithmetic probability curve showing traction, saltation and suspension population of Tipam sandstones of the study area (Visher, 1969).

5.3 STATISTICAL PARAMETERS OF GRAIN SIZE

5.3.1 Univariant Analysis

Graphic mean size (Mz), Inclusive graphic standard deviation (σ_1), inclusive graphic skewness (Sk_i) and graphic kurtosis (K_G) were calculated from the cumulative curves prepared in a log probability ordinates scale using the formulae of Folk and Ward, (1957). The percentile values from which the phi values are marked out are $\Phi 1$, $\Phi 5$, $\Phi 16$, $\Phi 25$, $\Phi 50$, $\Phi 75$, $\Phi 84$, and $\Phi 95$.

5.3.1.a Graphic Mean Size (Mz)

"The graphic mean size (Mz) indicates average size of the sediments which is influence by the source of supply, environment and average kinetic energy (velocity) of the depositing media (Sahu, 1964)". The graphic mean size is calculated by using the formula proposed by Folk and Ward, (1957) and is as follows:

$$M_Z = \frac{\phi_{16} + \phi_{50} + \phi_{84}}{3}$$

In the present study, the graphic mean size varies from 1.75 Φ to 3 Φ with an average of 2.16 Φ, i.e., the samples fall mostly within medium grain size to fine grain size sands (Table 5.2). 61% of the total samples are of medium-grained sand whereas 39% belong to fine-grained sand.

5.3.1.b Inclusive Graphic Standard Deviation (σ₁)

Fluctuation of kinetic energy of the depositing medium influence the sorting of sediments which is the main proxy for Inclusive graphic standard deviation or sorting coefficient (Lakhar, 2007). The modified formula of Folk and Ward, (1957) was used to find out the inclusive graphic standard deviation which is given below:

$$\sigma_1 = \frac{\phi_{84} - \phi_{16}}{4} + \frac{\phi_{95} - \phi_5}{6.6}$$

Inclusive graphic standard deviation values of the studied samples range from 0.59 Φ to 1.01 Φ. 5 % of the samples are well sorted, 45 % are moderately well sorted, 45 % are moderately sorted and 5 % are poorly sorted (Table 5.3). It can be observed here that, the sediments of the study area in general are moderately well sorted to moderately sorted. Beach sands are better sorted than river sands in general because of the effects of the bidirectional flow of thin sheets of water from the breaking waves (Friedman and Johnson, 1982).

The variation in sorting from moderately well sorted to moderately sorted in the samples of the study area can be an indicative of high energy fluctuation of the depositing agent in a mixed environment.

5.3.1.c Inclusive Graphic Skewness (Sk$_i$)

Inclusive graphic skewness measures frequency distribution stipulating the position of the mean with respect to median. It implies the supremacy of coarse grain over fine grain and vice versa since it is the outcome of two different normal populations in a proportion different from each other. Accordingly, the mean size

and standard deviation of two samples may be the same, but skewness may differ (Lahkar, 2007).

The kinetic energy of the depositing medium is also indicated by the values of skewness. "Coarsely skewed sediment is an indication of negative values of skewness which means the velocity of the depositing agent is higher than the average and works for a greater length of time than normal, while positive skewness values are indicative of finely skewed sediments and low energy of the median (Sahu, 1964)".

Skewness is represented by the following formula proposed by Folk and Ward (1957):

$$SK_1 = \frac{\phi_{84}+\phi_{16}-2\phi_{50}}{2(\phi_{84}-\phi_{16})} + \frac{\phi_{95}+\phi_5-2\phi_{50}}{2(\phi_{95}-\phi_5)}$$

The present samples show that skewness values vary from -3.30 to 3.29 and fall in the classes from very coarse-skewed to very fine-skewed. 90 % of the total 20 samples are very fine-skewed and the remaining samples fall under very coarse -skewed. This can be interpreted as a mixed environment of deposition where both marine and fluvial influences are present (Lakhar, 2007).

5.3.1.d Graphic Kurtosis (K_G)

Kurtosis, which measures the peakedness of the curves indicates concentration of grains in the size curves. "Kurtosis also measures the ratio between sorting in the "tails" (90%) of the distribution and sorting in the central (50%) portion of the distribution (Lindholm, 1987)". It is a sensitive and valuable parameter for testing normality's of the distribution (Sahu, 1964).

Kurtosis values are worked out by using the following formula proposed by Folk and Ward, (1957):

$$K_G = \frac{\phi_{95} - \phi_5}{2.44(\phi_{75} - \phi_{25})}$$

In the present work, kurtosis values range from 0.43 (very platykurtic) to 1.97 (Very Leptokurtic). The wide range of the kurtosis value is an indication of fluctuation in the energy of the depositing agent. 40 % of the total 20 samples fall under the class of very platykurtic, 20 % in platykurtic, 20 % in mesokurtic and 40 % in leptokurtic class. The leptokurtic and very leptokurtic nature of the sediments generally indicates that the source of sediments was nearer to depositional basin (Lahkar, 2007).

5.3.2 Bivariant Scatter Plots: Interrelationship between Grain Size Parameters

Steward in 1958 was one of the earliest attempts to identify the depositional environments by means of bivariate scatter-grams by plotting median against standard deviation and skewness in order to interpreting sediments from rivers, wave dominated zones and quiet water environments, and defined envelopes within which his analysis occurred (McManus, 1988). In the present work, interrelationship between the grain size parameters has been analyzed to deduced the depositional environment of the sediments by using bivariant scatter plots formulated by Folk and Ward, (1957), Sahu, (1964), Moiola and Weiser, (1968) and Thomson, (1972).

5.3.2.a Graphic Mean Size (Mz) Vs Inclusive Graphic Standard Deviation (σ_1)

A scatter plot of Graphic Mean Size (Mz) versus Inclusive Graphic Standard Deviation (σ_1) gives notable information about the depositional environment of the sediments (Inman, 1952).

A plot of graphic mean (Mz) versus graphic standard deviation (σ_1) according to Folk and ward, (1957) depict that most of the Tipam sandstones show fine sand of moderately sorted to moderately well sorted indicating continuous reworking of sediments by current and waves [(Figure 5.4(A)].

The scatter plot of Friedman, (1967) of graphic mean (Mz) against standard deviation (σ_1) in Figure 5.4(B) shows that 55 % of the sediments fall within the river field and 45 % of the samples fall in the beach field. It can also be seen that majority of the points clogged on the marginal line of the beach and river field. Form this plot, it can be inferred as mixed environment in the transitional zone where fluvial dominate with an influence of marine processes.
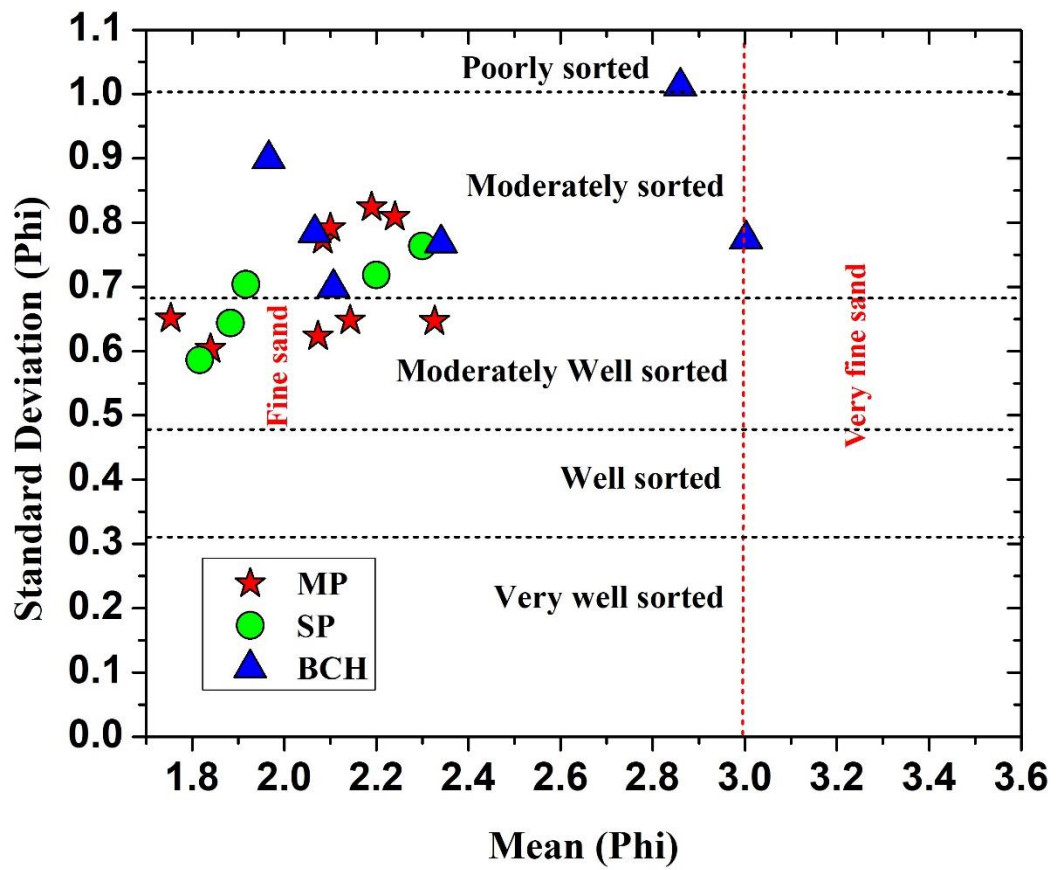
Figure 5.4(A): Binary plot of Mean (Mz) versus Standard deviation (σ_1) according to Folk and ward., (1957).
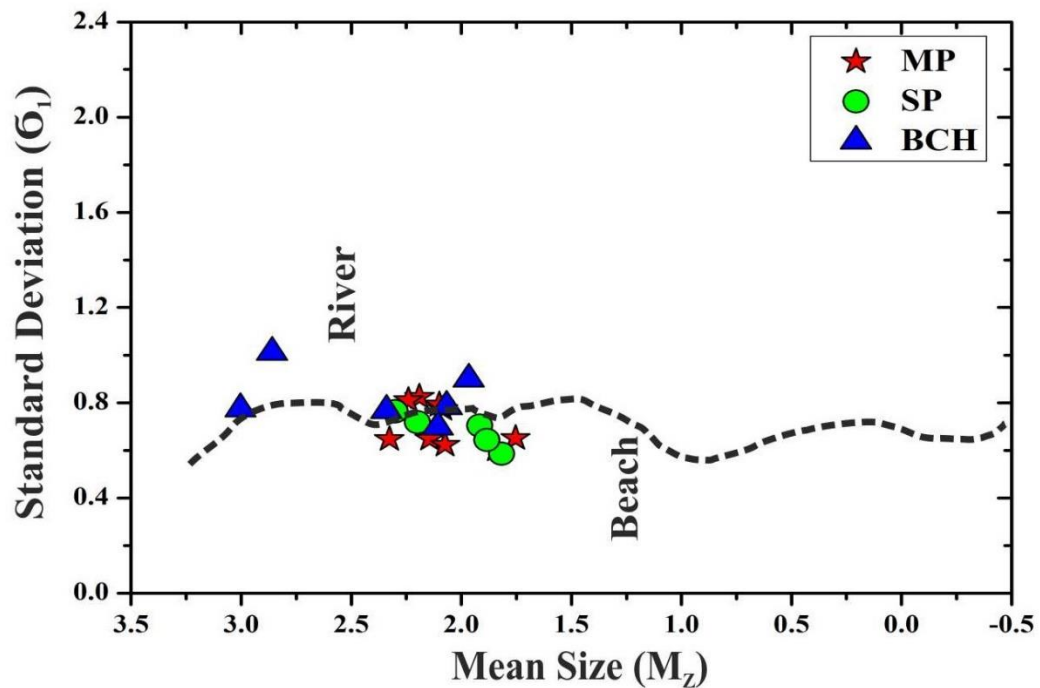
Figure 5.4 (B): Binary plot of Mean size Vs Standard deviation after Friedman., (1967).

5.3.2.b Graphic Mean Size (Mz) Vs Inclusive Graphic Skewness (Sk$_i$)

In the bivariant scatter plot proposed by Moiola and Weiser, (1968) between the two size parameters of graphic mean size and inclusive graphic skewness [Figure 5.4 (C)], the points in the scatter plot mainly concentrated at the river field of which only two samples from Buhchang section falls in the beach field. Since most of the samples are concentrated near the marginal line between the river field and the beach field, this may suggest a mixed influence of both fluvial and marine processes where fluvial process dominate over marine process.
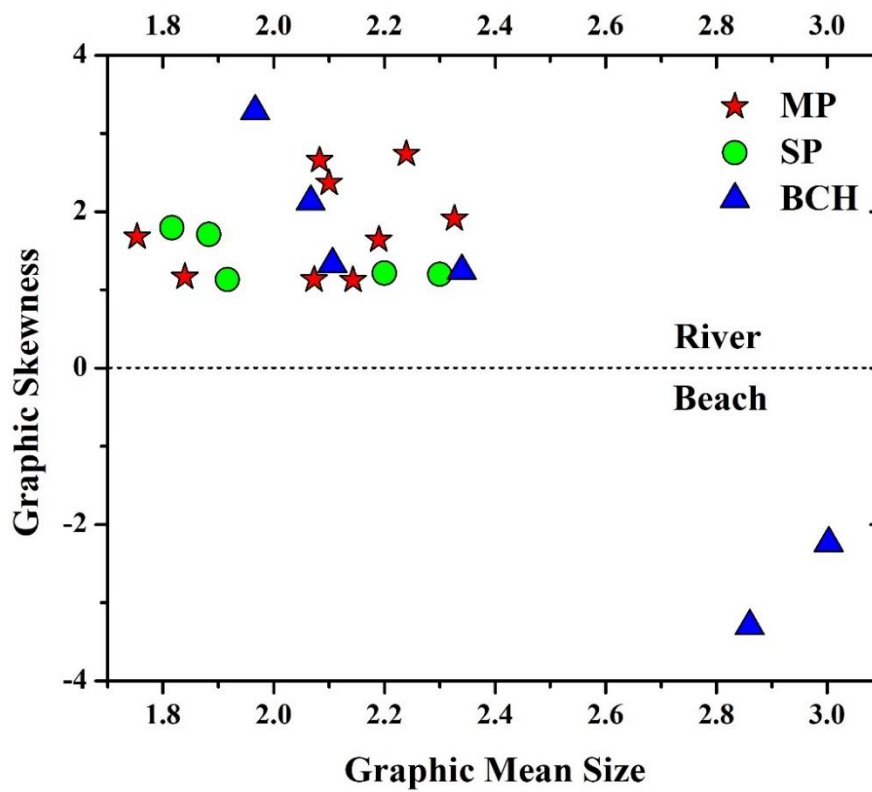
Figure 5.4 (C): Binary plot of Mean size Vs Standard deviation after Friedman, (1967).

5.3.2.c Inclusive Graphic Skewness (Sk$_i$) Vs Graphic Kurtosis (K$_G$)

The scatter plot of Thompson, (1972) between the inclusive graphic skewness and graphic kurtosis [Figure 5.4(D)] separate the condition of energy occurring at the time of deposition of sediments. Plotting of the studied samples all fall in the field of high energy zone where a mixture of fine to medium sand took place. This scatter plot indicates more of a fluvial environment with a transitional depositional setting.
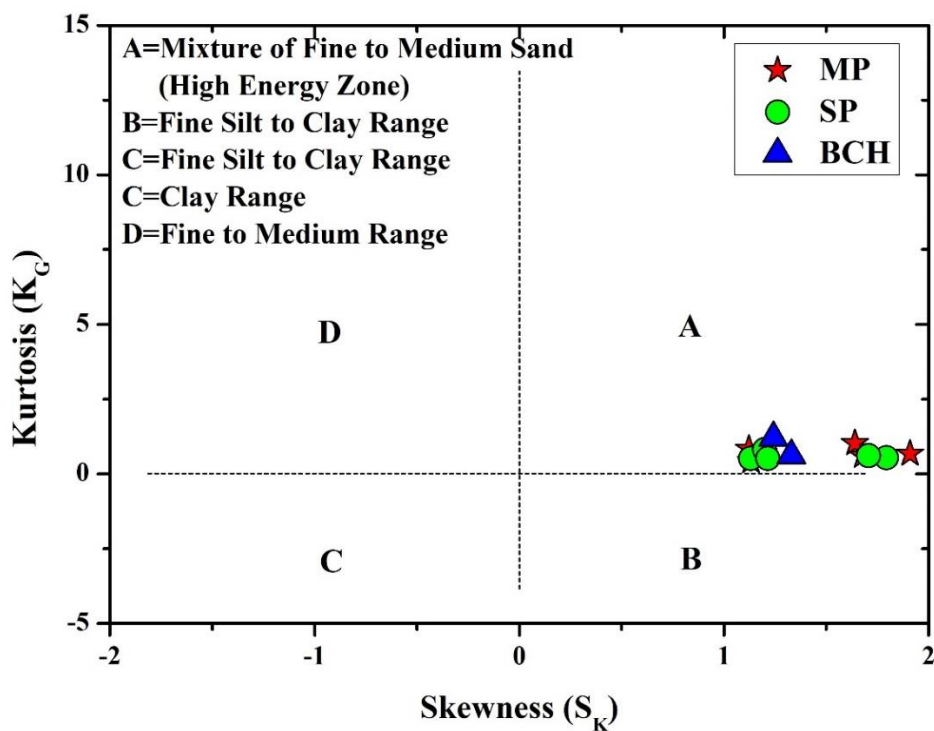
Figure 5.4 (D): Graphic skewness Vs Graphic kurtosis binary plot after Thompson., (1972).

5.3.2.d Log-Log Plot

Using the bivariant plot of $\sqrt{\sigma_1^{-2}}$ Vs $(K_G/M_Z)*\sigma_1^2$ on grain size values, Sahu in 1964 has work out a binary plot for discriminating depositional environment of sediments. Plotting of the samples of the studied Tipam sandstones reveals that 80 per cent of the samples fall in the field of Deltaic (fluvial) and only 15 % falls in Turbidites region while 0.05 % fall in shallow marine region [Figure 5.4(E)] indicating a mixed environment where fluvial depositional environment dominates over turbidites and shallow marine environment.
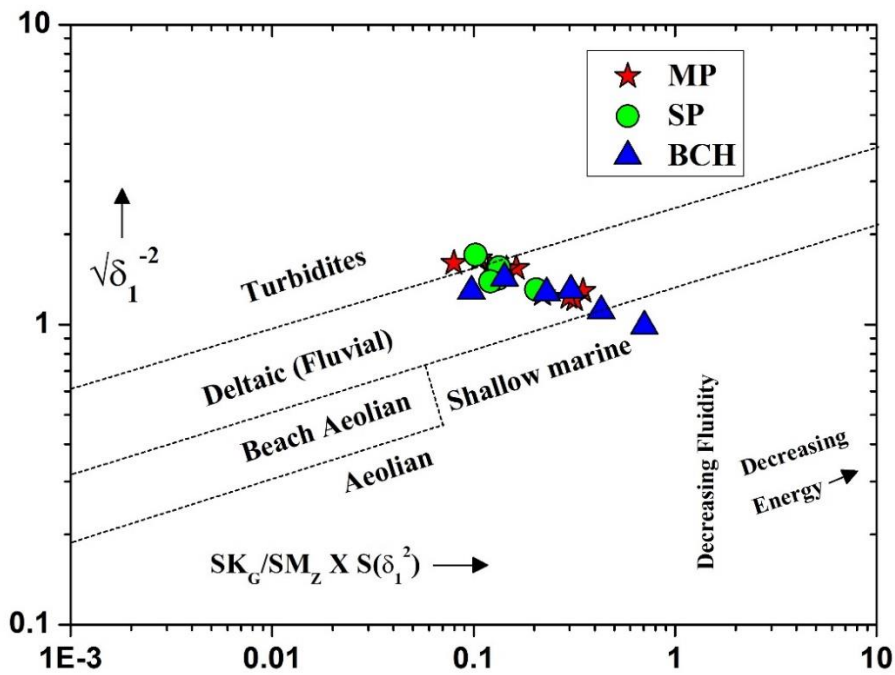
Figure 5.4 (E): Log-Log plot after Sahu, (1964).

5.3.2.e Linear Discriminate Function

Interpretation of variations in factors such as fluid and energy on or before the deposition of sediments using statistical analysis have a good correlation with different processes acting on the sediments and their depositional environment (Sahu, 1964). The linear discrimination function of Y_1, Y_2, Y_3 and Y_4 were modified and used by Sahu, (1964) to differentiate different processes and depositional environment of sediments as under:

$Y_1 = 15.6534Mz + 65.7091\sigma_1^{-}2 - 2.0766S_{ki} + 3.1135K_g$

$Y_{2=}15.6534M_{z+}65.7091\ \sigma_1^{-2} + 18.1071\ S_{ki} + 18.5043\ K_g$

$Y_3 = 0.2852\ Mz - 8.7604 - 4.8932\ S_{ki} + 0.0482\ K_g$

$Y_4 = 0.7215\ Mz - 0.4030\ \sigma_1^{-2} + 6.7322\ S_{ki} + 5.2927\ K_g$

63

Where,

Y_1 values < -2.7411 = Aeolian deposition

Y_1 values > -2.7411 = Beach deposition

Y_2 values < 65.3650 = Beach deposition

Y_2 values > 65.3650 = Shallow agitated marine deposition

Y_3 values < -7.4190 = Fluvial deposition

Y_3 values > -7.4190 = Shallow agitated marine deposition

Y_4 values < 9.8433 = Turbidity current deposition

Y_4 values > 9.8433 = Fluvial deltaic deposition

Calculation of the above Linear discrimination function of Tipam sandstones of the study area is given in table 5.4 (A & B). Based on the value of Y_1 all the samples of Tipam sandstone falls in aeolian deposits except for one sample which fall in beach deposition. Considering Y_2 values, 95 % of the studied sample fall in shallow agitated marine deposition except for one sample which fall in beach deposition. Binary plot of Y_1 versus Y_2 [(Sahu, 1964); Figure 5.4(F)] clearly shows the above discussion. The binary plot of Y_2 with respect to Y_1 [(Sahu, 1964); Figure 5.4(G)] along with the calculated value of Y_2 and Y_3 clearly shows that 95 % of the samples fall in shallow agitated marine deposition for Y_2 and 90 per cent falls under fluvial deposition with 10 % shallow agitated marine deposition for Y_3.

Again, calculation of Y_4 along with the binary plotting of Y_3 versus Y_4 [Figure 5.4(H)] depict that 90 % of Y_4 falls in fluvial deltaic with only 10 % falls in turbidity current deposition. From the study of linear discrimination function of

Tipam sandstones, it can be predicted that the sediments were deposited in a mixed environment where fluvial deposition dominates over the other.
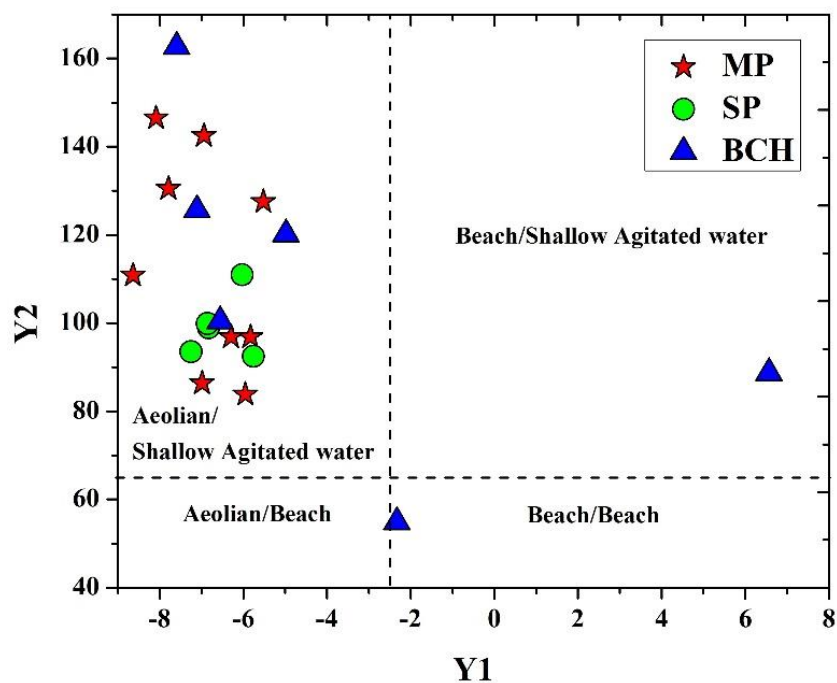
Figure 5.4 (F): Discrimination of environment based on Linear discrimination function plot of Y_2 against Y_1 (Sahu, 1964).
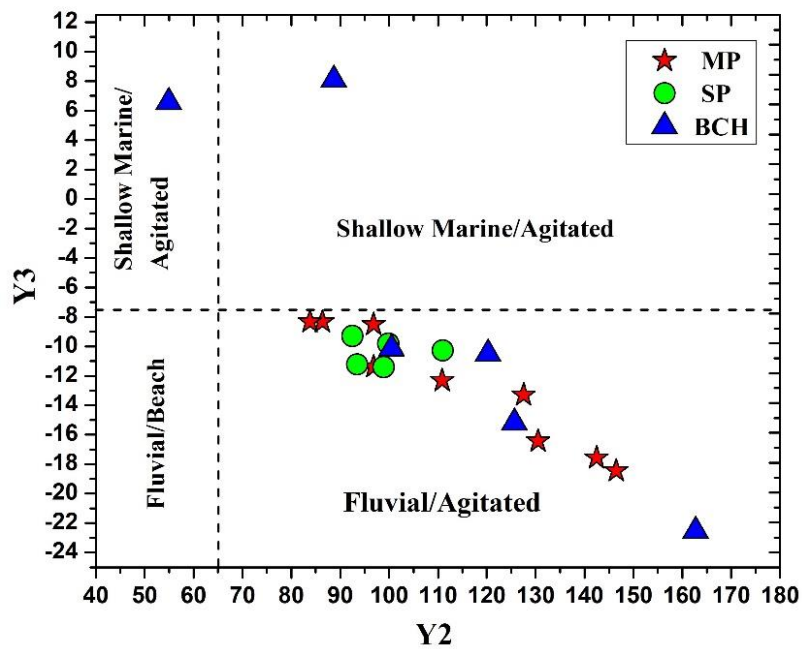
Figure 5.4(G): Discrimination of environment based on Linear discrimination functions plot of Y_3 against Y_2 (Sahu, 1964).
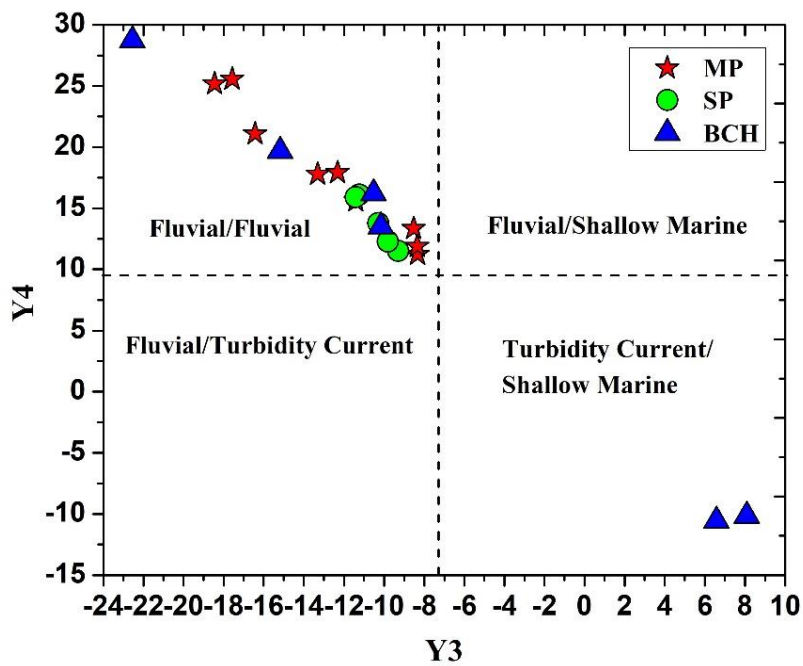
Figure 5.4(H): Discrimination of environment based on Linear discrimination functions plot of Y_4 against Y_3 (Sahu, 1964).

5.4 DISCUSSION AND INTERPRETATION

To assess the size distribution and depositional environment of a sediments, grain size analysis has been utilized in the present study. Graphical presentation of the size distribution in the form of histogram and frequency curve shows a unimodal nature with a sharp peak around 2 Φ to 2.5 Φ. From the one function histogram and frequency distribution curves alone, it can be inferred than the sediments were deposited in a mixed environment of marine and fluvial where marine processes are dominating over the river processes.

Plotting of the samples in a Log-probability curve shows that four sub populations are present which are produced mainly by four modes of transportation viz. rolling and sliding population, saltation population (1), saltation population (2) and suspension population (Figure 5.3). It can be observed here that, sorting is generally good in saltation population, whereas sorting is poor to fair in the suspended and rolling populations.

Grain size parameters such as Graphic mean, Graphic standard deviation, Graphic skewness and Graphic kurtosis shows that the Tipam sandstones of the study area are medium to fine sand with moderate to moderately well sorted which were deposited in a mixed environment where both marine and fluvial influences are present with high energy fluctuation.

Bivariant scatter plots using Inman., (1952), Folk and ward, (1957), Friedman, (1967) and Thompson, (1972) suggest that most of the Tipam sandstones falls in the field of river and few samples in the beach area with fine sand of moderately sorted to moderately well sorted indicating continuous reworking of

sediments by current and waves. Form this plot, it can be inferred as mixed environment in the transitional zone where fluvial dominate with an influence of marine processes.

Calculation of the above Linear discrimination function of Tipam sandstones of the study area is given in table 5.4 (A & B). Based on the calculation of Linear discrimination function value of Y_1, majority of the samples of Tipam sandstone falls in aeolian deposits. Y_2 values of the studied sample fall in shallow agitated marine deposition which is clearly supported by the binary plot of Y_1 versus Y_2 (Sahu, 1964); [Figure 5.4(F)]. The binary plot of Y_2 with respect to Y_1 (Sahu., 1964); [Figure 5.4(G)] along with the calculated value of Y_2 and Y_3 shows shallow agitated marine deposition. Again, calculation of Y_4 along with the binary plotting of Y_3 versus Y_4 [Figure 5.4(H)] depict a fluvial deltaic environment.

From the granulometric study of Tipam sandstones of the study area, it can be concluded that the sediments were deposited in a mixed environment where fluvial environment dominates over the other.

CHAPTER 6

PETROGRAPHY

6.1. INTRODUCTION

Petrographic analysis of sedimentary rocks enables us to classify the rocks, to understand the environment of deposition, diagenetic history, compaction, cementation, lithification, provenance and tectonic set up of the source area during their deposition. Crook, (1974) was the first to propose the method of determining the tectonic setting of sandstone using framework mineral composition, which, since then, has undergone considerable modifications.

The main assumption behind the study of sandstone provenance is that different tectonic settings contain their own rock types, which when eroded, produce sandstones with specific compositional ranges. Detrital modes of sandstone suits provide information on the tectonic setting of the basin of deposition and associated provenance (Dickinson, 1985). Petrographical studies also help in the reconstructing paleoclimate as existed during the time of deposition (Suttner and Dutta, 1986). Sandstone compositions have been widely used by sedimentoligists during the past few decades to interpret provenance and tectonic settings of the areas (Basu *et. al.,* 1975; Dickinson and Suczek, 1979; Dickinson, 1985; Uddin and Lundberg, 1998 and Das and Sarma, 2009).

Since, petrographic analysis as well as studies on composition of sandstones can reveal clues regarding provenance, tectonic history, paleoclimate and many others, a careful study has been carried out on petrography of the Tipam

sandstones exposed in the study area. Keeping these in mind, thin section studies under petrological microscope were done in order to know the mineralogical compositions, textural character, classification the sandstone, provenance, tectonic framework and paleoclimatic conditions prevailing at the time of deposition.

6.2. PETROGRAPHIC DESCRIPTION

The petrographic compositions of the Tipam sandstone exposed in the study area have been divided into four major groups.

      i) Primary detrital constituents

      ii) Miscellaneous detrital constituents

      iii) Matrix and cement

      iv) Accessory minerals

The primary detrital constituents are the main rock forming detrital components and minerals of the sandstones which include different varieties of Quartz, Feldspar and Lithic Fragments which are also known as Rock fragments. Miscellaneous detrital constituents include Mica such as biotite and muscovite along with chert. Matrix comprises of fine-grained components of clay and silt size particles and the cementing materials include siliceous, ferruginous and carbonate cement of the Tipam sandstones. The accessory minerals are those which occur as detrital constituent in very negligible or less amount, hence, serving limited significance with reference to general petrographic characterization of the rock. The detail petrography of the sandstone is discussed in the following section.

6.2.1. Quartz

It is the most abundant mineral having distinctive features like undulose extinction, strained action, inclusion etc. Broadly the quartz is grouped under two main classes such as Monocrystalline Quartz and Polycrystalline Quartz (Conolly, 1965; Blatt, 1967). The modal percentages of different quartz type are shown in Table 6.1.

The Monocrystalline Quartz is characterized by single crystal grain boundary and further classified into two types such as Unit Quartz or Non-Undulose Quartz and Undulose Quartz. The Unit quartz, also known as Non-Undulose quartz shows uniform extinction under crossed polars that vary from 1º - 3º. The grains are almost angular to sub-angular, though few grains are sub-rounded to rounded. The grain boundaries are straight, sutured or corroded. The grain may contain inclusions. The Unit quartz/Non-Undulose quartz of Tipam sandstone of the study area are medium to coarse grained and angular to sub-rounded in shape. The quartz grains sometimes sparsely contain inclusions of zircon. They show sutured and sometimes concavo-convex boundaries. The modal percentage of Non-Undulose quartz varies from 4.07 % to 21.92 %. [Table 6.1, Plate 6.2 (I)]. The Undulose quartz are, on the other hand, identifiable by their undulose extinction (wavy extinction) where extinction is not uniform and sweeps across the crystals. The quartz grains are almost angular to sub rounded and show sutured grain boundaries. Undulose quartz tends to break into small grains as compared to Non-Undulose quartz due to thermodynamically less stable. (Blatt *et. al.*, 1980). Undulose quartz is more prominent than Non-Undulose quartz in Tipam sandstones of the study area. The grains are

mostly angular and sutured and vary from 8.95 % to 11.84 % in Tipam sandstones. [Table 6.1, Plate 6.2(J)].

In Polycrystalline Quartz, the quartz grains are composite, showing two or more crystal units under cross-nicols (Conolly, 1965). Some grains of polycrystalline quartz are larger than monocrystalline quartz. Composite quartz may be either fine grained quartzites or microcrystalline chert or it could be coarse crystalline quart of either igneous or metamorphic origin. Polycrystalline quartz is further sub divided into two such as Polycrystalline Quartz 2-3 and Polycrystalline Quartz > 3. Polycrystalline quartz 2-3 are those in which the number of composite crystals varies between 2 to 3, The internal unit show both straight and undulose extinction. [(Plate 6.2 (K)]. The percentage of polycrystalline quartz 2-3 varies from 9.7 % to 14.84 %. When the number of composite crystals in polycrystalline quartz is greater than three, such type of quartz is known as polycrystalline quartz > 3. In such kind of polycrystalline quartz, one grain boundary is observed under plane polarized light but however under cross polar, the grain shows a number of microcrystalline units which generally exceeds three with sutured grain contact. The Tipam sandstone of the study area contain polycrystalline quartz > 3 characterized by a number of smaller interlocking grains of opaque and non-opaque inclusions arranged in a regular orientation showing mostly undulose extinction with boundaries from straight to curve. The grains are medium to fine and sub-angular to sub-rounded [Plate 6.2(L)] and varies from 14.05 % to 23.41 %.

6.2.2. Feldspar

Feldspar of the study area commonly shows cleavage. They rank second in dominance in the Tipam sandstones. Plagioclase and K-feldspar are both present in the Tipam sandstones. Plagioclase feldspar is easily recognized by lamellar twining. In K-Feldspar, the two varieties are common in the sandstones i.e. microcline and orthoclase. Microcline grains are easily observed by cross-hatched twinning whereas orthoclase grains show Carlsbad twinning. Untwined variety of orthoclase is more common as compared to twined variety and gives a cloudy appearance. Though their amount is less, Feldspar varieties are common in Tipam sandstones and constitute 7.14 % to 13.63 % with an average of 10.74%. Both plagioclase [Plate 6.1 (D)] and K-feldspar are presented with sub-angular to sub-rounded and weathered in nature. In a few samples, intergrowth of K-feldspar and plagioclase feldspar (Perthite) is observed [Plate 6.1 (G)].

6.2.3. Lithic Fragments

The Lithic Fragments are the pieces of sand size grains that are abraded particles of Igneous, Sedimentary or Metamorphic rocks and are of immense important in provenance study along with tectonic setting of the source area. Generally, black dotted nature under cross-nicols is shown by igneous rock-fragments while sedimentary rock-fragments show some sedimentary character. Preferred orientation and high interference color under cross-nicols are shown by metamorphic rock fragments. Rock fragments of sedimentary and metamorphic origin are sparsely distributed in the studied samples. Generally, in each of the samples of the study area,

metamorphic rock fragments are more common than sedimentary rock fragments. The rock fragments constitute 9.55% to 14.95% with an average of 11.27%.

6.2.4. Micas

Micas of the studied sandstone include muscovite, biotite and chlorite and commonly occur as flakes. The grains of biotite are mostly identified by their brown color, pleochroism and straight extinction while muscovite grains are easily identified by their red interference color. Chlorite is commonly found as varying degree of altered product of biotite. The mica group of minerals present in the Tipam sandstones includes mostly biotite and muscovite. [Plate 6.1 (C & E)]. They are flaky, slender, elongated showing cleavages. Biotite grains are light to deep brown, pleochroic and show straight extinction while muscovite grains are colorless, elongated and show red-green interference color. Some grains are fresh while some grains are weathered. Folding or Kink bending of mica grains is very common in the studied Tipam sandstone. The modal percentage of mica varies from 2.1% to 4.96 % (Table 6.1) with an average of 3.4%.

6.2.5. Chert

Chert is a dense rock and composed of microcrystalline aggregate of quartz grains or microcrystalline fibrous quartz (chalcedony) with minor impurities (Pettijohn, 1975). Chert grains exhibit pin point extinction and are mostly fine grained. Few chert grains are present in the Tipam sandstones of the study area. Under deep burial environment, the chert grains may be formed due to conversion of detrital matrix and interstitial clay minerals (Dapples, 1979). The modal percentage of chert varies from 1.1% to 2.22 % with an average of 1.53%.

6.2.6. Matrix and Cement

Matrix in sedimentary rocks is a fine grained argillaceous and siliceous materials with 0.03 mm diameter or lesser without grain boundaries trapped within framework grains. They consist of both detrital as well as authigenic grains and may include silt or clay minerals, fine size mica and feldspar. Clay as well as silt sized matrix containing fine grained quartz were observed in the Tipam sandstones constituting 5.33 % to 14.46 % with an average of 9.95%.

The Siliciclastic framework grains are bind together by some types of secondary minerals which are formed after deposition and diagenesis of sandstone known as cement. This cementing material may be silicate minerals such as quartz or non-silicate minerals such as calcite or dolomite. The most common cementing materials to act as cement in sandstones are quartz. Next to quartz is the carbonate mineral which is commonly found as cement in siliciclastic sedimentary rocks. Among the carbonate minerals, calcite is more common than dolomite and siderite (iron carbonate) minerals and found to precipitates in the pore spaces of framework grains. Hematite, limonite, anhydrite, goethite, gypsum, barite and clay minerals are less commonly found as cement in sandstones. Calcareous cement is the most common cement followed by ferruginous and silica cement in Tipam sandstone of the study area constituting 5.92 % to 12.45 % with average of 8.4%.

6.2.7. Accessory Minerals

Minerals with a small percentage of grains in sedimentary rocks are referred as accessory minerals. These include clay minerals, chlorite, and heavy minerals which are denser than quartz. Zircon, tourmaline, epidote (colorless, pistachio

green), rutile (blood red) are the dominant detrital accessory minerals present in the Tipam sandstone of the study area and constitute 1.05% to 4.4 % with an average of 2.5%.

6.3. MICROSTRUCTURES

Microstructures which are identified under petrological microscope reflect diagenesis of the present sandstones. These structures are as follows:

6.3.1 Kink band

Compaction of the sandstone due to pressure effect results in the development of Kink band structure. Mica flakes in the present Tipam sandstone exhibit this kind of structure [Plate 6.1 (C)].

6.3.2. Overgrowth

Quartz cement which is chemically attached to the existing quartz grains forming a rim known as overgrowths and are particularly common in quartz-rich sandstones. In the present sandstones, overgrowth can be recognized by a line of impurities or bubbles that mark the surface of the original grain (Boggs, 2009), [Plate 6.2 (M)].

Sl. No.	Sample No.	Quartz Types						Total $Q=(Q_{mt}+Q_{pt})$	Feldspar	Rock Fragment	Chert	Cement	Matrix	Micas	Others
		Monocrystalline Quartz			Polycrystalline Quartz										
		Q_{Mnu}	Q_{Mu}	Q_{Mt}	Q_{P2-3}	$Q_{P>3}$	Q_{pt}								
1	MP-7	4.07	11.12	15.19	12.03	23.41	35.44	50.63	11.96	10.22	1.32	7.32	15.4	2.45	2.02
2	MP- 9	10.15	10.22	20.37	11.33	17.81	29.14	49.51	10.68	10.48	2.2	8.05	14.46	3.6	3.22
3	MP- 11	13.14	11.84	24.98	14.2	19.92	34.12	59.1	8.94	11.27	1.1	8.89	6.81	3.14	1.85
4	MP- 16	10.9	10.87	21.77	12.39	22.18	34.57	56.34	11.57	10.04	1.05	8.53	8.58	3.89	1.05
5	MP-17	13.32	10.95	24.27	17.82	18.67	36.49	60.76	7.14	10.15	1.67	9.12	8.13	2.6	2.1
6	MP-19	9.23	10.71	19.94	18.34	16.43	34.77	54.71	9.27	10.54	1.14	8.91	9.12	4.12	3.33
7	MP-20	14.49	9.63	24.12	12.56	15.12	27.68	51.8	13.48	9.86	2.22	8.99	9.36	4.96	1.55
8	MP-21	15.18	10.96	26.14	13.39	17.69	31.08	57.22	7.84	11.78	1.47	7.85	9.15	3.96	2.2
9	MP-22	14.5	10.24	24.74	12.3	15.55	27.85	52.59	12.26	9.58	1.04	12.45	9.8	2.47	0.85
10	SP-1	15.3	9.75	25.05	14.84	14.01	28.85	53.9	10.9	10.4	1.46	12.23	6.13	3.34	3.3
11	SP-2	13.67	8.96	22.63	10.9	14.67	25.57	48.2	13.12	10.17	1.54	7.36	13.24	3.79	4.12
12	SP-3	16.76	18.76	27.11	9.7	18.89	28.59	55.7	9.85	12.22	1.68	7.34	10.19	2.9	1.8
13	SP-4	16.12	9.04	25.16	10.54	14.05	24.59	49.75	11.3	10.8	1.45	6.46	13.69	4.25	3.75
14	SP-6	11.46	10.4	21.86	14.4	14.1	28.5	50.36	8.44	14.95	2.17	10.1	10.54	4.11	1.5
15	BCH-1	9.87	9.35	19.22	12.32	20.91	33.23	52.45	13.04	10.95	1.88	7.19	11.24	2.88	2.25
16	BCH-2	21.92	8.95	30.87	11.84	17.49	29.33	60.2	12.23	9.55	1.47	7.57	5.33	2.47	2.65
17	BCH-3	12.85	10.1	22.95	12.4	16.15	28.55	51.5	11.41	14.27	1.08	7.78	10.02	3.58	1.44
18	BCH-4	13.98	11.56	25.54	10.68	20.88	31.56	57.1	9.85	12.66	1.94	6.77	7.12	2.1	4.4
19	BCH-5	15.86	10.87	26.73	12.38	15.57	27.95	54.68	8.22	13.37	1.25	5.92	10.17	3.34	4.3
20	BCH-6	9.4	11.52	20.92	10.55	16.75	27.26	48.18	13.63	12.22	1.63	9.12	10.59	4.13	2.13
Average				22.17			30.26	53.73	10.74	11.27	1.53	8.4	9.55	3.4	2.5

Table 6.1: Modal count of petrographic study of thin sections of Tipam Sandstone (where, Q_{Mu}: monocrystalline undulatory quartz, Q_{Mnu}: monocrystalline non undulatory quartz, Q_{P2-3}: polycrystalline quartz with 2-3 grains per quartz, $Q_{P>3}$: polycrystalline quartz with >3 grains)

77

Table 6.2: Table showing Recalculated percentile values of total quartz, feldspar and rock fragments of Tipam sandstone of the study area

Sample No.	Quartz (Total)	Feldspar	Rock Fragments	Sum (Qtot+F+RF)	Total Quartz (Recalculated %)	Feldspar (Recalculated %)	Rock Fragments (Recalculated %)
MP-7	50.63	11.96	10.22	72.81	69.54	16.43	14.04
MP- 9	49.51	10.68	10.48	70.67	70.06	15.11	14.83
MP- 11	59.1	8.94	11.27	79.31	74.52	11.27	14.21
MP- 16	56.34	11.57	10.04	77.95	72.28	14.84	12.88
MP-17	60.76	7.14	10.15	78.05	77.85	9.15	13.00
MP-19	54.71	9.27	10.54	74.52	73.42	12.44	14.14
MP-20	51.8	13.48	9.86	75.14	68.94	17.94	13.12
MP-21	57.22	7.84	11.78	76.84	74.47	10.20	15.33
MP-22	52.59	12.26	9.58	74.43	70.66	16.47	12.87
SP-1	53.9	10.9	10.4	75.2	71.68	14.49	13.83
SP-2	48.2	13.12	10.17	71.49	67.42	18.35	14.23
SP-3	55.7	9.85	12.22	77.77	71.62	12.67	15.71
SP-4	49.75	11.3	10.8	71.85	69.24	15.73	15.03
SP-6	50.36	8.44	14.95	73.75	68.28	11.44	20.27
BCH-1	52.45	13.04	10.95	76.44	68.62	17.06	14.32
BCH-2	60.2	12.23	9.55	81.98	73.43	14.92	11.65
BCH-3	51.5	11.41	14.27	77.18	66.73	14.78	18.49
BCH-4	57.1	9.85	12.66	79.61	71.72	12.37	15.90
BCH-5	54.68	8.22	13.37	76.27	71.69	10.78	17.53
BCH-6	48.18	13.63	12.22	74.03	65.08	18.41	16.51

| Sl. No	Sample No.	Monocrystalline Quartz	Feldspar	Rock Fragments	Sum $(Q_{mt}$ $+F+RF)$	Monocrystalline Quartz (Recalculated %)	Feldspar (Recalculated %)	Rock Fragments (Recalculated %)
1	MP-7	15.19	11.96	10.22	37.37	40.65	32.00	27.35
2	MP- 9	20.37	10.68	10.48	41.53	49.05	25.72	25.23
3	MP- 11	24.98	8.94	11.27	45.19	55.28	19.78	24.94
4	MP- 16	21.77	11.57	10.04	43.38	50.18	26.67	23.14
5	MP-17	24.27	7.14	10.15	41.56	58.40	17.18	24.42
6	MP-19	19.94	9.27	10.54	39.75	50.16	23.32	26.52
7	MP-20	24.12	13.48	9.86	47.46	50.82	28.40	20.78
8	MP-21	26.14	7.84	11.78	45.76	57.12	17.13	25.74
9	MP-22	24.74	12.26	9.58	46.58	53.11	26.32	20.57
10	SP-1	25.05	10.9	10.4	46.35	54.05	23.52	22.44
11	SP-2	22.63	13.12	10.17	45.92	49.28	28.57	22.15
12	SP-3	27.11	9.85	12.22	49.18	55.12	20.03	24.85
13	SP-4	25.16	11.3	10.8	47.26	53.24	23.91	22.85
14	SP-6	21.86	8.44	14.95	45.25	48.31	18.65	33.04
15	BCH-1	19.22	13.04	10.95	43.21	44.48	30.18	25.34
16	BCH-2	30.87	12.23	9.55	52.65	58.63	23.23	18.14
17	BCH-3	22.95	11.41	14.27	48.63	47.19	23.46	29.34
18	BCH-4	25.54	9.85	12.66	48.05	53.15	20.50	26.35
19	BCH-5	26.73	8.22	13.37	48.32	55.32	17.01	27.67
20	BCH-6	20.92	13.63	12.22	46.77	44.73	29.14	26.13

Table 6.3: Table showing Recalculated percentile values of Monocrystalline quartz, feldspar and rock fragments of Tipam sandstone of the study area (where Qmt: Monocrystalline Quartz total).

PLATE 6.1
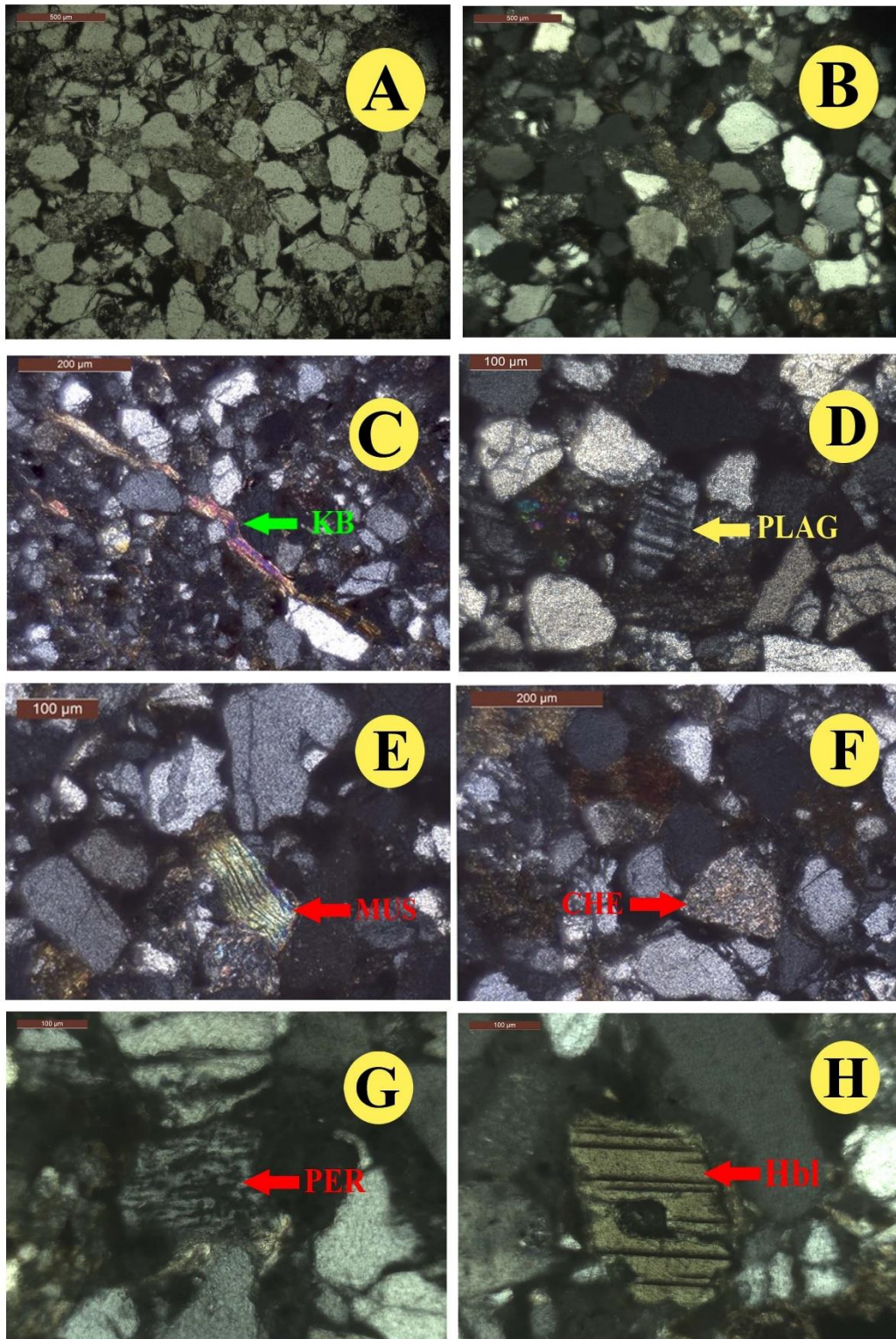
Where; KB = Kink band, Plag = Plagioclase, MUS = Muscovite, CHE = Chert,

PER = Perthite, Hbl = Hornblende

PLATE 6.2
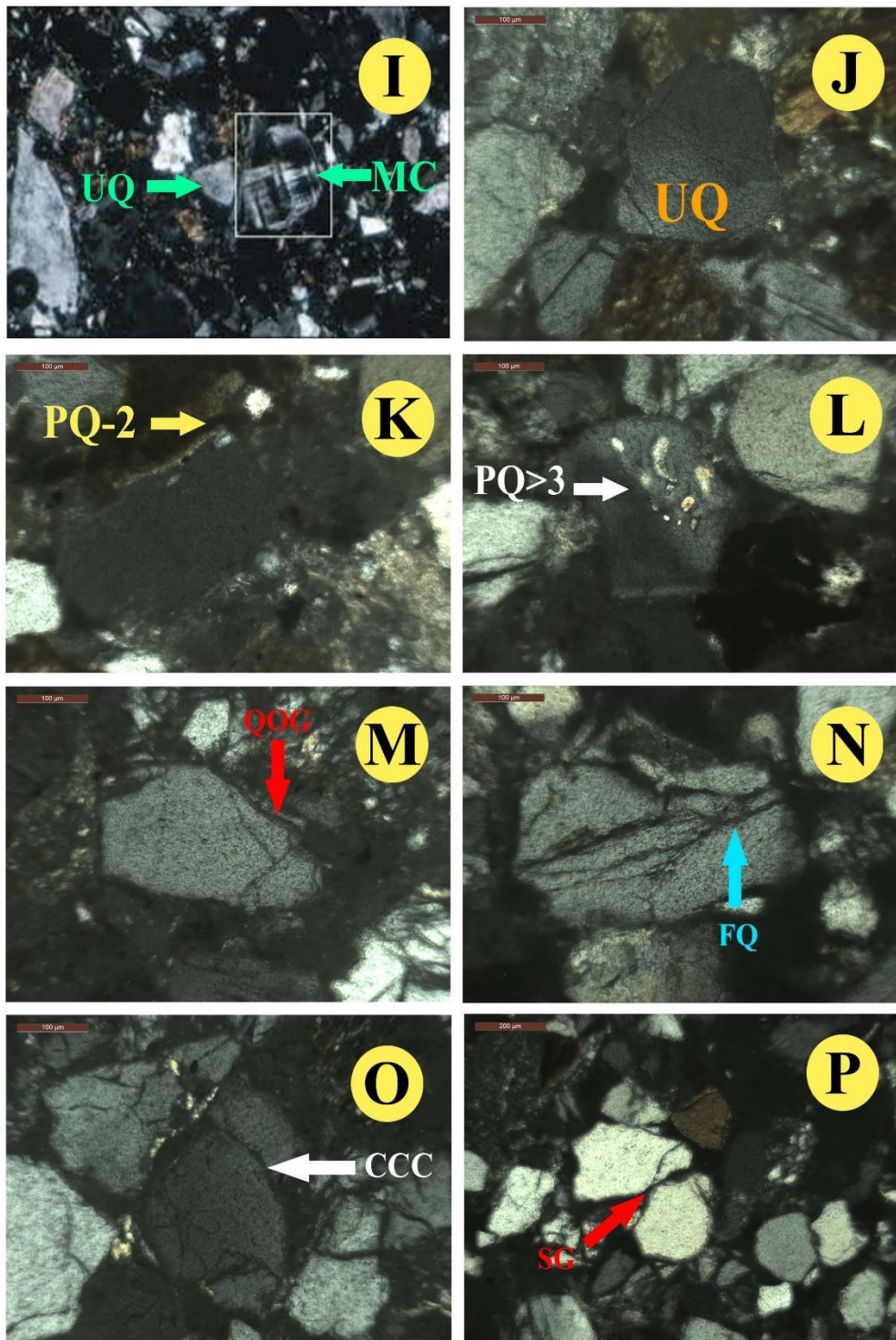
Where; Plag = Plagioclase, UQ = Undulatory quartz, PQ-2 = Polycrystalline quartz-2, PQ>3 = Polycrystalline quartz >3, QOG = Quartz overgrowth, FQ = Fracturing of quartz, CCC = Concavo-Convex contact and SQ = Sutured quartz.

6.4. Sandstone Classification

To classify sandstones using petrography, quantitative modal analysis (modal counting) of rock thin section is commonly used (Pettijohn *et. al.*, 1972; Folk, 1980). In the present study, classifications of Tipam sandstone were done according to ternary plot of Pettijohn, (1975) and Q-F-R plot after Folk, (1980). Table of Modal count petrographic study and recalculated percentile values of framework grains are shown in table 4.1 and 4.2. Quartz is the dominant mineral (48.18 – 60.76 %) in the present study followed by rock fragments (9.55 – 14.95 %) and feldspars (7.14 – 13.63 %,). Majority of the Tipam sandstone samples fall in the field of sublith-arenite while few samples fall in the field of sub-arkose according to Pettijohn, (1975) as represented in Figure 6.1(A). In the Q-F-R ternary plot of sandstone classification after Folk, (1980), the studied samples fall in the field of both lith-arkose and Feldspathic lithic arenites while only two samples fall in the field of sub-litharenite as represented in the Figure 6.1(B).
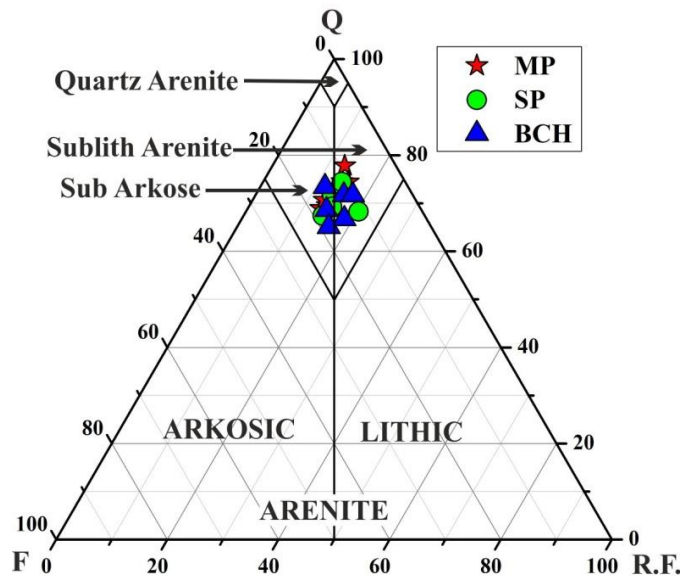
Figure 6.1(A): Petrographic classification of Tipam Sandstones after Pettijohn, (1972).
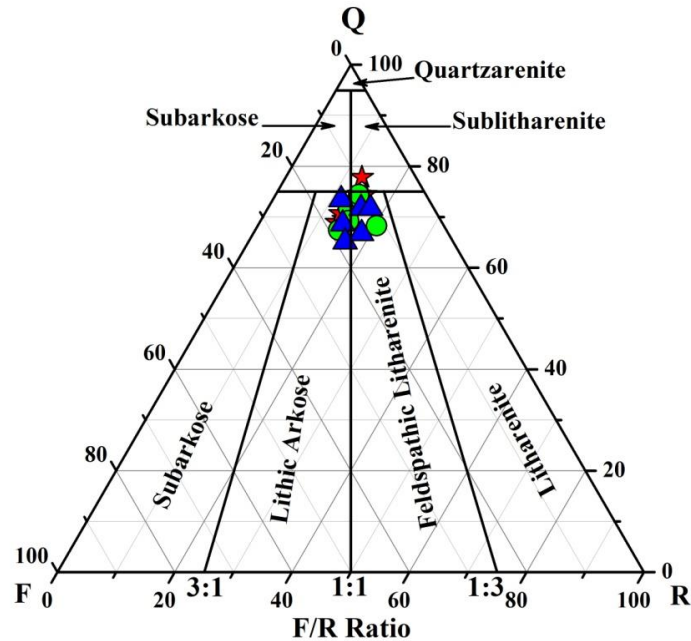
Figure 6.1(B): Petrographic classification of Tipam Sandstones after Folk, (1980).

6.5. Provenance

In order to decipher the nature and type of source rock, quartz varieties viz. monocrystalline (undulatory and non-undulatory) and polycrystalline (2-3 grains and >3 grains per quartz) are commonly used in the present study. Thin section analysis shows the abundance of Polycrystalline >3 ($Q_{P>3}$: 14.01 - 23.41% with an average of 17.51%) followed by Non-Undulatory Quartz (Q_{mnu}: 4.07 – 21.92% with an average of 13.11%) followed by Polycrystalline 2-3 grains per Quartz (Q_{P2-3}: 9.7-18.34% with an average of 12.75%) and Monocrystalline Undulatory Quartz (Q_{mu}: 8.95-18.76%, with an average of 10.79%). Using quartz varieties such as monocrystalline and polycrystalline varieties of quartz, Basu *et. al*., (1975) proposed the diamond diagram in order to discriminate source rock into 'plutonic', 'low, middle and upper rank metamorphic' types.

Using the data obtained from recalculated value of quartz varieties of Tipam sandstone of the study area, diamond diagram according to Basu *et. al*., (1975) was plotted [Figure 6.2(A)] and is observed that all the samples fall at low rank metamorphic rock which signifies that some quartz grains are derived from metamorphic terrain. The undulatory quartz grain of the present studied samples shows strain effect (wavy extinction) under petrological microscope which could be due to the compression experienced by the source rock.

Modified diamond diagram of Basu *et. al*., (1975) was proposed by Tortosa *et. al*., (1991) by keeping the same parameters of quarts varieties like Basu *et. al*., (1975) but introducing new fields of source rocks. Quartz varieties of the studied samples were plotted employing Tortosa *et. al*., (1991) and almost all the samples fall in the field of slate and schist [Figure 6.2(B)]. Hence, based on the two provenance discrimination plots, it can be stated that Tipam sandstone of the study area is derived from slate and schist of low rank metamorphic rock. Moreover, modal analysis of the present study indicates low abundance of feldspar (7.14-13.63% with average of 10.74%) showing moderate distance of transportation or moderate reworking of sediments.
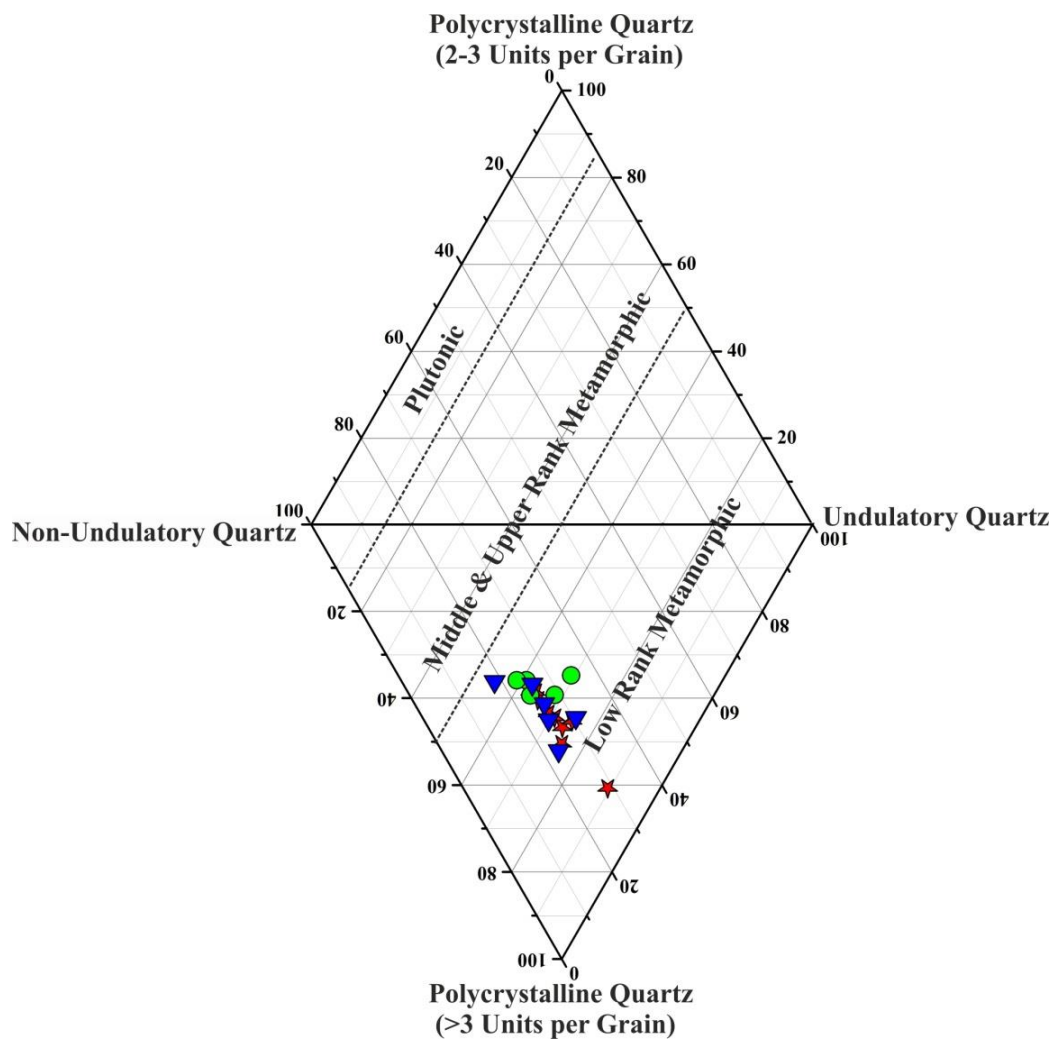
Figure 6.2(A): Diamond diagram for interpretation of provenance of Tipam sandstone of the study area after Basu *et. al*., (1975).
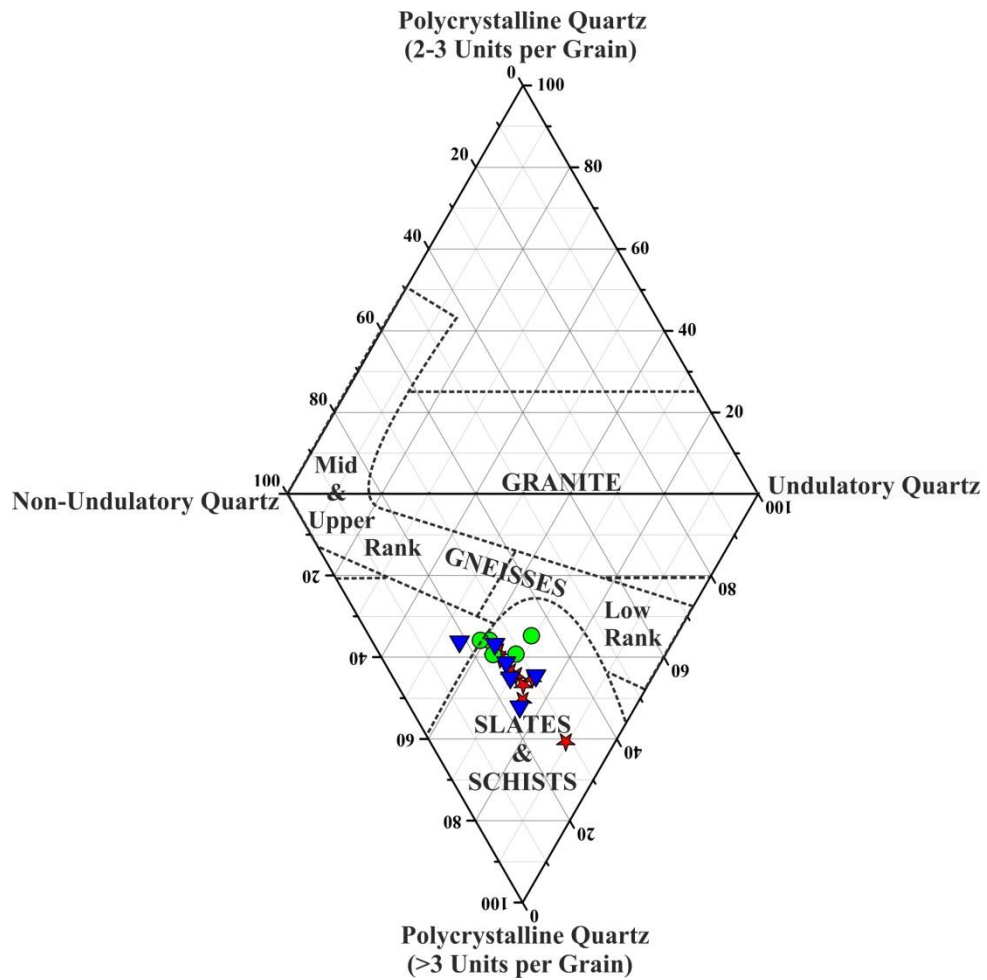
Figure 6.2(B): Diamond diagram for interpretation of provenance of Tipam sandstone of the study area after Tortosa _et. al_., (1991).

6.6. TEXTURAL MATURITY

Well sorted, well rounded sand free of interstitial clay is defined as matured sand (Folk, 1954). Textural maturity is controlled by the final depositional environment. Thus, a matured sand may be mixed with deep-water clay fractions which may produce framework textural inversion. "Textural maturity was subdivided by Folk, (1954) into four stages: the immature sands having >5% clay, poorly sorted, angular grains; the sub-mature sands 5% clay, moderately sorted, sub-angular to sub-

rounded grains; the mature sands are well sorted with <5% clay and rounded grains and the super-mature sands in which the clay fraction is almost absent and grains are well sorted and well rounded". From the petrographical analysis, the Tipam sandstones of the study area are immature to mature with 5% to >5% clay; sub angular to sub rounded.

6.7. MINERALOGICAL MATURITY

Maturity in sedimentary geology is described as the composition and texture of grains in clastic rocks, mostly of sandstones resulting from different amounts of sediment transportation. Among the mineral composition of sandstones, the most resistant mineral is Quartz and survive prolonged weathering and erosion. The index of mineralogical maturity of clastic rock can be somehow determined from the ratio of quartz to feldspar and unstable rock-fragments. In order to eliminate all the unstable fractions of minerals to produce a matured first cycle quartz sand, combination of extreme climate, relief and transportation. High quartz content with well-rounded and good sorting which are displayed by the orthoquartzitic sandstones are indicative of a high degree of mineralogical and textural maturity. From petrographical analysis, the Tipam sandstones of the study area are immature.

6.8. DIAGENESIS

Von Gumbel in 1888 was the first to introduce the term 'Diagenesis' (Pettijohn, 1975). Diagenesis is a process of compaction, cementation and lithification of loose sand grains. Any changes in terms of physical, chemical and biological undergone by loose sediments after deposition and during and after its lithification is termed as diagenesis (Dapples, 1962). Process of aging begins on sand very shortly after deposition and profoundly modifies its character. It is no longer rather it is

transformed into a dense lithified rock. It is a complex and long process that conversion of newly deposited loose sediments into indurated rocks by the process of diagenesis is a long and complex processes.

"Diagenesis of sandstone depends upon temperature, pressure, pore-water chemistry fluid influx, sand-shale ratio, texture and mineralogy of the rock and time (Blatt, 1980)". Diagenetic process is generally temperature controlled. Many of these factors appear to have been released to pre-burial tectonic setting, provenance and depositional environment (Mc Bridge, 1985). Diagenesis is the process undergone by sediments from deposition to lithification under normal temperature-pressure conditions. (Sengupta, 1994). Much importance is given on the study of diagenesis as it directly affects porosity and permeability which influence directly the accumulation of hydrocarbon and natural gas on sedimentary reservoir.

Diagenesis has been extended to a depth of 4-7 km and temperature of 120^0-220^0 C) where metamorphism began to sets in. Diagenesis is being divided into three stages as Near-surface (*telegenetic*), shallow depth (*eogenetic*) and deeper level (*mesogenetic*) changes (Sengupta, 2004). Authegenic growth and replacement of quartz grains, alteration of feldspar to clay minerals, crenulations of grain boundary, more silica and iron cementing materials and replacement of biotite mineral by chlorite are the effects of diagenesis.

Thin section study of the present Tipam sandstone samples reveled that all samples have undergone three stages of diagenesis in varying degree. During the early stage of diagenesis, mechanical compaction is the dominant process forming point and long contact due to rearrangement of the framework grains. Bending of mica flakes due to mechanical compaction of sediments [Plate 6.1 (C)], fracturing of ductile grains

of feldspar suggest post depositional tectonic disturbance of the sediments which reflects moderate compaction of the studied sandstone. Presence of fracturing of quartz grains also indicates the effect of tectonic activity after deposition of sediments [Plate 6.2 (N)]. Overgrowth of quartz [Plate 6.2 (M)] and presence of dissolution of feldspar grains by cementing materials suggests telegenetic stage of diagenesis. Presence of long contact, cancavo-convex contact and few sutured grain contacts indicate moderate pressure solution (Blatt, 1980) of the studied sandstone [Plate 6.2 (O) and Plate 6.2 (P)] Presence of point contact between quartz grains with precipitation of secondary chert [Plate 6.1 (F)] represent locomorphic stage of diagenesis under oxidizing condition (Dapple, 1967).

Ferric oxides, which are produced by oxidation of ferruginous sediments under humid climate, impart a red coloration to sediments at shallow depths. So, presence of ferruginous cement due to weathering and leaching of unstable ferromagnesian minerals in some thin section of the present study which is observed as void filling, coating around the detrital quartz grain is an indication of early burial reaction at shallow depth of diagenesis (eogenetic). Presence of fracturing and wrapping of quartz grains by mica flakes in the studied sandstones infer deeper level (mesogenetic) of diagenesis.

6.9 PALEOCLIMATIC CONDITIONS

The effects of climate on sand composition is reflected from the framework mineralogy. The nature of framework grains and its abundance give clues to the climatic condition prevailing during the time of deposition of sediments. According to Suttner *et. al*., (1981), high abundance of quartz, less amount of feldspar and rock fragments designate that the sediments are derived from metamorphic source

under humid climatic condition. Following Suttner *et. al*., (1981), QFR diagram was plotted for the present study and majority of the samples fall in metamorphic humid region and a few samples fall in plutonic humid region. Thus, it can be observed that the Tipam sandstone constitute a mixed nature of plutonic and metamorphic origin under humid climatic condition.
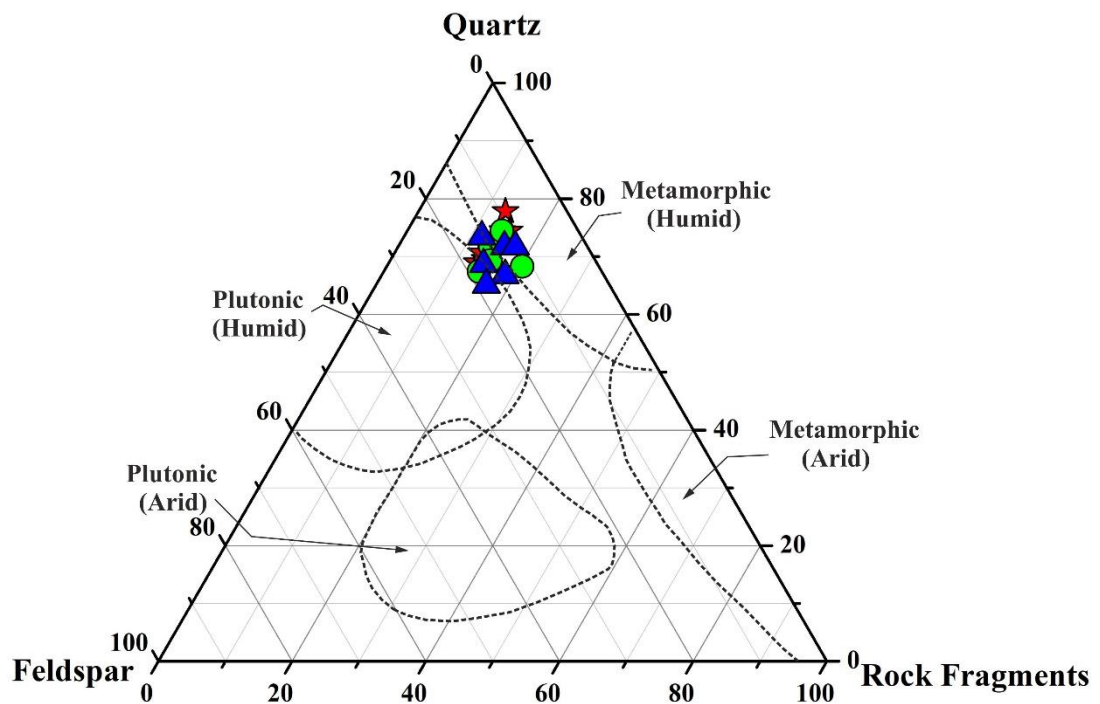
Figure 6.3(A): Triangular diagram for plots of QFR for climatic conditions after Suttner *et. al*., (1981).

Bivariate plot of ln(Q/R) vs ln(Q/F) (Weltje, 1994), **Figure 4.3(B)** and weathering index (Grantham and Velbel, 1988): WI=C x R (WI-Weathering index, C-Climate and R-Relief) also represents similar nature of paleoclimatic conditions. Bivariant plot of Tipam sandstones represent a plutonic source with the weathering indices at 1 suggesting a moderate hills relief under sub-humid climatic conditions.

Figure 6.3(B): Semi Quantitative Weathering Index after Weltje, 1994;
Grantham and Velbel, (1988).

4.10. TECTONIC SETTINGS

Tectonic history of the source area along with the site of deposition is directly related to the mineralogical composition of sediments (Krynine, 1984). The connection of sandstone composition to tectonic setting has been notable workout by Dickinson & Suczeck, (1979) and Dickinson *et. al*., (1983) to name a few. They

proposed QFL and Q_mFL_t compositional diagrams to delineate the tectonic settings of the source areas. QFL plot of the present study clustered in the field of recycled orogen [Figure 6.4(A)] while majority of the samples fall in mixed setting with only a few samples falling in dissected arc setting in Q_mFL_t plot [Figure 6.4(B)].

Presence of monocrystalline quartz with wavy extinction suggests a metamorphic source while plutonic source is evident by the presence of non-undulatory monocrystalline quartz and slightly curved inter-crystal boundaries of polycrystalline quartz (>3 crystal unit per grain). Granite or pegmatite sources are evident by the presence of perthite. Few Rounded quartz grains stipulate recycled origin while angular grains and present of rock fragments indicate textural immaturity of the rock.
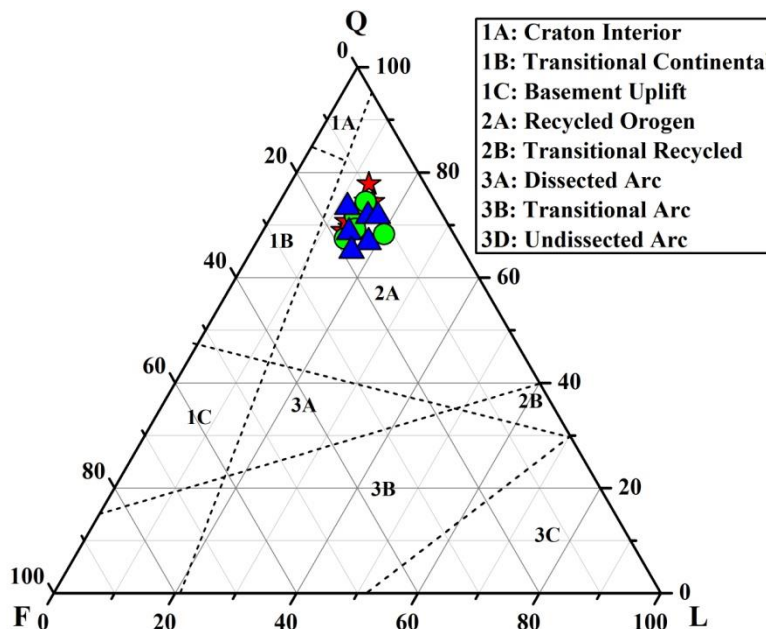
Figure 6.4(A): Q-F-L triangular plot for tectonic settings after Dickinson & Suczeck, (1979).
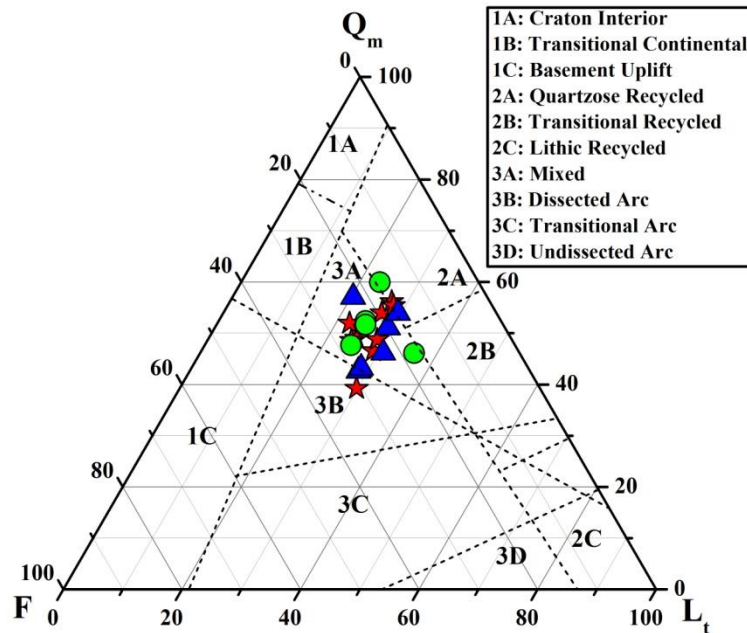
Figure 6.4(B): Q_m-F-L_t triangular plot for tectonic settings after Dickinson *et. al.*, (1983).

6.11 DISCUSSION AND INTERPRETATION

Thin section studies of Tipam sandstones reveal that quartz is the most abundant minerals among the framework grains (Avg: 53.73) followed by Lithic fragments and feldspar. Plotting of the samples for classification in QFR according to Pettijohn *et. al.*, (1972) and Folk, 1980 fall in the field of sublith-arenite to sub-arkose and Feldspathic lithic arenites to lithic arkose.

Using the data obtained from recalculated value of quartz varieties of Tipam sandstone of the study area, diamond diagram according to Basu *et. al.*, (1975) and modified diamond diagram was plotted [Figure 6.2(A)] and is observed that all the samples fall at low rank metamorphic rock of slate and schist. Following Suttner *et. al.*, (1981), QFR diagram was plotted for the present study and majority of the samples

fall in metamorphic humid region and a few samples fall in plutonic humid region. Thus, it can be observed that the Tipam sandstone constitute a mixed nature of plutonic and metamorphi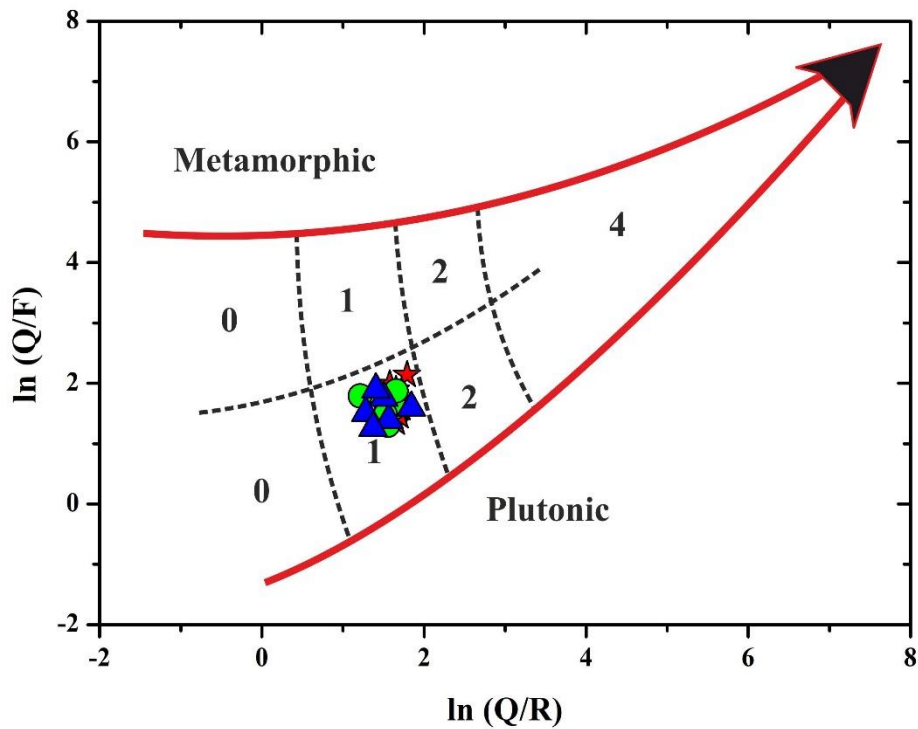c origin under humid climatic condition. Bivariate plot of ln(Q/R) vs ln(Q/F) (Weltje, 1994), Figure 6.3(B) and weathering index (Grantham and Velbel, 1988): WI=C x R (WI-Weathering index, C-Climate and R-Relief) also suggesting a moderate hills relief under sub-humid climatic conditions. QFL and Q_mFL_t ternary plot for tectonic settings according to Dickinson & Suczeck, (1979) and Dickinson *et. al.*, (1983) suggests recycled orogen [Figure 6.4(A)] and mixed setting.

Presence of monocrystalline quartz with wavy extinction suggests a metamorphic source while plutonic source is evident by the presence of non-undulatory monocrystalline quartz and slightly curved inter-crystal boundaries of polycrystalline quartz (>3 crystal unit per grain). Granite or pegmatite sources are evident by the presence of perthite. Few Rounded quartz grains stipulate recycled origin while angular grains and present of rock fragments indicate textural immaturity of the studied Tipam sandstones.

CHAPTER 7

HEAVY MINERALS

7.1 INTRODUCTION

Sedimentary rocks contain a lot of information to their origin and the environment in which they were deposited. Heavy mineral is an important and useful tool as it brings character of the source rocks from which they are derived. Heavies are those accessory minerals having specific gravity higher than 2.89 and are volumetrically minor population, usually less than 1% by weight of a terrigenous rock (Folk, 1980).

Heavy minerals can supply information regarding provenance by supplementing the overall modal analysis of sandstones in defining changes with respect to time in source areas. Although the distribution of heavy minerals is controlled by a variety of factors (such as specific gravity , grain size of the sediments; abrasion; weathering experienced by the source area; distance of transport, and post-depositional changes), these data can be useful in determining provenance and evaluating temporal changes in detritus shed from sedimentary sources. Morton, (1985) stated that "The heavy mineral suites are not only controlled by provenance, but also affected by weathering, transportation, deposition and post-depositional alteration". Heavy mineral assemblages may reflect the petrology of source-area rock suites in the case of relatively proximal synorogenic sediments, which are typically eroded prior to extensive weathering, transported over relatively brief intervals, and deposited rapidly. One of the first person to stress on the need to study the heavy

minerals in order to know the history of sedimentation which has useful implications for the exploration of hydrocarbons was Von Andel, (1959). Morton, (1985) stated that "The heavy mineral suites are not only controlled by provenance, but also affected by weathering, transport, deposition and post-depositional alteration". Heavy mineral study is useful for interpreting composition and tectonic history of provenance (Pettijohn *et. al*, 1987).

Until the 1950s, heavy minerals were studied and used as a tool for stratigraphic correlation, particularly of the oil field areas. Nowadays, they are used to determine provenance since origin of many heavy minerals is limited to certain rock types. Besides these, the heavy minerals are considerable important for studying transportation and weathering history of sediments and also in palaeo-geographic studies.

Heavy minerals normally include many kinds of opaque and transparent minerals. The opaque minerals usually predominate and include oxides, sulphides and other ore minerals. The transparent minerals include rock forming silicates. Heavy minerals have been widely used for studying provenance and for demarcating the mechanism of transportation (King, 1972; Frihy and Kumar, 1993).

7.2 DESCRIPTION OF HEAVY MINERALS

A number of heavy mineral species have been recorded from the study area. The common heavy mineral assemblages of Tipam sandstone of the study area consist of zircon, tourmaline, rutile, Hornblende, garnet, staurolite, sillimanite, kyanite, Epidote and opaque minerals.

Zircon

It is one of the most common heavy minerals which are found in almost all the samples analyzed. They are mostly colourless or slightly greyish in colour under plane polarized light but a few pinkish to yellowish brown varieties are also reported. Well rounded grains are rare in occurrence. They are identified by their high order interference colour and zoning and absence of cleavage. They occur mostly as prismatic, sub-angular to sub-rounded in shape and also contain inclusion of other minerals. Zircon percentage varies from 6.59 to 11.98 with an average of 8.60. [Plate 7.1 (2a-2f)]

Tourmaline

Tourmaline grains are Prismatic, angular and sub-rounded and show pleochroism from pale green to dark green, pale brown to dark brown and light green to dark green. The colour ranges from pale green to pale brown. It is found in all the samples of the present study. In a few samples, Inclusions of non-opaque minerals are observed. Tourmaline percentage varies from 90.14 to 15.93 with an average of 12.56. [Plate 7.1 (3a-3d)].

Rutile

They are easily identified by their blood red to dark brownish red color and are abundant in almost all the samples. High refractive index, absence of cleavage and slight pleochroism are some of the distinguishing optical properties seen in the samples. Rutile percentage varies from 3.89 to 7.12 with an average of 5.21. Prismatic, irregular and angular to sub-angular grains are usually shown by rutile of the present study [Plate 7.2 (1a-1f)].

Hornblende

Grains are anhedral, prismatic and irregular in shape and exhibit perfect prismatic cleavage. They show distinct Pleochroism from green to pale green under plane polarized light. Inclined extinction and second order greenish interference color are the distinguishing properties under cross polar. The percentage varies from 1.10 to 2.96 with an average of 1.98 [Plate 7.3 (3a-3c)].

Garnet

Garnet shows high relief and are isotropic in nature which make them easily identifiable. They are represented by a colorless, sub-angular to sub-rounded grains with conchoidal fracture. Inclusions are common in the sample grains. The percentage varies from 3.63 to 6.60 with an average of 5.16 [Plate 7.3 (2a-2d)].

Staurolite

Staurolite grains are light yellowish to straw yellow in color and reveal Strong pleochroism (pale yellow to golden yellow) with moderately high relief. The percentage varies from 3.15 to 6.42 of the total heavies with an average of 4.51 [Plate 7.2 (3a-3d).

Sillimanite

Sillimanite occurs as needle shape or elongated shape, prismatic with a prominent cleavage parallel to the direction of elongation. Under cross polar, they show straight extinction and second order greenish/bluish interference color.

Sillimanite percentage varies from 1.10 to 3.50 with an average of 2.10 [Plate 7.2 (2a-2d)].

Kyanite

Kyanite grains show elongated or prismatic texture with irregular terminations and mostly colorless with excellent cleavage producing nearly rectangular grains. Weak pleochroism and inclined extinction are clearly observed in the grains. The percentage varies from 7.31 to 12.89 with an average of 9.32 [Plate 7.3 (1a-d)].

Epidote

Colorless to pale greenish yellow with some inclusions are shown by grains of epidote. It shows a faint pleochroism with Moderate relief. Color appears almost same as ordinary light due to low interference color. The grains are sub-angular to sub-rounded. The percentage varies from 4.14 to 10.15 with an average of 7.07 [Plate 7.4 (1a-d)].

Opaque Minerals

Opaque minerals represent an ample part of the heavies under study. They are mostly oxides of iron (hematite and magnetite) with irregular shape and size and also with broken surfaces and are usually black to brownish black in color. The percentage of opaque minerals varies from 32.65 to 48.17 with an average of 41.04 [Plate 7.1 (1a-b)].

PLATE 7.1
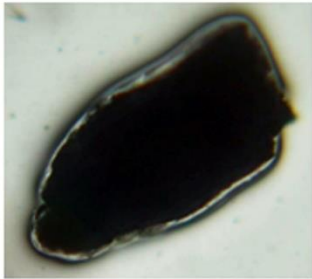
1a

1b
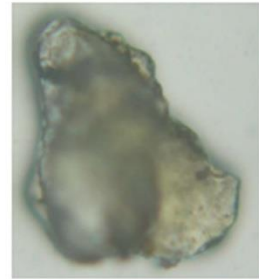
2a
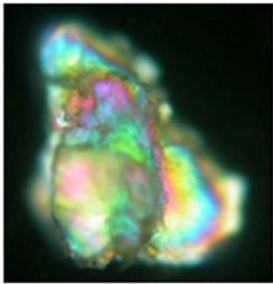
2b

2c
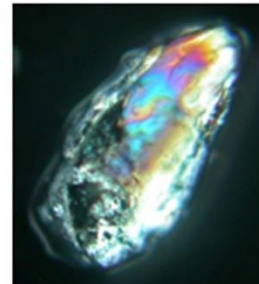
2d
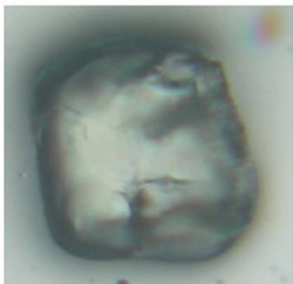
2e
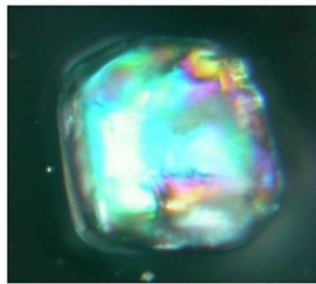
2f
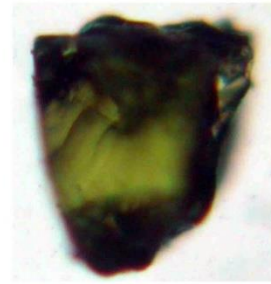
3a
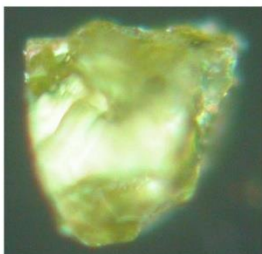
3b
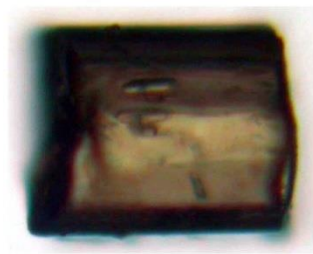
3c
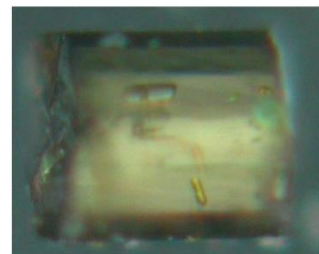
3d

PLATE 7.2
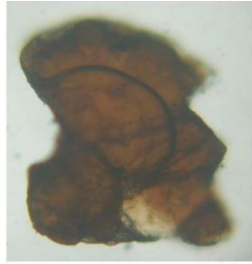
1a
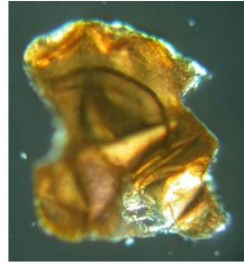
1b
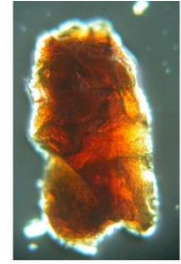
1c
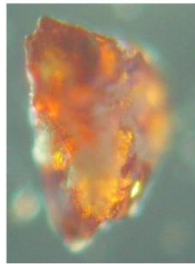
1d
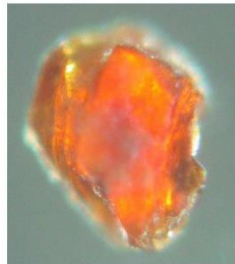
1e
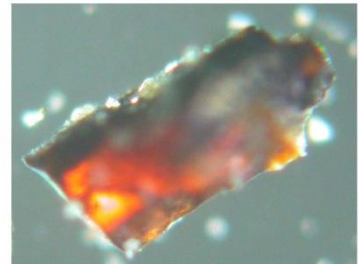
1f
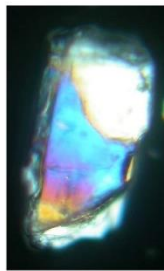
2a

2b

2c
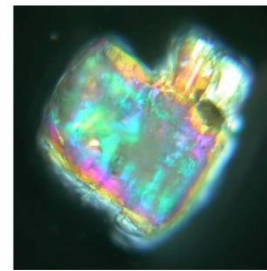
2d
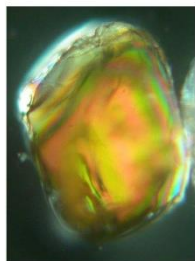
3a
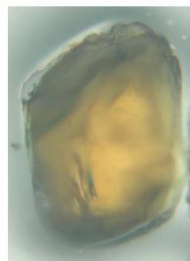
3b

3c
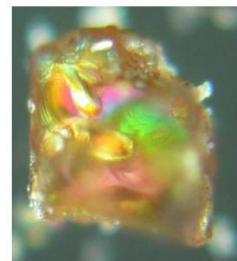
3d

PLATE 7.3

1a

1b

1c

1d

2a
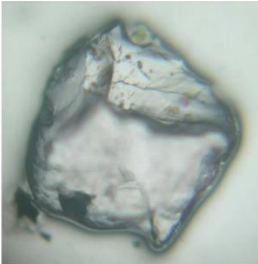
2b
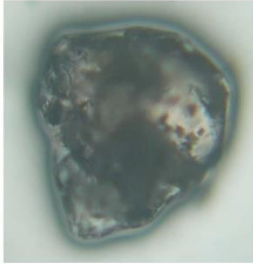
2c

2d
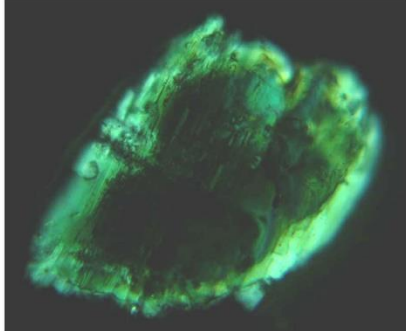
3a
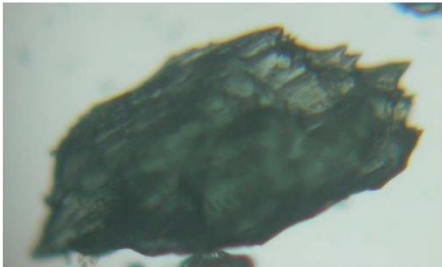
3b
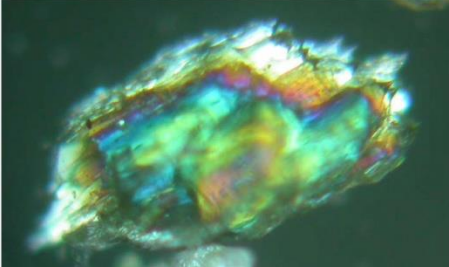
3c

PLATE 7.4
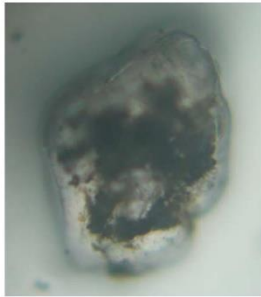
1a
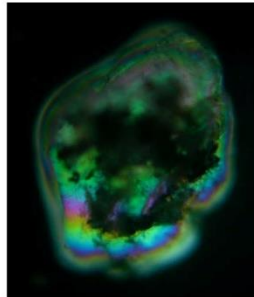
1b
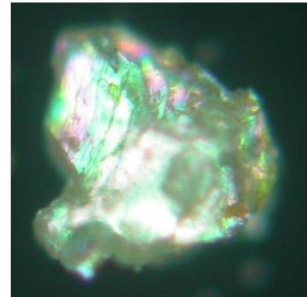
1c
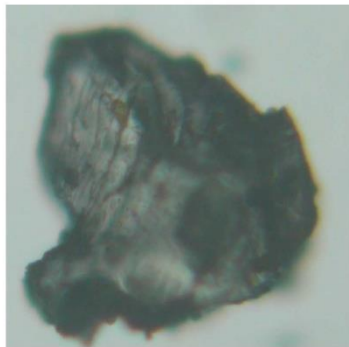
1d
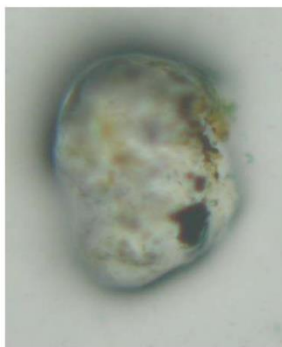
2a
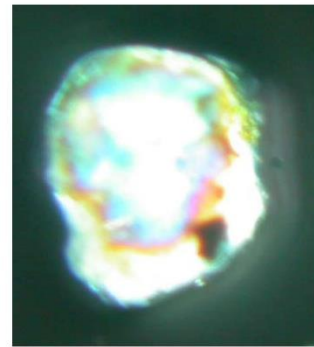
2b

3a
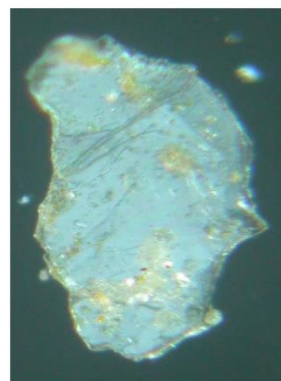
3b

DESCRIPTION OF PLATE 7.1-7.5 (Magnification 40X)

Plate 7.1 (2a-2f):   Photomicrograph of Zircon (Under ppl and Xpl)

Plate 7.1 (3a-3d):   Photomicrograph of Tourmaline (Under ppl and Xpl)

Plate 7.2 (1a-af):   Photomicrograph of Rutile (Under ppl and xpl)

Plate 7.3 (3a-3c):   Photomicrograph of Hornblende (Under ppl and Xpl)

Plate 7.2 (3a-d):   Photomicrograph of Staurolite (Under ppl and Xpl)

Plate 7.2 (2a-d):   Photomicrograph of Sillimanite (Under ppl and Xpl)

Plate 7.3 (1a-d):   Photomicrograph of Kyanite (Under ppl and Xpl)

Plate 7.4 (1a-d):   Photomicrograph of Epidote (Under ppl and Xpl)

Plate 7.1 (1a-b):   Photomicrograph of Opaque minerals (Under ppl and Xpl)

Sample No.	Zr	Tr	Rt	Hb	Gr	Si	St	Ky	Ep	Ch	En	Op
SP-1	7.20	10.75	6.25	2.15	6.60	3.50	4.00	7.50	4.25	2.15	1.55	45.25
SP-2	8.25	12.75	5.65	1.42	5.20	1.75	5.15	7.69	9.21	1.20	1.29	46.09
SP-3	8.73	14.45	4.63	2.07	4.30	2.17	3.31	9.45	7.23	1.68	-	42.25
SP-4	11.02	12.51	4.34	1.33	5.12	2.78	4.45	11.15	6.49	1.45	1.32	38.04
SP-6	9.35	11.32	7.12	2.16	7.46	1.89	4.12	8.13	5.59	2.67	1.06	39.13
MP-7	7.11	9.14	5.27	1.87	3.68	1.10	6.42	10.61	9.75	1.98	-	43.07
MP-9	6.76	10.61	3.89	1.58	4.14	1.33	5.76	7.39	8.61	1.76	-	48.17
MP-11	10.14	15.27	6.79	2.17	4.63	2.19	3.15	9.47	5.25	2.05	1.46	37.43
MP-16	8.15	12.27	4.62	2.21	5.15	1.20	4.31	8.22	6.65	1.06	1.02	45.14
MP-17	7.65	11.86	5.98	2.94	4.27	2.21	5.10	7.31	10.15	1.46	2.21	38.86
MP-18	8.45	9.14	4.30	2.07	6.29	2.09	4.04	11.34	4.14	1.37	1.63	45.14
MP-19	6.95	13.07	6.10	2.25	4.63	2.13	3.25	12.89	5.17	1.11	-	42.45
MP-20	6.80	9.90	4.24	1.76	5.51	1.67	4.75	8.75	7.93	1.14	1.05	46.50
MP-21	6.59	12.98	4.10	1.45	3.63	2.24	3.57	7.89	8.63	1.61	1.32	45.99
MP-22	7.45	12.80	5.86	2.14	5.12	2.19	5.23	8.22	9.42	1.33	1.61	38.63
BCH-1	10.97	14.85	6.24	2.15	6.20	2.77	5.13	7.47	7.50	2.02	1.05	33.65
BCH-2	8.40	15.45	4.15	1.77	4.45	2.71	3.17	10.12	6.78	2.17	1.40	39.97
BCH-3	11.98	15.93	3.95	1.10	5.12	2.14	4.89	11.24	7.84	2.13	1.33	32.65
BCH-4	9.83	12.59	5.70	2.13	6.22	2.28	4.22	9.37	6.32	1.85	1.24	38.25
BCH-5	10.27	13.63	5.20	2.96	5.54	1.84	6.37	12.23	4.55	2.27	1	34.14
AVERAGE	**8.60**	**12.56**	**5.21**	**1.98**	**5.16**	**2.10**	**4.51**	**9.32**	**7.07**	**1.72**	**1.07**	**41.04**

Table 7.1: Table showing heavy mineral percentage of the study area. (Where; Zr: Zircon, Tr: Tourmaline, Rt: Rutile, Hb: Hornblende, Gr: Garnet, Si: Sillimanite, St: Staurolite, Ky: Kyanite, Ep: Epidote, Ch: Chlorite, En: Enstatite and Op: Opaque minerals).

Table 7.2: Table showing average of all the heavies of the study area.

HEAVY MINERALS	Zircon	Tourmaline	Rutile	Hornblende	Garnet	Sillimanite	Staurolite	Kyanite	Epidote	Chlorite	Enstatite	Opaque
AVERAGE	8.6	12.56	5.21	1.98	5.16	2.1	4.51	9.32	7.07	1.72	1.07	41.04
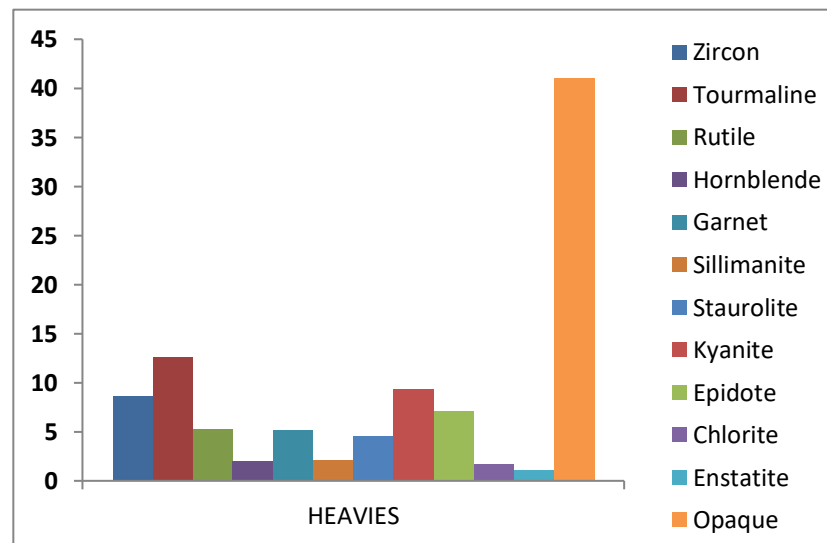
Figure 7.1 Histogram showing average of all the heavies of the study area

7.3 ZTR MATURITY INDEX

Z.T.R. maturity index quantitatively can define whether the heavy mineral assemblages of a particular region are mature or not. "The Z.T.R. maturity index is the percentage of the combined zircon, tourmaline and rutile grains among the transparent, non-micaceous and detrital heavy minerals" (Hubert, 1962). Among the heavies; Zircon, tourmaline, rutile and non-micaceous heavy mineral assemblage are stable (Pettijohn *et. al*., 1973). In the present study, the recalculate percentage values of ZTR were plotted in the triangular graphs (modified after Hazarika, 1984) to obtain the ZTR maturity index of Tipam sandstone of the study area (Figure7.2).

ZTR maturity index of Tipam sandstone of the study area varies from 38.25% to 58.81 % with a mean of 48.53%. Individually zircon value ranges from 6.59% to 11.98%, tourmaline from 9.14% to 15.13% while rutile value ranges from 3.89% to 7.12% of Tipam sandstone. The recalculated percentile value of zircon ranges from 27.84% to 39.54%, tourmaline from 40.73% to 55.18% and rutile varies from 12.40% to 25.83%. In the present study, plotting of the recalculated individual value of zircon, tourmaline and rutile all falls in the C_1 tier which shows that the proportion of Tourmaline is the highest and followed by zircon and rutile. Moderate maturity and dominating metamorphic provenance are indicative of C_1 tire. So it can be concluded that the sediments of Tipam sandstone is almost matured.

SAMPLE NO.	ZIRCON	TOURMALINE	RUTILE	TOTAL
SP-1	29.75	44.42	25.83	100
SP-2	30.96	47.84	21.20	100
SP-3	30.96	47.84	21.20	100
SP-4	31.39	51.96	16.65	100
SP-6	39.54	44.89	15.57	100
MP-7	33.65	40.73	25.62	100
MP-9	33.04	42.47	24.49	100
MP-11	31.80	49.91	18.30	100
MP-16	31.49	47.42	21.09	100
MP-17	32.55	49.00	18.45	100
MP-19	30.01	46.53	23.46	100
MP-20	38.60	41.75	19.64	100
MP-21	26.61	50.04	23.35	100
MP-22	32.47	47.28	20.25	100
BCH-1	27.84	54.84	17.32	100
BCH-2	28.53	49.02	22.44	100
BCH-3	34.22	46.32	19.46	100
BCH-4	30.00	55.18	14.82	100
BCH-5	37.60	50.00	12.40	100
BCH-6	34.96	44.77	20.27	100

Table 7.3: Recalculated Zircon, Tourmaline and Rutile Percentage of the study area.
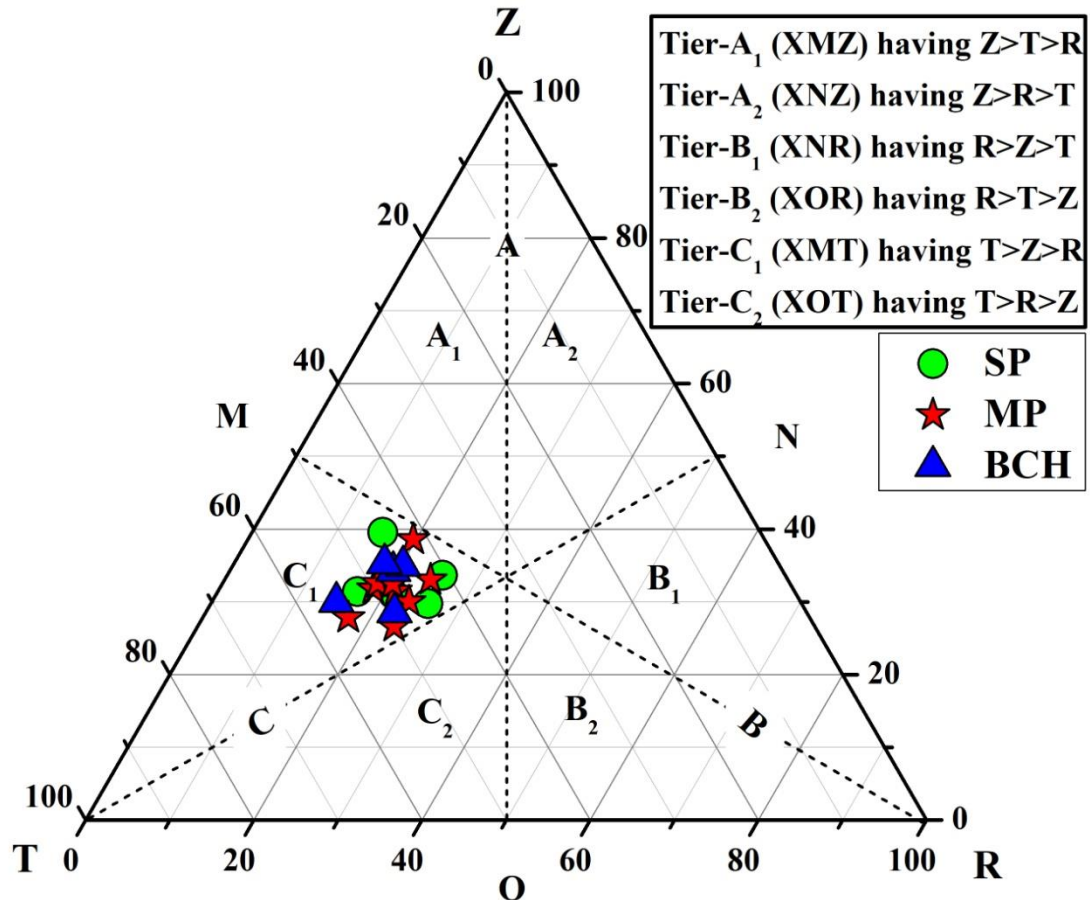
Figure 7.2: ZTR maturity of Tipam sandstone.

7.4 DISCUSION AND INTERPRETATION

Abundance of both opaque and non opaque mineral such as zircon, tourmaline, rutile, hornblende, garnet, sillimanite, staurolite, Kyanite, epidote, chlorite and enstatite are shown by the heavy mineral assemblages of the present study. Of these, opaque minerals, zircon, tourmaline, rutile, kyanite, epidote and garnet are abundant. The bulk dominance of zircon, tourmaline and rutile along with the dominance of opaque

minerals indicate portion of the sediments originate from acid plutonic rock. Presence of few colourless euhedral zircon grains suggests an acidic igneous source with short transportation. Presence of a few perfect euhedral grain of tourmaline may also indicate silicic igneous source with short distance of transportation. According to Heinrich, (1956) presence of epidote along with tourmaline suggests low to medium grade metamorphic source.

"The zircon grains in sandstones are diverse types and regarded as the best provenance indicator and one of the most resistant minerals among all the heavy minerals" (Pettijohn, 1975). Presence of subhedral grains of zircon not only suggest igneous source, but also reworked sediments. Presence of green and brown tourmaline indicate granite and pegmatite derivation (Krynine, 1946). Sub-angular to sub-rounded blood red color rutile indicate derivation not only from igneous but also reworked sediments and metamorphic provenance of mainly schist. Presence of few hornblende with irregular shape reflect an acidic igneous source as well as metamorphic source. Occurrence of chlorite, epidote, kyanite and sillimanite suggest low to high rank metamorphic origin.

Based on the observation of heavy mineral suite and ZTR maturity index, it can be concluded that the Tipam sandstone of the study area show moderate maturity and are derived from mixed source where major portion of the sediments were derived from metamorphic source and also from igneous source. However, presence of sub rounded grains of heavies also suggest contribution from reworked sediments.

CHAPTER 8

GEOCHEMISTRY

8.1 INTRODUCTION

Clastic Sedimentary rock originate from weathering, erosion, transport and deposition of pre-existing rocks and are an important source of information about previous orogenic conditions and may contain detritus that describes the evolution of orogenic settings (Johnsson, 1993). Minerals of pre-existing rock are disintegrated, dissolved and are carried by various agents to produce sediments during the process of weathering (Krishnamurthy *et. al*., 1986; Laird *et. al*., 2003; Rose *et. al*., 2004). The chemical composition of sandstone has been used to determine relationships between tectonic setting and provenance (Dickinson and Suczek, 1979; Johnsson, 1993).

Thin section studies of sedimentary rock can disclose transportation of sediments, diagenesis, provenance and depositional environment (Dickinson and Suczek, 1979; Ingersoll and Suczek, 1979; Dickinson, 1985). However, framework grains can likely be modified due to deep burial and compaction of the sediments. In contrast to thin section study, the precision of geochemical data gives a precise information of sedimentary rocks (McLennan *et. al.,* 1993; Kroonenberg, 1994; Armstrong and Altrin, 2014). The chemical composition of source rock is the main controlling factor on the chemistry of sedimentary rocks. However, the composition of clastic sedimentary rocks can be greatly modified by several factors, which include weathering, erosion, hydraulic sizing, deposition, transport, burial, and diagenesis

(Bhatia and Crook, 1986; Johnsson, 1993; Cullers and Podkovyrov, 2000). Chemical changes during deposition depend on the depositional environment, which is chiefly controlled by subsidence rate. The most important factors noted by Johnsson, (1993) are source rock composition, chemical weathering, abrasion, sorting during transport, and diagenesis. These factors are affected by three main interrelated components, namely, tectonic setting, climate and the nature of the depositional system. Each of these factors affects the characteristics of the others, producing different clastic compositions. As sediments are transported long distances from the source area, lithics become separated from relict quartz, and are chemically broken down. This results in quartz-rich sandstones that are characteristic of continental interiors and passive margin platform settings, and massive, mud-rich deltas characteristic of passive continental margin slope settings. In contrast, magmatic arc depositional systems tend to have short transport distances, which reduce physical sediment sorting and chemical weathering, and results in quartz deficient sandstones and more abundant in lithics. "For characterizing the weathering profile of a source rock, chemical weathering indices are commonly used by incorporating the bulk major element oxide chemistry into a single metric (Jason *et. al*, 2003)".

The chemical compositions of the sediments due to these complex interactions are sometimes difficult to match back the compositions of source rock (Johnsson, 1993). However, relationship between sandstone composition, provenance and tectonic setting has been observed (Dickinson and Suczek, 1979; Dickinson *et. al*., 1983). Even though the interactions between these factors are complex, this suggests that they typically behave in similar ways in any given setting. Moreover, the influence

112

of these factors upon sediment composition varies from one setting to another, hence producing similar and consistent compositional groups in each setting (Seiver, 1979).

The rare earth elements (REE, from La - Lu) are a logical group characterized by a single oxidation state: REE (III) except for cerium and europium. In order to understand and describe the chemical evolution of the earth's continental crust, REE have become important geochemical tracers during the last few decades (Goldstein and Jacobsen, 1988; McLennan, 1989; Dupre *et. al.*, 1996). "Terrigenous sediments may reflect the features of their source rocks on the assumption that some elements (particularly rare earth elements, Th, Zr, Hf and Sc) are transformed from the site of weathering to the terrigenous component of the sediments, and their abundances are not significantly modified during weathering, sediment transport, diagenesis or metamorphism; Taylor and McLennan, (1985), McLennan, (1989), McLennan and Taylor, (1991).

Based on peculiar Th/La, Th/Sc and other elemental pairs, Bhatia, (1983) grouped sandstones into four tectonic settings: oceanic arc, continental arc, active and passive continental margins. The effects of chemical weathering on trace element distributions suggested that the conventionally immobile elements could also be re-distributed to some extent (Nesbitt, 1979; Cullers *et. al.*, 1987). Further studies showed that chemical weathering can even change the REE patterns and Eu anomalies in sediments (Condie *et. al.*, 1995). Other processes, such as heavy mineral assemblage fractionation and the degree of diagenesis to some extent have an influence on REE and elemental concentrations of high field strength element (HFSE, Nb, Ta, Zr and Hf) (Ohr *et. al.*, 1994).

The geochemical composition of sedimentary rocks is a multiplex function of various variables like source material, weathering, transportation, physical sorting and diagenesis (Middle-ton 1960; Bhatia 1983; McLennan 1989; Cox and Lowe 1995). "Several trace elements, such as the rare earth elements (REE; e.g., La,Ce, Nd, Gd, Yb), Y, Th, Zr, Hf, Nb, and Sc are most suited for discriminations of provenance and tectonic setting because of their relatively low mobility during sedimentary processes and their short residence times in sea water (Holland, 1978; Taylor and McLennan 1985)". So, due to their low mobility, they are transferred quantitatively into clastic sediments during weathering and transportation, thus reflecting the impression of the parent materials, and hence are more useful in differentiating tectonic environment and source-rock compositions than the major elements (Bhatia and Crook, 1986; McLennan, 1989; Condie, 1993).

8.2 WHOLE ROCK CHEMISTRY

The whole rock chemistry studies of Tipam sandstone includes major elements in terms of wt % of oxides, trace elements and REE in terms of ppm and are represented in Table 8.1(A-C).

Litho-Unit	Sample	SiO$_2$	Al2O$_3$	Fe$_2$O$_3$	MnO	MgO	CaO	Na$_2$O	K$_2$O	TiO$_2$	P$_2$O$_5$	SiO$_2$/Al$_2$O$_3$	Al$_2$O$_3$/TiO$_2$	K$_2$O/Al$_2$O$_3$	K$_2$O/Na$_2$O
TIPAM SANDSTONE	MP-7	78.88	10.84	2.77	0.03	1.26	1.04	1.16	1.71	0.54	0.07	7.28	20.26	0.16	1.48
	MP-9	82.52	8.02	2.61	0.04	1.54	1.06	1.05	1.42	0.35	0.05	10.29	22.77	0.18	1.35
	MP-11	78.23	11.44	2.47	0.04	2.67	1.02	0.84	1.39	0.32	0.04	6.84	35.53	0.12	1.65
	MP-16	80.33	11.44	2.20	0.04	1.74	0.76	0.42	1.30	0.27	0.04	7.02	42.21	0.11	3.10
	MP-17	81.83	10.85	1.59	0.01	1.48	0.47	0.16	1.44	0.24	0.02	7.54	45.40	0.13	8.88
	MP-19	81.56	10.05	2.30	0.04	1.50	0.76	0.36	1.37	0.29	0.05	8.12	35.12	0.14	3.83
	MP-20	78.95	11.77	1.82	0.03	2.54	1.07	0.35	1.25	0.23	0.03	6.71	50.73	0.11	3.55
	MP-21	79.05	11.72	1.68	0.03	2.70	1.28	0.23	1.18	0.26	0.03	6.74	45.96	0.10	5.13
	MP-22	79.44	10.56	2.85	0.04	2.65	1.07	0.33	1.37	0.33	0.06	7.52	31.61	0.13	4.21
	SP-1	79.69	8.17	3.00	0.04	3.04	1.32	1.07	1.46	0.41	0.05	9.76	19.87	0.18	1.37
	SP-2	79.70	10.81	2.45	0.04	1.49	0.92	0.97	1.27	0.33	0.04	7.38	32.55	0.12	1.31
	SP-3	80.85	10.93	1.79	0.02	1.73	0.76	0.86	1.41	0.24	0.03	7.40	45.73	0.13	1.65

Table 8.1 (A): Table showing major oxides in terms of wt% and their corresponding elemental ratios (where, GSR-4: Chinese Sandstone Standard from Xeujing *et. al.*, 2007 and UCC: Upper continental crust from Rudnick and Gao, 2003, 2005).

Litho-Unit	Sample	SiO$_2$	Al2O$_3$	Fe$_2$O$_3$	MnO	MgO	CaO	Na$_2$O	K$_2$O	TiO$_2$	P$_2$O$_5$	SiO$_2$/Al$_2$O$_3$	Al$_2$O$_3$/TiO$_2$	K$_2$O/Al$_2$O$_3$	K$_2$O/Na$_2$O
TIPAM SANDSTONE	SP-4	79.44	10.74	2.46	0.03	2.40	0.91	0.79	1.38	0.33	0.04	7.40	32.25	0.13	1.73
	SP-6	77.56	10.78	4.53	0.06	2.25	0.56	0.62	1.67	0.53	0.11	7.20	20.34	0.15	2.71
	BCH-1	75.67	10.48	2.28	0.04	3.32	4.09	0.47	1.59	0.39	0.04	7.22	27.01	0.15	3.36
	BCH-2	76.29	8.65	1.35	0.02	4.45	5.64	0.46	1.55	0.26	0.03	8.82	32.89	0.18	3.36
	BCH-3	78.90	8.79	1.54	0.02	3.25	3.97	0.45	1.49	0.28	0.03	8.97	31.18	0.17	3.28
	BCH-4	74.51	9.69	3.27	0.07	3.92	5.06	0.27	1.06	0.54	0.06	7.69	17.87	0.11	3.90
	BCH-5	82.51	11.60	1.72	0.03	0.39	0.23	0.36	1.56	0.32	0.01	7.12	36.24	0.13	4.37
	BCH-6	78.75	12.46	2.51	0.05	1.04	0.71	0.78	1.73	0.53	0.07	6.32	23.54	0.14	2.20
	GSR-*	90.31	3.55	3.24	0.02	0.06	0.28	0.06	0.64	0.24	0.20	25.44	14.98	0.18	11.23
	UCC	66.6	0.64	15.4	5.04	0.1	2.48	3.59	3.27	2.8	0.15	4.32	24.06	0.18	0.86

Table 8.1 (A) Continue: Table showing major oxides in terms of wt% and their corresponding elemental ratios (where, GSR-4: Chinese Sandstone Standard from Xeujing *et. al.*, 2007 and UCC: Upper continental crust from Rudnick and Gao, 2003, 2005).

Table 8.1(B): Table showing trace elements in terms of ppm with their corresponding elemental ratios (where, GSR-4: Chinese Sandstone Standard from Xeujing *et. al.*, 2007 and UCC: Upper continental crust from Rudnick and Gao, 2003, 2005)

Elements/Ratio	Tipam Sandstone						
	MP7	MP9	MP11	MP16	MP17	MP19	MP-20
Sc	9.44	7.24	7.02	6.35	5.07	7.22	3.58
V	69.71	54.13	55.00	45.96	30.74	50.55	31.56
Cr	66.29	68.23	93.42	80.07	55.54	101.17	53.97
Co	5.83	10.17	11.69	9.15	6.98	9.98	7.54
Ni	23.76	27.92	33.24	31.52	28.88	28.41	28.70
Cu	9.56	9.63	11.95	8.66	9.24	10.96	7.05
Zn	20.05	19.64	26.97	25.62	28.00	31.84	19.69
Ga	12.36	10.45	10.29	8.80	7.043	9.51	6.30
Rb	90.67	68.69	83.39	71.39	58.20	76.56	54.54
Sr	137.58	137.28	107.99	77.26	44.93	88.72	63.14
Y	22.39	20.52	20.88	17.34	16.21	19.31	10.42
Zr	141.31	104.64	112.48	98.81	82.31	101.19	81.88
Nb	13.76	8.79	9.33	8.20	5.45	7.41	4.34
Ba	353.33	301.81	338.72	318.19	266.17	326.87	267.73
Pb	14.71	12.55	16.23	9.99	11.35	13.83	10.11
Th	13.69	19.11	6.68	8.95	5.95	10.33	3.56
U	1.69	2.02	1.37	1.20	0.89	1.37	0.79
Rb/Sr	0.66	0.50	0.77	0.92	1.30	0.86	0.86
Y/Ni	0.94	0.73	0.63	0.55	0.56	0.68	0.36
Co/Th	0.43	0.53	1.75	1.02	1.17	0.97	2.12
Th/Co	2.35	1.88	0.57	0.98	0.85	1.04	0.47
Cr/Th	4.84	3.57	13.98	8.95	9.34	9.79	15.18
Cr/Ni	2.79	2.44	2.81	2.54	1.92	3.56	1.88
Th/Cr	0.21	0.28	0.07	0.11	0.11	0.10	0.07
Zr/Cr	2.13	1.53	1.20	1.23	1.48	1.00	1.52
Th/Sc	1.45	2.64	0.95	1.41	1.17	1.43	0.99
Zr/Sc	14.97	14.45	16.02	15.56	16.25	14.01	22.88
Cr/V	0.95	1.26	1.70	1.74	1.81	2.00	1.71
Cr/Zr	0.47	0.65	0.83	0.81	0.67	1.00	0.66
Th/U	8.09	9.45	4.87	7.44	6.65	7.53	4.49

Table 8.1(B): Table showing trace elements in terms of ppm with their corresponding elemental ratios (where, GSR-4: Chinese Sandstone Standard from Xeujing *et. al.*, 2007 and UCC: Upper continental crust from Rudnick and Gao, 2003, 2005).

Elements/Ratio	Tipam Sandstone						
	MP-21	MP-22	SP-1	SP-2	SP-3	SP-4	SP-6
Sc	6.80	6.34	9.87	6.39	4.85	6.44	14.20
V	43.74	54.87	73.05	58.09	42.40	47.67	88.18
Cr	138.35	108.81	111.92	64.40	57.13	75.65	70.76
Co	8.51	10.36	13.90	8.37	8.38	8.93	15.39
Ni	44.36	37.96	41.15	27.32	28.18	25.60	25.60
Cu	9.11	9.80	21.70	13.99	9.91	10.71	24.79
Zn	25.46	31.70	34.19	28.11	21.51	19.38	26.19
Ga	8.09	10.20	12.52	9.97	7.98	8.62	15.07
Rb	56.51	79.76	89.04	71.14	70.16	60.94	100.88
Sr	78.44	81.05	133.83	123.03	89.16	80.33	92.05
Y	18.53	18.55	22.68	25.53	12.70	17.05	40.01
Zr	99.48	144.99	119.79	89.16	84.10	86.12	154.13
Nb	6.41	9.33	12.91	9.22	6.28	5.83	14.28
Ba	294.06	324.60	339.05	307.83	282.13	259.76	368.63
Pb	11.53	11.37	19.53	16.17	11.98	10.79	24.17
Th	9.18	8.14	14.62	10.12	7.11	7.74	14.72
U	1.15	1.80	1.81	1.48	0.89	1.17	3.26
Rb/Sr	0.72	0.98	0.67	0.58	0.79	0.76	1.10
Y/Ni	0.42	0.49	0.55	0.93	0.45	0.67	1.56
Co/Th	0.93	1.27	0.95	0.83	1.18	1.15	1.05
Th/Co	1.08	0.79	1.05	1.21	0.85	0.87	0.96
Cr/Th	15.07	13.36	7.66	6.37	8.04	9.77	4.81
Cr/Ni	3.12	2.87	2.72	2.36	2.03	2.96	2.76
Th/Cr	0.07	0.07	0.13	0.16	0.12	0.10	0.21
Zr/Cr	0.72	1.33	1.07	1.38	1.47	1.14	2.18
Th/Sc	1.35	1.28	1.48	1.58	1.47	1.20	1.04
Zr/Sc	14.62	22.86	12.13	13.96	17.35	13.38	10.86
Cr/V	3.16	1.98	1.53	1.11	1.35	1.59	0.80
Cr/Zr	1.39	0.75	0.93	0.72	0.68	0.88	0.46
Th/U	7.96	4.52	8.07	6.85	7.95	6.61	4.51

Table 8.1(B): Table showing trace elements in terms of ppm with their corresponding elemental ratios (where, GSR-4: Chinese Sandstone Standard from Xeujing *et. al.*, 2007 and UCC: Upper continental crust from Rudnick and Gao, 2003, 2005).

Elements/ Ratio	Tipam Sandstone						Standard	
	BCH-1	BCH-2	BCH-3	BCH-4	BCH-5	BCH-6	GSR-4	UCC
Sc	7.79	5.72	4.18	11.16	6.69	10.28	4.21	14
V	61.58	43.25	36.09	80.57	46.85	73.23	33.03	97
Cr	46.27	32.06	27.67	93.29	34.62	84.39	20.06	92
Co	7.57	6.40	5.38	6.11	5.88	11.42	6.42	17.3
Ni	21.16	18.68	15.46	18.36	16.82	24.61	16.69	47
Cu	10.15	10.12	8.86	10.52	9.73	14.16	19.10	28
Zn	24.99	18.90	15.36	20.67	27.61	22.84	20.30	67
Ga	11.76	9.62	7.42	12.29	10.49	13.26	5.24	-
Rb	84.31	81.03	61.79	51.80	77.35	92.18	29.08	82
Sr	98.07	85.41	73.45	82.71	80.26	126.59	58.09	320
Y	19.52	15.87	11.76	25.80	17.92	24.74	21.38	21
Zr	109.77	108.33	76.18	115.18	112.79	151.98	213.52	193
Nb	8.72	6.68	5.67	13.74	7.15	15.13	5.86	12
Ba	403.03	372.96	315.26	299.00	380.91	403.75	142.99	628
Pb	14.68	11.19	10.04	10.62	11.77	14.80	7.57	17
Th	14.42	7.01	6.98	29.15	9.08	19.13	7.00	10.5
U	2.05	1.23	1.68	2.58	1.55	2.38	2.08	2.7
Rb/Sr	0.86	0.95	0.84	0.63	0.96	0.73	0.50	0.26
Y/Ni	0.92	0.85	0.76	1.40	1.06	1.00	1.28	0.45
Co/Th	0.52	0.91	0.77	0.21	0.65	0.60	0.92	1.65
Th/Co	1.91	1.10	1.30	4.77	1.54	1.68	1.09	0.61
Cr/Th	3.21	4.57	3.97	3.20	3.81	4.41	2.86	8.76
Cr/Ni	2.19	1.72	1.79	5.08	2.06	3.43	1.20	1.96
Th/Cr	0.31	0.22	0.25	0.31	0.26	0.23	0.35	0.11
Zr/Cr	2.37	3.38	2.75	1.23	3.26	1.80	10.65	2.1
Th/Sc	1.85	1.23	1.67	2.61	1.36	1.86	1.66	0.75
Zr/Sc	14.08	18.92	18.21	10.32	16.86	14.78	50.76	13.79
Cr/V	0.75	0.74	0.77	1.16	0.74	1.15	0.61	0.95
Cr/Zr	0.42	0.30	0.36	0.81	0.31	0.56	0.09	0.48
Th/U	7.04	5.71	4.16	11.31	5.85	8.03	3.36	3.89

Table 8.1(C): Table showing rare earth elements in terms of ppm and their corresponding elemental ratios (where, GSR-4: Chinese Sandstone Standard from Xeujing *et. al.*, 2007 and UCC: Upper continental crust from Rudnick and Gao, 2003, 2005).

Oxides/ Elements	MP-7	MP-9	MP-11	MP-16	MP-17	MP-19	MP-20	MP-21
La	39.402	43.262	30.377	27.160	25.706	30.310	15.174	29.209
Ce	80.967	91.770	61.970	52.029	42.069	61.608	30.717	54.563
Pr	9.743	11.219	7.604	6.658	7.006	7.320	3.702	7.083
Nd	36.026	40.724	28.536	24.389	28.202	27.220	13.948	26.150
Sm	7.242	8.037	5.825	4.731	6.065	5.380	2.922	5.181
Eu	1.202	1.142	1.223	0.960	1.171	1.132	0.714	1.107
Gd	5.293	6.012	4.825	3.903	4.304	4.476	2.474	4.195
Tb	0.862	0.941	0.813	0.656	0.631	0.748	0.423	0.716
Dy	4.414	4.590	4.224	3.454	3.044	3.759	2.098	3.610
Ho	0.830	0.797	0.772	0.629	0.552	0.687	0.377	0.675
Er	2.373	2.084	2.120	1.760	1.503	1.902	1.022	1.834
Tm	0.346	0.291	0.293	0.247	0.204	0.269	0.142	0.256
Yb	2.554	2.056	2.052	1.759	1.404	1.934	0.999	1.815
Lu	0.389	0.310	0.317	0.262	0.215	0.285	0.158	0.274
(La/Yb)N	10.43	14.22	10.00	10.43	12.37	10.59	10.26	10.87
(La/Sm)N	3.42	3.39	3.28	3.61	2.67	3.55	3.27	3.55
(Gd/Yb)N	1.68	2.37	1.91	1.80	2.48	1.88	2.01	1.87
Eu/Eu*	0.57	0.48	0.69	0.66	0.67	0.69	0.79	0.70
(La/Lu)N	10.53	14.47	9.94	10.77	12.42	11.05	9.98	11.06

Table 8.1(C): Table showing rare earth elements in terms of ppm and their corresponding elemental ratios (where, GSR-4: Chinese Sandstone Standard from Xeujing _et. al_., 2007 and UCC: Upper continental crust from Rudnick and Gao, 2003, 2005).

Oxides/ Elements	MP-22	SP-1	SP-2	SP-3	SP-4	SP-6	BCH-1	BCH-2
La	28.514	40.411	41.878	19.080	24.069	43.749	33.555	25.087
Ce	50.316	81.384	83.270	39.288	50.172	90.759	66.608	45.664
Pr	7.017	9.759	9.737	4.856	6.017	11.005	7.777	5.859
Nd	25.978	35.502	34.988	18.157	22.391	41.533	28.376	21.248
Sm	5.069	6.832	6.604	3.788	4.532	9.066	5.329	4.018
Eu	1.059	1.257	1.193	0.809	0.962	2.077	1.163	0.895
Gd	4.135	5.445	5.305	2.979	3.775	8.151	4.398	3.391
Tb	0.693	0.912	0.880	0.482	0.635	1.479	0.753	0.582
Dy	3.573	4.580	4.610	2.470	3.303	7.960	3.926	3.004
Ho	0.669	0.854	0.883	0.452	0.613	1.494	0.731	0.563
Er	1.820	2.344	2.522	1.240	1.737	4.154	2.023	1.593
Tm	0.260	0.332	0.358	0.176	0.246	0.578	0.291	0.228
Yb	1.885	2.379	2.579	1.272	1.764	4.084	2.123	1.651
Lu	0.295	0.351	0.384	0.196	0.263	0.617	0.304	0.245
(La/Yb)N	10.22	11.48	10.97	10.14	9.22	7.24	10.68	10.27
(La/Sm)N	3.54	3.72	3.99	3.17	3.34	3.04	3.96	3.93
(Gd/Yb)N	1.78	1.85	1.67	1.90	1.73	1.62	1.68	1.66
Eu/Eu*	0.69	0.61	0.60	0.71	0.69	0.72	0.71	0.72
(La/Lu)N	10.03	11.95	11.33	10.11	9.50	7.36	11.45	10.63

Table 8.1(C): Table showing rare earth elements in terms of ppm and their corresponding elemental ratios (where, GSR-4: Chinese Sandstone Standard from Xeujing *et. al*., 2007 and UCC: Upper continental crust from Rudnick and Gao, 2003, 2005).

Oxides/ Elements	BCH-3	BCH-4	BCH-5	BCH-6	GSR-4*	UCC
La	20.560	60.953	33.203	49.098	21.00	31
Ce	38.857	132.843	48.989	98.235	48.00	63
Pr	4.861	14.219	7.436	11.679	5.40	7.1
Nd	17.759	50.201	26.703	42.316	21.00	27
Sm	3.371	9.383	4.870	8.019	4.70	4.7
Eu	0.744	1.663	1.023	1.391	1.02	1
Gd	2.761	6.613	3.887	6.151	4.50	4
Tb	0.455	1.044	0.619	0.999	0.79	0.7
Dy	2.316	5.080	3.293	4.981	4.10	3.9
Ho	0.436	0.951	0.632	0.902	0.75	0.83
Er	1.170	2.575	1.760	2.481	2.00	2.3
Tm	0.168	0.371	0.248	0.347	0.32	0.3
Yb	1.229	2.710	1.768	2.462	1.92	2
Lu	0.183	0.398	0.266	0.380	0.30	0.31
(La/Yb)N	11.30	15.20	12.69	13.47	7.39	10.47
(La/Sm)N	3.84	4.09	4.29	3.85	2.81	4.15
(Gd/Yb)N	1.82	1.98	1.78	2.02	1.90	1.62
Eu/Eu*	0.72	0.61	0.70	0.58	0.67	0.69
(La/Lu)N	11.65	15.89	12.94	13.43	7.27	10.38

8.2.1 Major Oxides

The study of major oxides is crucial in order to know the source rocks and tectonic settings occurring at the time of deposition. The concentration of SiO_2 varies between 74.51- 82.52 wt % with an average of 79.23% which is high and show a weakly positive correlation with Al_2O_3 (R:0.06) because of the differentiation of quartz and clay during diagenesis. [Figure 8.1(A)]. Comparing the value of SiO_2 of the studied samples, it is much higher than UCC (Rudnick and Gao, 2003). The concentration of Al_2O_3 varies between 8.02-12.46 wt % with an average of 10.49 wt % which is much lower than the UCC (Rudnick and Gao, 2003, 2005). The low MnO wt % concentration of all the samples reflects low Eu. The low value of Na_2O (Avg: 0.6) can be attributed to a small amount of Na- rich plagioclase; Saeed *et. al.,* (2011) which are also less in the petrographic data (Table 6.1). The ratio of Na_2O/ K_2O (Avg: 0.42) which are very low (Na_2O/ K_2O<1) can also be attributed to the dominance of K-feldspar over Plagioclase which are also consistent with the petrographic observations [Plate 6.2(I)]. Oxides such as K_2O (R: 0.02) and P_2O_5 (R: 0.01) also shows positive correlation while MgO (R: -0.48), CaO (R: -0.5), MnO (R: -0.07), Fe_2O_3 (R: -0.07), Na_2O (R: -0.22) and TiO_2 (R: -0.01) shows a weakly negative correlation with Al_2O_3. Positive correlation of as K_2O and P_2O_5A signifies the presence of these elements in the rock fragments of sandstone and clay minerals. The positive correlation of K_2O indicate the enrichment of clay minerals and also indicate the influence of weathering (Feng and Kerrich, 1990). A moderate positive correlation is shown by TiO_2 Vs Fe_2O_3 (R: 0.77) indicating the presence of Titanium and Iron bearing heavy minerals. Fe_2O_3 show only a weak negative correlation with Al_2O_3 which sometimes occurred due

enrichment of Fe_2O_3 during the process of compaction and cementation of the sediments which is evident by the low concentration of Cr, Ni and V representing the precipitation of Fe in an early diagenetic stage.
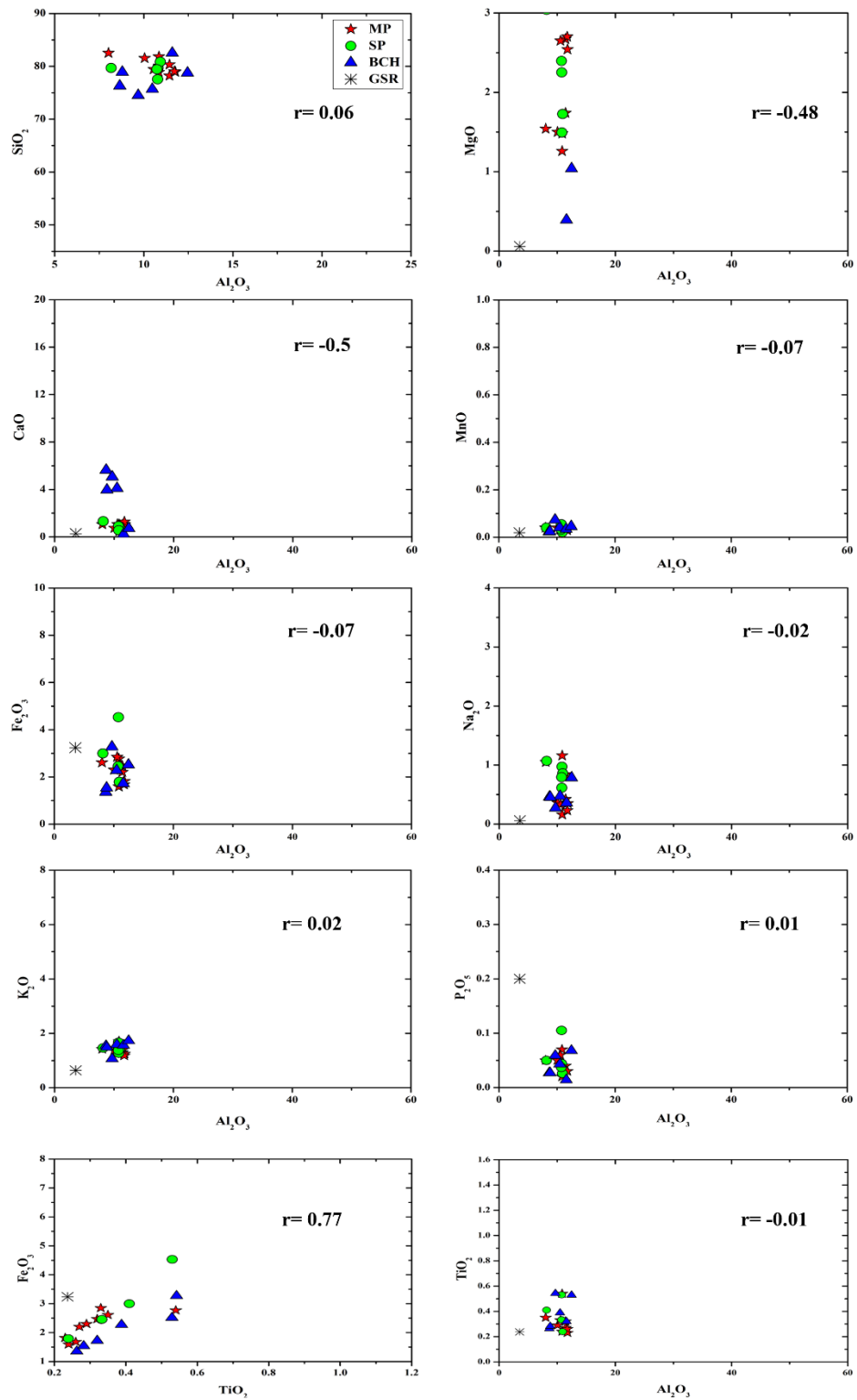
Figure 8.1(A): Correlation between various Major Oxides of Tipam sandstones
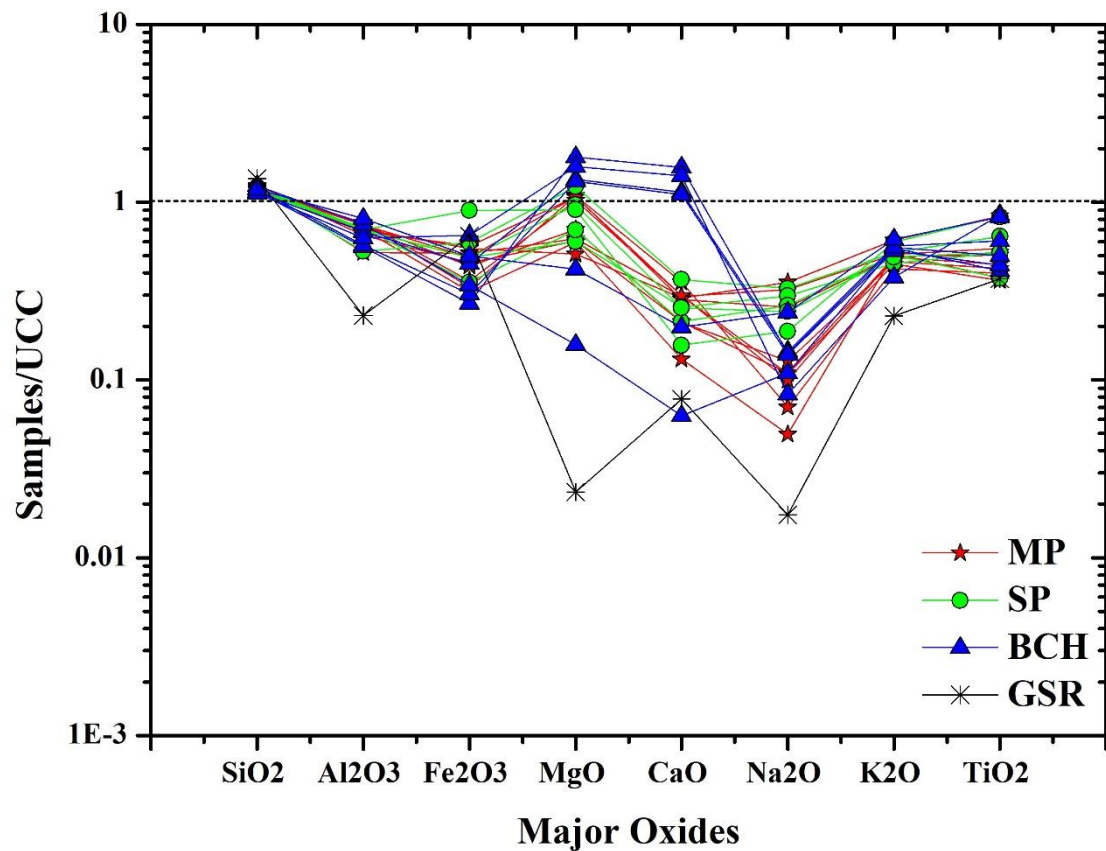
Figure 8.1(B): UCC normalized major elemental spider diagram of Tipam sandstones. (UCC values after Taylor and McLennan, 1993).

8.2.2 Trace Elements

The content of Large ion lithophile elements such as Rb (Avg: 74.02), Sr (Avg: 94.06), Ba Avg:326.2, and U (Avg: 1.62) are much lesser as compared to UCC while Th (Avg: 11.28) is higher than UCC. Rb (r: 0.01) and Zr (r: 0.13) are showing positive correlation with Al_2O_3. The positive correlation and higher concentration of Zr is due to the enrichment of zircon grains which is also supported by the high population of zircon [Average: 8.60; and photomicrograph Plate 7.1 (2a-2f) in heavy mineral analysis]. Sr (r: -0.25), Nb (r: -0.02), V (r: -0.08) and Th (r: 0.25) are showing

a weak negative correlation with Al_2O_3. Sr preserves signature of provenance that is similar to other REE even though not enriched (McLennan, 1989). Negative correlation of Sr with Al_2O_3 and depletion of Cao indicate removal of calcic plagioclase during the process of diagenesis causing less abundance of calcic plagioclase which is even observed in thin section studies. The very weak negative correlation of Nb indicate its decoupling from Zr. [Figure 8.2(A)]. The overall ratio of Zr/Hf ranges from 28.65 to 34.25 suggesting the presence of heavy minerals in the studied Tipam sandstones. Positive correlation between Rb and K_2O suggests the presence of K bearing clay minerals such as kaolinite, illite etc.
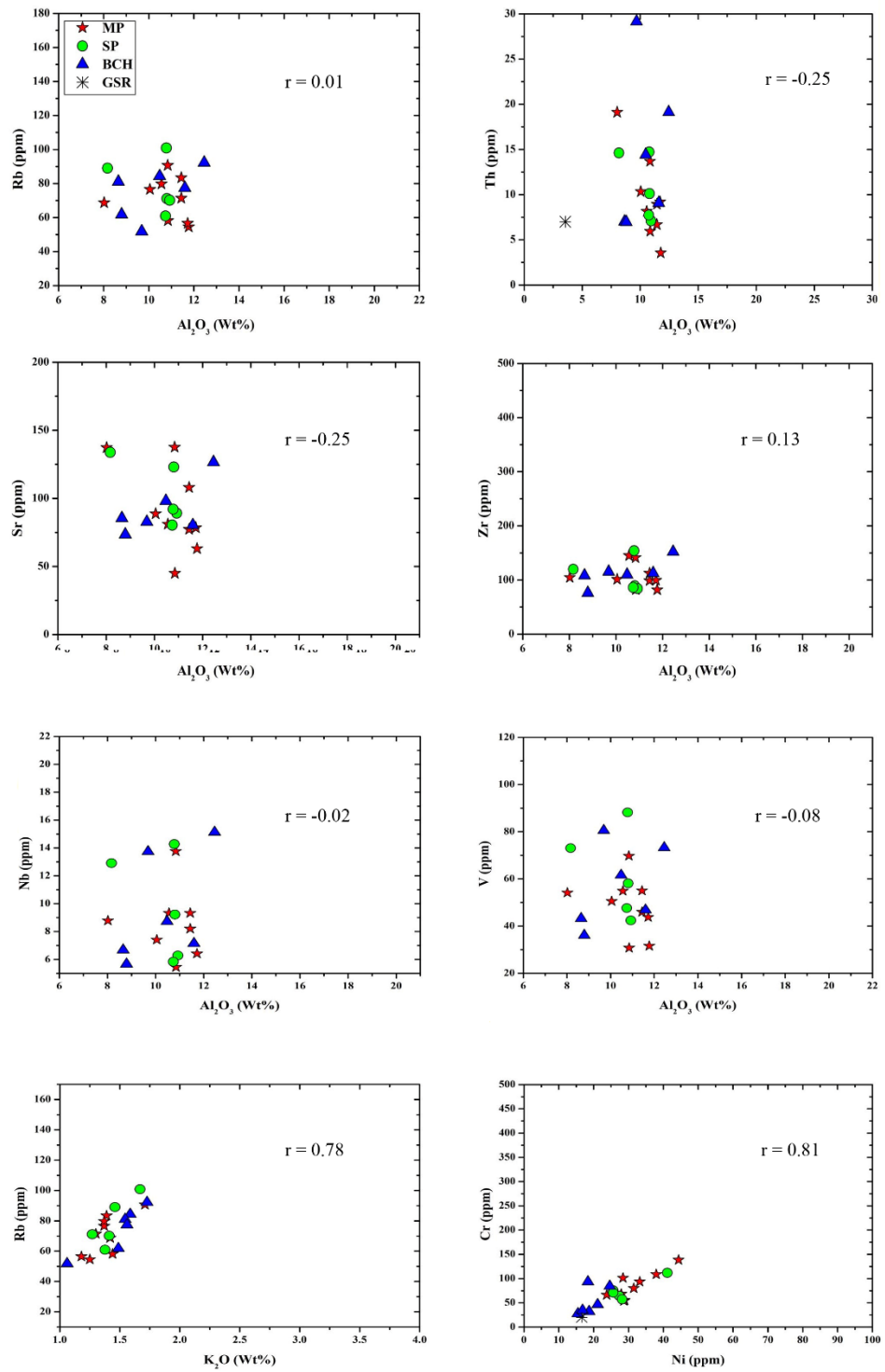
Figure 8.2(A): Correlation of Al₂O₃ w.r.t. various trace elements. (Pearson, 1895)
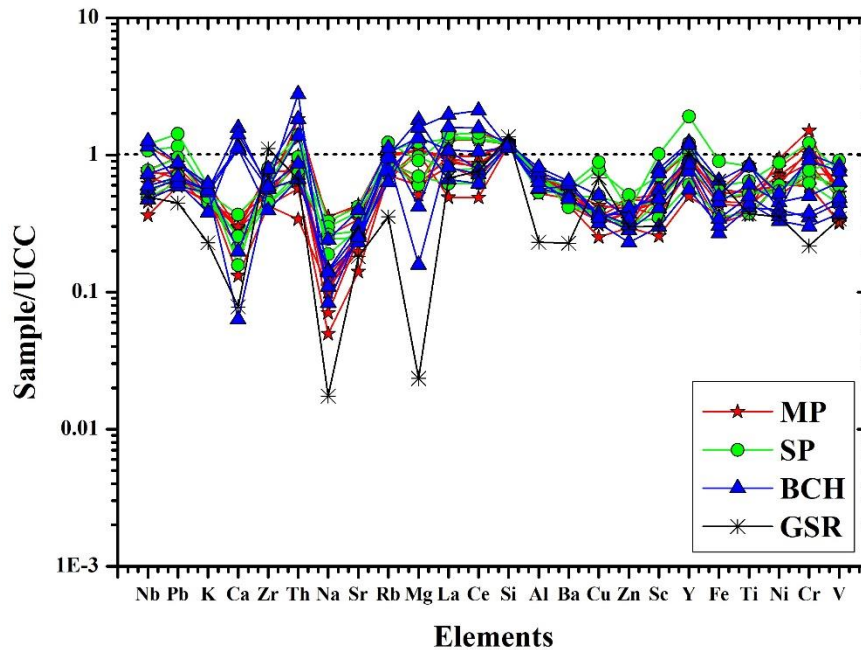
Figure 8.2(B): UCC normalized elemental pattern of Tipam sandstones.

8.2.3 Rare Earth Elements (REE)

The concentration of REE along with some elemental ratios of Tipam sandstones are represented in Table 8.1 (C). Chondrite normalized REE pattern (Figure 8.3) display a very similar pattern to UCC with slight enrichment and depletion as compared to UCC. Plotting of Chondrite normalized average REE of the studied sample represent a relative enrichment of Light Rare Earth elements (LREE: La-Sm); a depleted Heavy Rare Earth Elements (HREE: Gd-Lu). Ratio of $(La/Yb)_N$ (Avg: 10.93) and negative Eu anomalies (Range from 0.48 to 0.79 with an average of 0.67) almost resembling the UCC standard and shows fractionation of Tipam sandstones of the study area. Fractionation of LREE is also shown by $La/Sm)_N$ with an average of 3.54 and high value of ratio of LREE/HREE i.e. $(La/Lu)_N$=(Ranges from 7.27-14.47) also show fractionation of HREE. Furthermore, the high ratio of $(Gd/Yb)_N$ (Ranging

from 1.62 to 2.48 with an average of 1.88) represent a depleting pattern of HREE. The overall features suggest that the original source rock is mainly of fractionated felsic source akin to granite and granitoid (Slack and Stevens, 1994).
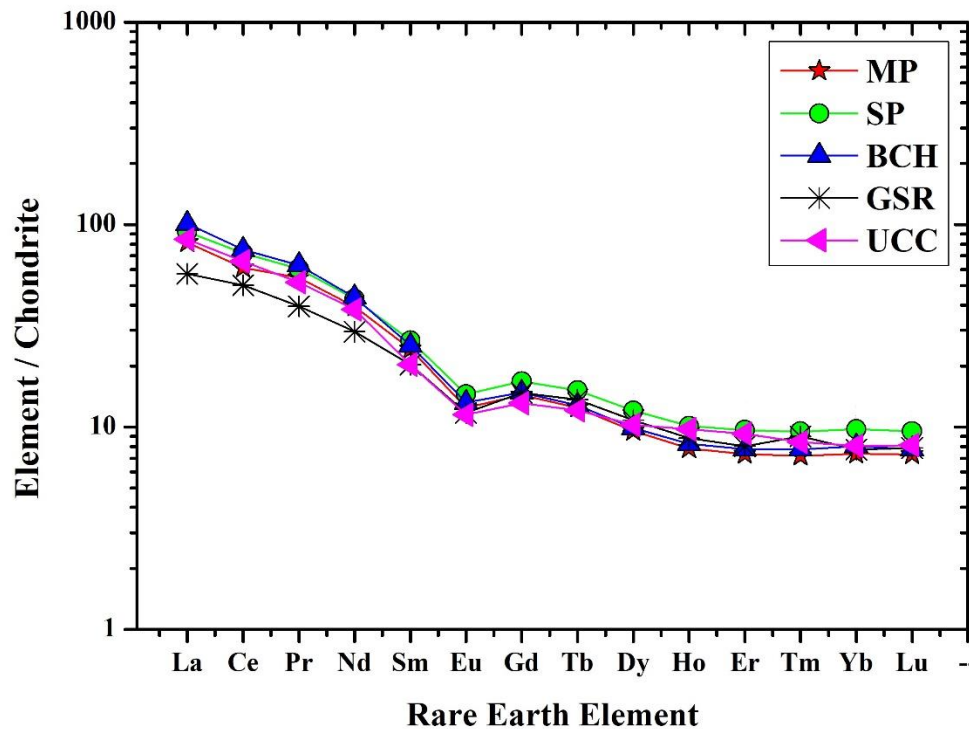
Figure 8.3: Chondrite normalized REE elemental pattern of Tipam sandstones. (Chondrite values after Taylor and McLennan, 1985).

8.3 GEOCHEMICAL CLASSIFICATION

To classify the various types of sandstones, geochemistry is often helpful based on major oxides. Using this major elemental data, geochemical classification of terrigenous sedimentary rocks has been proposed by several workers including Pettijohn *et. al.*, 1972, Blatt *et. al.*, 1980 and Herron, 1988. The logarithmic values of ratio of SiO_2/Al_2O_3 Vs the logarithmic values of ratio Na_2O/K_2O was proposed by

Pettijohn *et. al.*, 1972 as a method of classifying sandstone where majority of the samples falls within the arkose while few samples fall in the field of litharenite. [Figure 8.4(A)]. Herron, 1988 modified the diagram of Pettijohn *et al.*, 1972 and used the log ratio of SiO_2/Al_2O_3 in the x-axis Vs the log ratio of Fe_2O_3/K_2O instead of log ratio of Na_2O/K_2O in the y-axis to classify sandstones into two categories viz Fe rich (Fe-shale and Fe-sandstone) and Fe-poor (shale, wacke, litharenite, sublitjarenite, arkose and subarkose) sandstone. Samples of the study area mostly falls in the field of litharenite while only a few samples fall within arkose of Heron, 1998 [Figure 8.4(C)]. Blatt *et al.*, 1980 classify the sandstones into greywacke, arkose and lithic sandstone using ternary plot w.r.t. the wt% values of Na_2O, (Fe_2O_3+MgO) and K_2O. Most of the samples of Tipam sandstone clustered in the field of lithic sandstone while only three samples fall in the field of arkose as represented in the [Figure 8.4(B)].

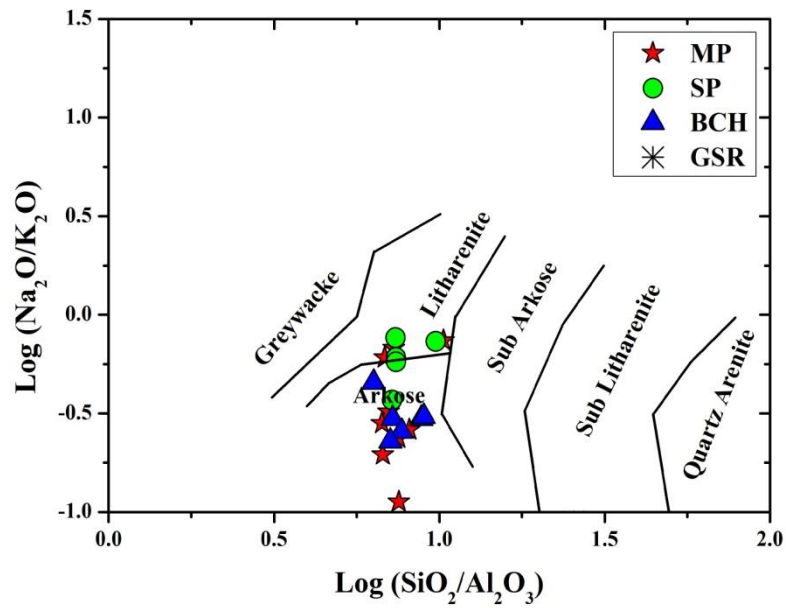**Figure 8.4 (A): Log(SiO$_2$/Al$_2$O$_3$) vs Log(Na$_2$O/K$_2$O) classification scheme of Tipam sandstone after Pettijohn *et. al.*, 1972**
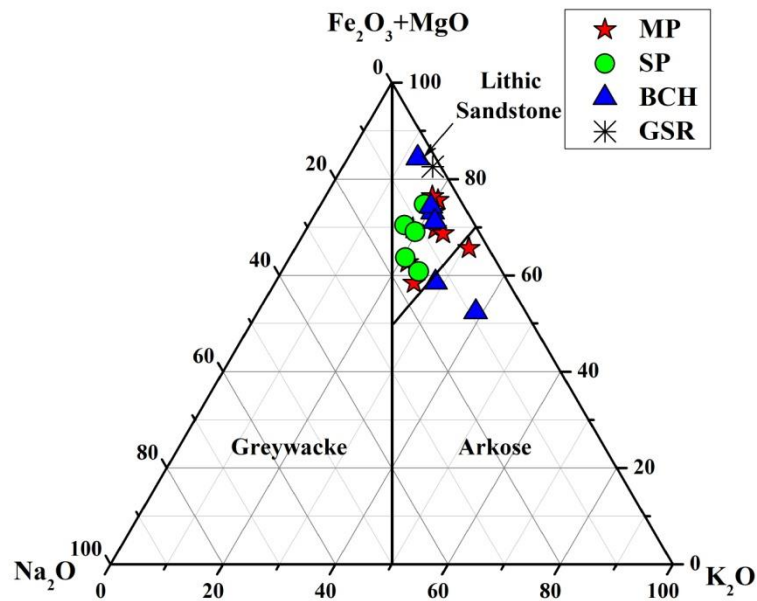
Figure 8.4 (B): Na$_2$O-(Fe$_2$O$_3$+MgO)-K$_2$O ternary plot for sandstone classification after Blatt *et. al.*, 1980.
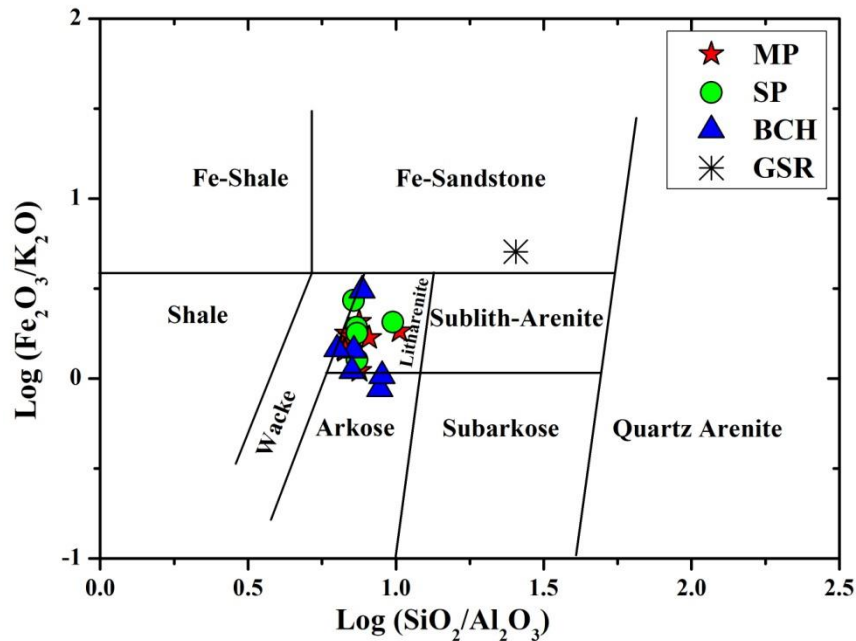
Figure 8.4 (C): Log(SiO₂/Al₂O₃) vs Log(Fe₂O₃/K₂O) classification scheme of Tipam sandstone after Herron, 1998

8.4 GEOCHEMICAL PROVENANCE

Composition of source rock, the nature and kind of dispersal pattern within the depositional basin mainly influenced the composition of clastic sedimentary rocks (Dickinson and Suczek, 1979). In order to identify the nature and type of source rock, geochemistry is widely used and is one of the most accurate tools. The study of trace elements has become an important part in modern petrology since they are more competent in discriminating between petrological processes rather than major elements which also plays an important part for identification of provenance of clastic rocks. Among the trace elements, some trace elements like Cr, Co, Th, Sc, Zr and REE (La- Lu) are callous to the process of sedimentation such as transportation, diagenesis and lithification (Taylor and McLennan, 1985; Bhatia and Crook, 1986; McLennan *et.*

al., 1993). Certain trace elements like Zr, Nb and Y along with REE are conceded to be immobile but unusual during the last stage of diagenesis on permeable clastic rocks of fluvial and Aeolian origin (Hole *et. al*., 1992). In the present study, geochemical plots proposed by Bhatia, (1983), Bracciali *et. al*., (2007), Floyd *et. al.* (1989), Hayashi *et. al*., (1997), Jinliang and Xin, (2008), Schoenborn and Fedo, (2011), Mongelli *et. al*., (2009) and McLennan *et. al*., (1993) are used.

Using the wt % of major oxides CaO, Na_2O and K_2O in ternary plot, Bhatia, 1983 represents the derivation of sediments from various sources where fields are represented using the standard average values of andesite, dacite, granodiorite and granite after Le Maitre, (1976). Plotting of the samples of the study scattered in different region where majority of the samples falls in andesite field suggesting that the sediments have been sourced from andesitic terrain with intermixing of dacite [Figure 8.5(A)].
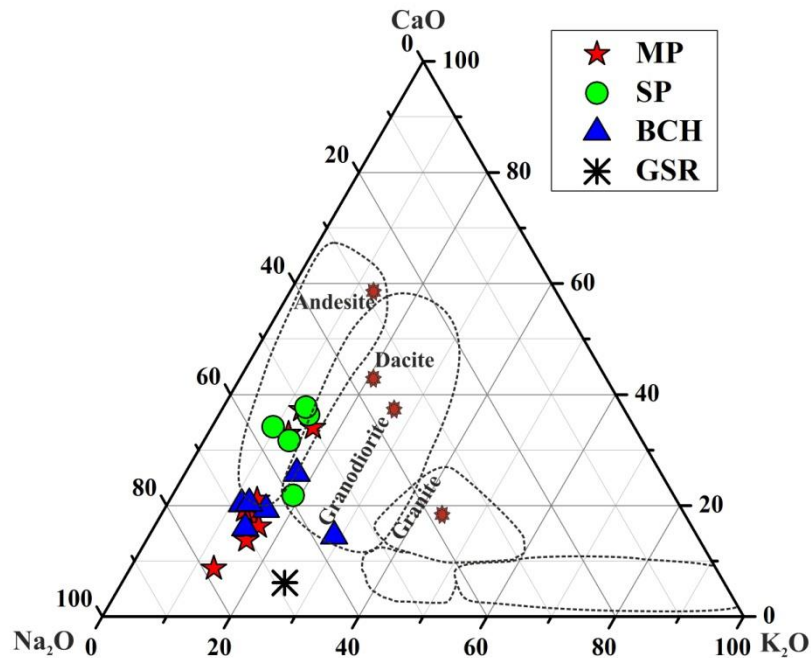
Figure 8.5(A): Na₂O-CaO-K₂O ternary plot after Bhatia, 1983

Ternary plot of V-Ni-Th X 10 after Bracciali *et. al*., (2007) is often used to recognize provenance for clastic sediments due to the immobility nature of trace elements in sedimentation processes. Some trace elements like V and Ni are assembled in the mafic and ultramafic rocks while Th is usually concentrated in felsic rocks. Ternary plot after Bracciali *et. al*., (2007) shows that the Tipam sandstones are rich in Th and on the same time depleted in V and Ni, thus resulting in the concentration of the samples near the field of felsic [Figure 8.5(B)]. Plotting of the samples of the study area using bivariate plot of TiO_2 Vs Ni after Floyd *et. al*., (1989) represents an acidic source [Figure 8.5(C)]. Hayashi *et al*., in 1997 noticed that "the ratio of TiO_2/Zr decreases with the increasing concentration of SiO_2" and suggested that "the ratio of TiO_2/Zr is > ~200 for mafic source, 195-55 for intermediate source and < 55 for felsic source rock for clastic sediments". Based on the ratio of TiO_2/Zr (Hayashi *et. al*., 1997)

the Tipam sandstone of the study area depict felsic source [Figure 8.5(D)]. The ternary plot of La-Th-Sc proposed by Jinliang and Xin, (2008) represent intermixing of source sediments essentially for sandstones by intermixing between Granite (with Eu/Eu*: 0.5 and Th/Sc: 1.18) and Granodiorite (with Eu/Eu*: 0.7 and Th/Sc: 0.5). Due to enrichment of La, plotting of the Tipam sandstones (average Eu/Eu*: 0.67 and average Th/Sc: 1.58) clustered near the granitic field as represented in [Figure 8.5(E)].
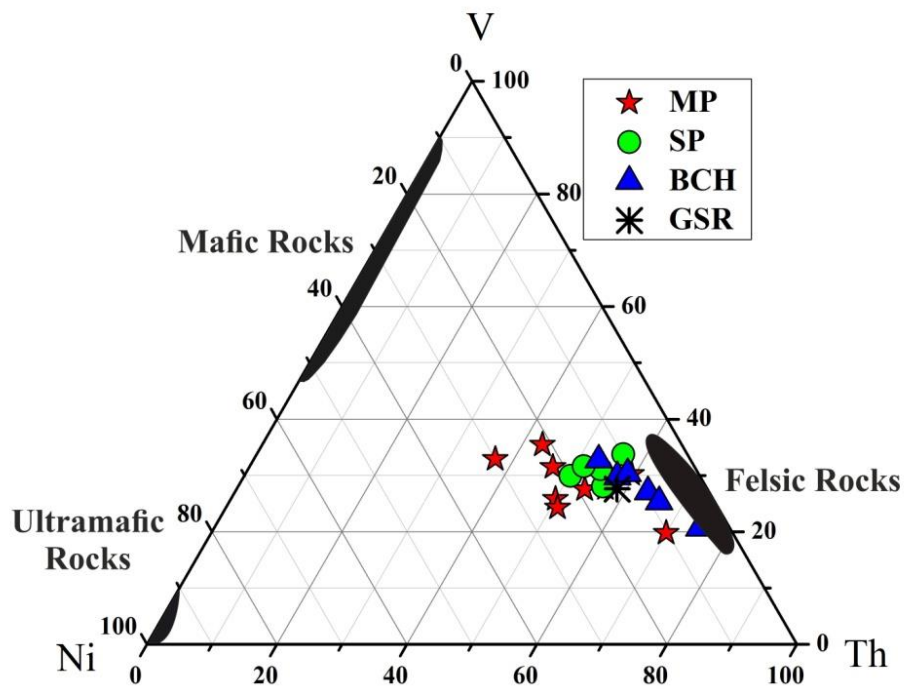
Figure 8.5(B): Provenance plot of V-Ni-Th X 10 after Bracciali *et. al*., (2007).
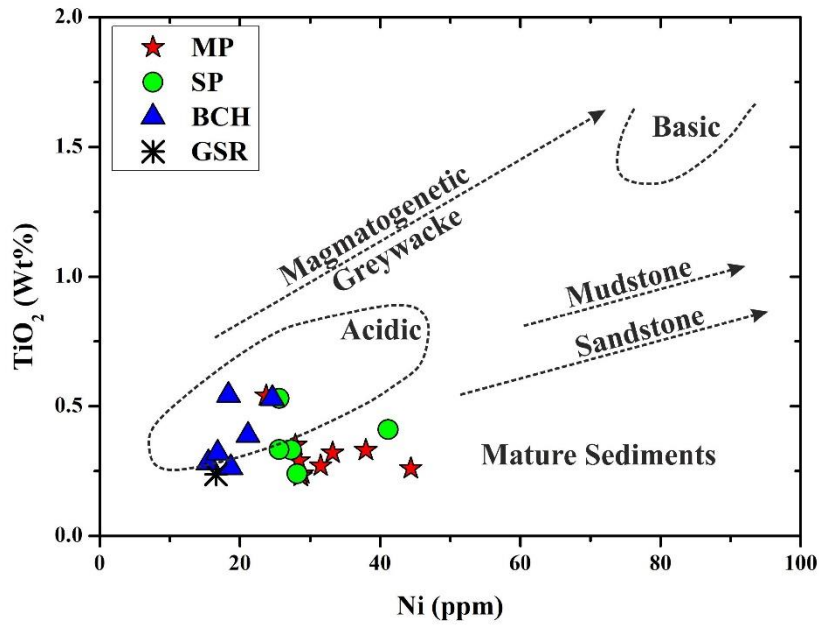
Figure 8.5(C): Provenance plot of Ni Vs Tio$_2$ after Floyd *et. al*., (1989).
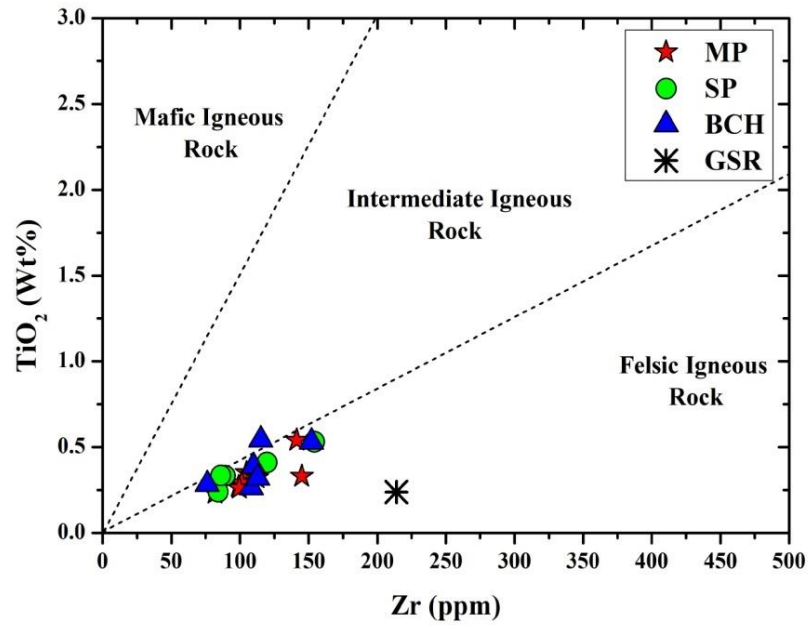
Figure 8.5(D).: Zr Vs Tio2 bivariate provenance plot after Hayashi *et. al*., (1997).
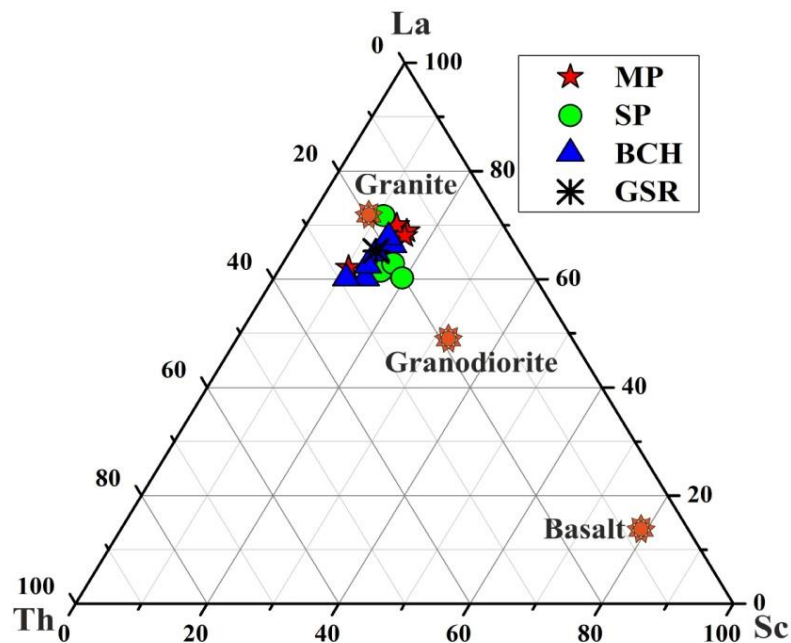
Figure 8.5(E): Ternary provenance plot of La-Th-Sc after Jinliang and Xin, (2008).

The quantitative estimation of source rock can also be ruled out using binary plot of Sc vs Th/Sc after Schoenborn and Fedo, 2011. The provenance plot of Sc vs Th/Sc (Schoenborn and Fedo, 2011) is represented in the [Figure 8.5(F)] where majority of the studied samples of Tipam sandstones are clustered near 90% Granodiorite+10% high K-Granite field which is a suggestive of the input of intermixing of granodioritic and granitic source rocks which is also supported by presence of higher K-feldspar than plagioclase feldspar in thin section study [Plate 6.2 (I)].
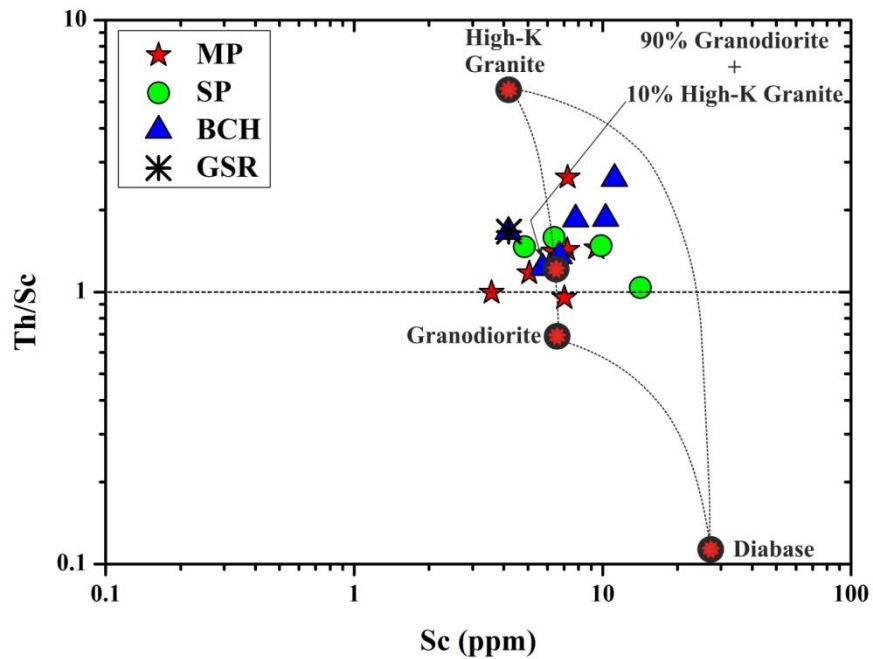
Figure 8.5(F): Sc vs Th/Sc plot for Bhuban Sandstones representing mixing of source rocks after Schoenborn & Fedo, (2011).

Using the ratios of Y/Ni vs Cr/V, Mongelli *et. al*., (2006) put forward a binary mixing model curve between granite and ultramafic end-members in order to represent a mixing of source rocks. The lower ratio of Cr/V (avg. 1.4) represents a probable derivation of source rocks from granitic terrain with few handouts from the ultramafic sources. Samples from Buhchang section of Tipam sandstone represents lower Cr/V ratio than samples of Meidum, accordingly are plotted more towards the granitic field [Figure 8.5(G)].
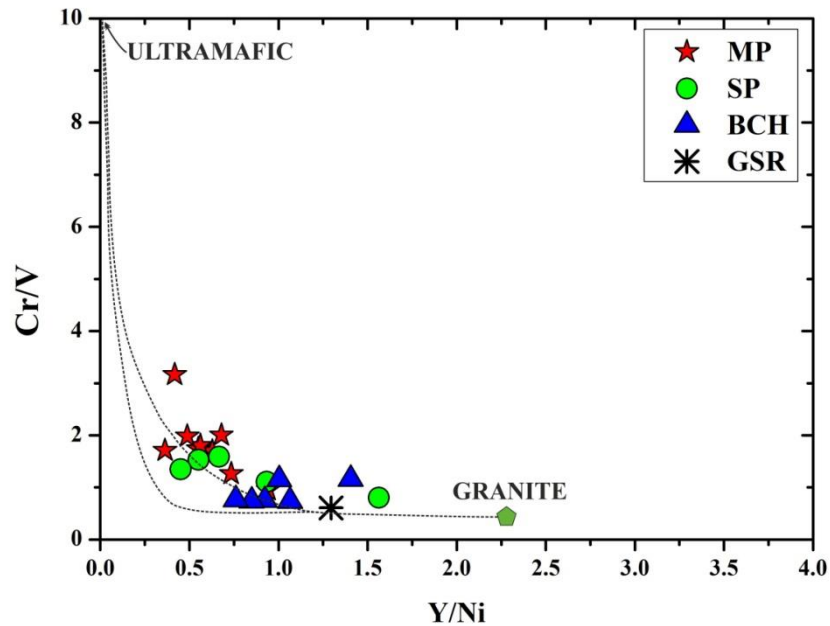
Figure 8.5(G): Binary plot of Y/Ni Vs Cr/v for Granite-Ultramafic end member mixing after Mongelli et al., (2006).

Bivariant plot of ratios of trace elements i.e. Zr/Sc vs Th/Sc proposed by McLennan *et. al*., (1993) [Figure 8.5(H)] constitute two patterns regarding the composition of source rock and effects on source due to sedimentation processes in which the straight trend represents composition of the original source rocks and the effect of sedimentation processes is represented by the diversion trend. Plotting of the samples all follow the straight trend following the original composition of the source rock i.e. a trend compatible with igneous differentiation (provenance) but near the diversion trend thus representing the original source composition. Medium concentration of Zr in Tipam sandstone (avg. 108.73) is mainly due to the leaching of the mobile alkali element and enrichment of immobile Zr during sedimentation. Besides, the concentration of detrital zircon from heavy mineral analysis is also high

and stood next to tourmaline in ZTR percentage which indicates a few recycled source provenance.
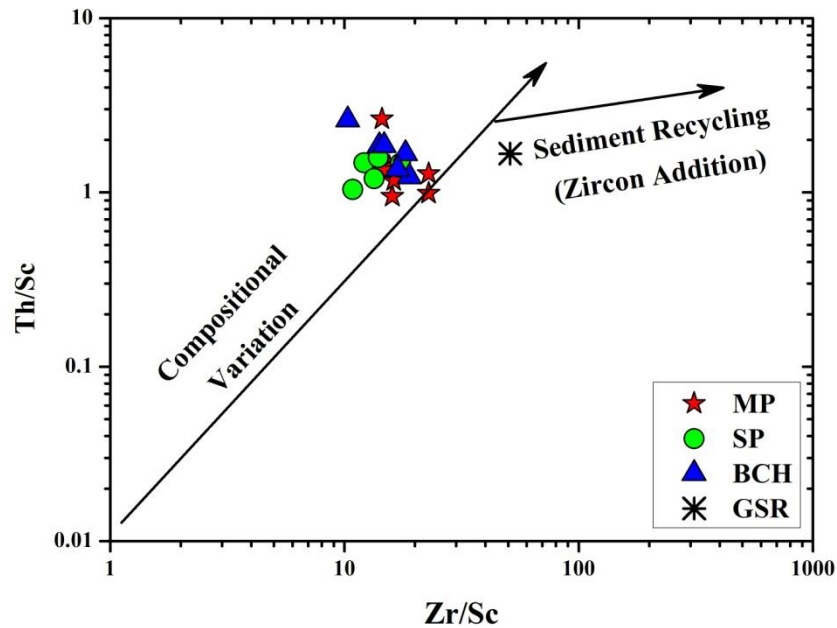
Figure 8.5(H): Zr/Sc vs Th/Sc binary plot after McLennan et al., 1993.

In order to predict provenance of clastic sedimentary rocks, certain trace and REE ratios are advantageous since trace and rare earth elements in most cases are insensitive to the process of sedimentation. Cullers, (1994, 2000) and Cullers and Podkovyrov, (2002) put forward the standard values of certain elemental ratios of trace and rare earth elements as presented in the Table 8.2. The ranges of elemental ratios of Tipam sandstone are: (La/Lu: 7.27-15.89, La/Sc: 7.27-15.89, La/Co: 2.01-9.97, Th/Sc: 0.95-2.64, Th/Co: 0.57-4.77 and Cr/Th: 2.86-15.18), which represents the contribution of sediments basically from felsic source rocks. Furthermore,

incompatible ferromagnesian trace elements such as Sc, Cr, Ni and V are considerably

low to moderate indicating the felsic source.

Table 8.2: Table showing certain Trace and REE elemental ratios representing provenance; where, Felsic & Mafic sources: Cullers, (1994, 2000); Cullers & Podkovyrov, (2000); UCC: Upper continental crust after Rudnick and Gao, (2003, 2005)

Elemental Ratio	Range of Tipam Sandstone	Felsic Sources	Mafic Sources	UCC
Eu/Eu*	0.48-0.79	0.32-0.83	0.70-1.02	0.69
La/Lu	7.27-15.89	3.00-27.0	1.10-7.00	10.38
La/Sc	3.08-6.56	0.70-27.7	0.40-1.1	2.21
La/Co	2.01-9.97	1.4-22.4	0.14-0.38	1.79
Th/Sc	0.95-2.64	0.64-18.1	0.05-0.4	0.75
Th/Co	0.57-4.77	0.30-7.5	0.04-1.40	0.6
Cr/Th	2.86-15.18	4.00-15.0	25-500	8.76

Chondrite-normalized REE patterns and Eu anomaly gives additional

information in order to conclude the nature and types of source rock (Basu *et. al*., 1975;

Armstrong-Altrin, 2009). Higher LREE/HREE ratio with negative Eu anomalies are

shown by felsic rock (Cullers, 1994, 2000), while lower LREE/HREE ratios are shown

by mafic rocks. Plotting of Chondrite-normalized REE (Figure 8.3) shows that the

concentration of LREE is much higher as compared to HREE. The higher ratio of

LREE/HREE indicates the derivation of sediments of Tipam sandstone from

granitoids. The ratio of $(La/Lu)_N$:7.27-15.89 indicate fractionation of source rock

which results in the higher concentration of K. Negative Eu anomaly delineate a post

Archean source which is supported by the enrichment of potassium. Fractionation of

Ca-rich plagioclase of source rocks results in the negativity of Eu which is obviously

shown by the less concentration of Sr (avg: 94.06).

Based on the above plotting and consideration it can be inferred that the sediments of Tipam sandstones were primarily derived from the uplifted and eroded Himalayan felsic terrain with input from neighboring orogen such as Indo-Burmese Range.

8.5 WEATHERING AND PALEOCLIMATIC CONDITIONS

The extent of chemical weathering may be imprinted in the record of sedimentary rock (Nesbit and Young, 1982), which act as a powerful tool for examining the condition of source area weathering. The varying degree of weathering in the source area results in the diversification and content of alkali and alkaline earth elements of terrigenous rocks. Weathering indices are very helpful for evaluating the paleoclimatic conditions occurring during the time of deposition of sediments. Of the number of geochemical weathering indices proposed by many workers, the most widely used chemical index by using major element concentrations in order to measure the potency of source area weathering are Weathering Index of Parker (WIP; Parker, 1970), Chemical Index of Alteration (CIA; Nesbitt and Young, 1982), Plagioclase Index of Alteration (PIA; Fedo *et. al*., 1995), Chemical Index of Weathering (CIW; Harnois, 1988), Index of Chemical Variability (ICV; Cox *et. al*., 1995) with their mathematical derivations are as under: (where, CaO* indicates Ca incorporated from the silicate bearing minerals; # indicates by using Molecular Proportions and ^ indicates by using Weight Percentage)

$$\textbf{CIA}^{\#} = \left[\frac{\text{Al}_2\text{O}_3}{\text{Al}_2\text{O}_3 + \text{CaO}^* + \text{Na}_2\text{O} + \text{K}_2\text{O}}\right] \times 100$$

$$\textbf{PIA}^{\#} = \left[\frac{\text{Al}_2\text{O}_3 - \text{K}_2\text{O}}{\text{Al}_2\text{O}_3 + \text{CaO}^* + \text{Na}_2\text{O} - \text{K}_2\text{O}}\right] \times 100$$

$$\textbf{CIW}^{\#} = \left[\frac{\text{Al}_2\text{O}_3}{\text{Al}_2\text{O}_3 + \text{CaO}^* + \text{Na}_2\text{O}}\right] \times 100$$

$$\textbf{WIP}^{\#} = \left[\left\{2\frac{\text{Na}_2\text{O}}{0.35}\right\} + \left\{\frac{\text{MgO}}{0.9}\right\} + \left\{2\frac{\text{K}_2\text{O}}{0.25}\right\} + \left\{\frac{\text{CaO}^*}{0.7}\right\}\right] \times 100$$

$$\textbf{ICV}^{\wedge} = \left[\frac{\text{Fe}_2\text{O}_3 + \text{K}_2\text{O} + \text{Na}_2\text{O} + \text{CaO}^* + \text{MgO} + \text{MnO} + \text{TiO}_2}{\text{Al}_2\text{O}_3}\right]$$

Table 8.3: Geochemical weathering parameters of Tipam Sandstones (where, CIA: Chemical Index of Alteration after Nesbitt and Young, 1982; PIA: Plagioclase Index of Alteration after Fedo *et. al.*, 1995; CIW: Chemical Index of Weathering after Harnois, 1988; WIP: Weathering Index of Parker after Parker, 1970; ICV: Index of Chemical Variability after Cox *et. al.*, 1995; where, GSR-4: Chinese Sandstone Standard from Xeujing *et. al.*, 2007 and UCC: Upper continental crust after Rudnick and Gao, 2003, 2005)

Litho-Unit	Sample	CIA	PIA	CIW	WIP	ICV
Tipam Sandstones	MP-7	65.75	70.31	74.06	31.33	0.79
	MP-9	60.65	63.89	68.66	28.75	1.01
	MP-11	70.72	75.45	77.96	29.48	0.76
	MP-16	76.74	82.94	84.72	21.59	0.59
	MP-17	80.21	89.24	90.64	18.98	0.5
	MP-19	74.41	81.28	83.59	21.02	0.66
	MP-20	75.21	80.49	82.34	23.61	0.62
	MP-21	74.69	79.48	81.3	22.81	0.63
	MP-22	72.69	78.53	80.98	24.71	0.82
	SP-1	58.76	61.34	66.3	33.99	1.26
	SP-2	69.9	74.21	76.73	26.22	0.69
	SP-3	71.64	77.06	79.61	26.6	0.62
	SP-4	70.67	75.71	78.35	27.95	0.77
	SP-6	73.72	81.51	84.12	27.48	0.95
	BCH-1	51.34	51.61	56.05	37.4	1.16
	BCH-2	40.56	38.8	44.01	44	1.59
	BCH-3	47.87	47.42	52.47	35.9	1.25
	BCH-4	47.31	46.97	50.12	35.21	1.47
	BCH-5	81.19	90.85	92.07	18.2	0.4
	BCH-6	73.68	80.4	82.84	26.57	0.59
	Average	**66.89**	**71.37**	**74.35**	**28.09**	**0.86**
Standard	GSR-4	73.26	82.58	85.48	6.83	1.28
	UCC	50.17	50.22	55.81	69.91	1.19

Tipam sandstones shows a moderate value of Chemical Index of Alteration (Avg: 66.89) which is a bit higher than UCC (50.17) which generally represents low to moderate degree of weathering of source rock. Moreover, moderate values of CIA together with negative Eu anomaly also indicates some contribution of juvenile sediments from local/near sources with moderate to higher rate of mechanical weathering and short transportation, poor sorting, rapid sedimentation and exhibits less amount of alkali bearing minerals (Camiré *et. al.,* 1993). Based on the CIA value, sediments of the study area were derived from Himalayan ranges and transported by paleo-Brahmaputra with a minor contribution from Indo Burmese Arc etc [(Najman and Garzanti, 2000 and Bracciali *et. al.*, 2015) (Govind *et al.*, 2018)]. The ternary plot of CIA using wt% of Al_2O_3-(CaO+Na_2O)-K_2O after Nesbitt and Young., 1982 is given in [Figure 8.6(A)]. In the ternary plot of CIA, the samples are following a parallel trend of the A-CN line near the feldspar join (CIA Avg: 66.89) indicating the beginning of chemical weathering (Feedo *et. al.*, 1995) suggesting that weathering effect has not yet reached to the removal stage of alkali and alkaline earth elements from clay minerals (Taylor and Mc Lennan, 1985) suggesting the breakdown of plagioclase. On conditions of intense weathering, CaO and Na_2O completely leaches which can avert the trend towards the A-K line revealing enrichment of K. Total removal of K will happen under extreme weathering and the trend will redirect to Al_2O_3 apex. Metasomatism of K also reflects the concentration of K, which involves the removal of K. At the same time, K-rich pore fluids may also add potassium. K-Addition of K will head the trend towards the K apex. In some case conversion of plagioclase into K-feldspar or to clay minerals might occur due to enrichment of K by the process of metasomatism (Fedo *et. al.*, 1995).
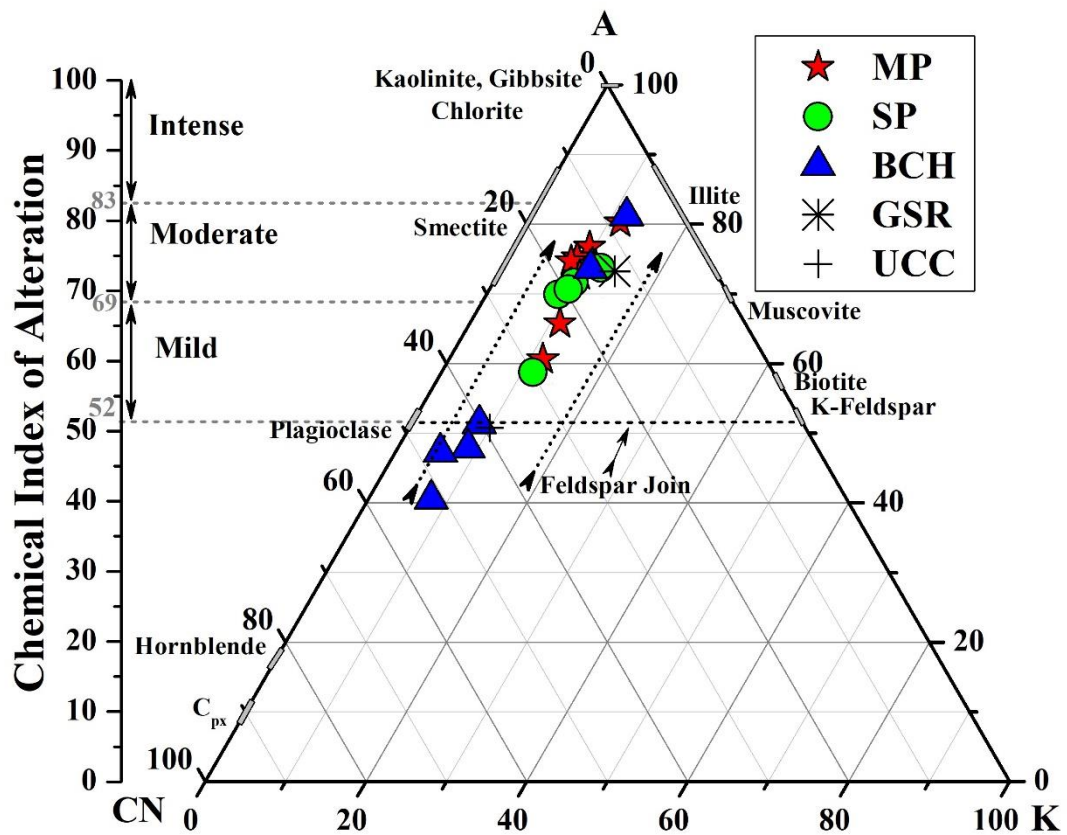
Figure 8.6(A): A-CN-K plot after Nesbitt & Young, (1983) for Tipam Sandstone.

CIA, which is considered as one of the most important indexes for measuring the nature and degree of weathering, it does have a major drawback since remobilization of K occurs during the process of sedimentation and metamorphism. To overcome such problem, Chemical Index of Weathering (CIW; Harnois, 1988) is commonly used in which wt% of alkalis are employed excluding K_2O in order to avoid metasomatism. Since K^+ ion is related with pore solution and higher exchange capacity, it can form K-bearing clay minerals instead of Na^+ and Ca^+ during the process of sedimentation (Harnois, 1988). The Tipam sandstones of the study area shows moderate to high (Avg: 74.35) nature of weathering (Table 8.3) which is much higher than UCC.

Fedo *et. al*., in 1995 proposed another weathering index for Plagioclase by using the wt% of alkalis in order to put forth the extent of source rock weathering known as Plagioclase Index of Weathering (PIA). Totally weathered products like kaolinite, gibbsite etc will show a maximum PIA value i.e. 100 and un-weathered plagioclase will show PIA value of 50. The Sandstones of Tipam are showing moderate average value of PIA (Range: 38.8 to 90.85, Avg: 71.37) which is higher than UCC (50.22) thus showing a moderate weathering of plagioclase.
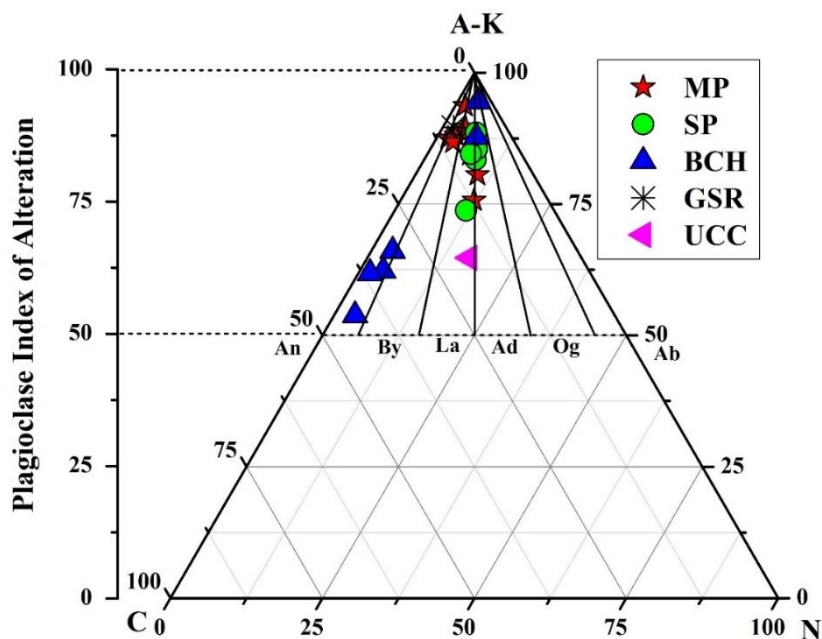
Figure 8.6(B): AK-C-N plot for Tipam Sandstones after Fedo *et. al*., (1995).

The first chemical weathering index by using alkali and alkaline elements was introduced by Parker, (1970) which is known as Parker Index or Weathering Index of Parker (WIP). It is mainly based on the proportion of mobile alkali and alkaline earth elements such as sodium, magnesium, potassium and calcium present in a rock. WIP also consider individual mobilities of Na, K, Ca and Mg based on their bond strength with oxygen. Most of the alkali and alkaline elements are removed during the

process of hydrolysis and Si serve as mobile elements during weathering nevertheless with irregular movement within the profile resulting in less amount of leaching. Hence, mobile elements like Na, Mg, K and Ca served as the base to represent the weathering index (Parker, 1970). The studied Tipam Sandstones are showing high WIP value (Avg: 71.37) indicating immense weathered source rocks.

Based on the proportion of Al_2O_3 for discrimination between clay and non-clay minerals, an important geochemical parameter known as Index of Chemical Variability (ICV) is commonly used which measures the richness of alumina (Cox *et. al.*, 1995). A lower proportion of Al_2O_3 is found in the non-clay minerals. As a consequence, the value of ICV is increasing meaning the non-clay minerals have a high CIV. According to Cox *et. al.*, (1995), "the range of ICV is between 0.6-1.0 for feldspars, illite and muscovite while K_2O/Al_2O_3 ranges between 0-0.3 for clay minerals and 0.3-1.0 for feldspars". Tipam sandstones of the study area are showing an average of ICV= 0.89 and K_2O/Al_2O_3= 0.16 indicating immature in nature and may be derived from tectonically active settings. Thin section studies in addition reveal evidences about the less occurrence of feldspars, muscovite and glauconite [Table 6.2]. The CIA vs ICV proposed by Long et al., (2012) expresses the maturity and the nature of weathering of clastic sedimentary rocks. From the plotting [Figure 8.6(C)], majority of the samples have the ICV value ~1 with average CIA (Avg: 66.89) and can be said that the sediments are mostly chemically mature, with moderate to intense weathering and of recycled nature with bit amount of weathered product of Kaolinite, smectite, illite etc. Only a few samples fall in the region of immature with weak weathering.
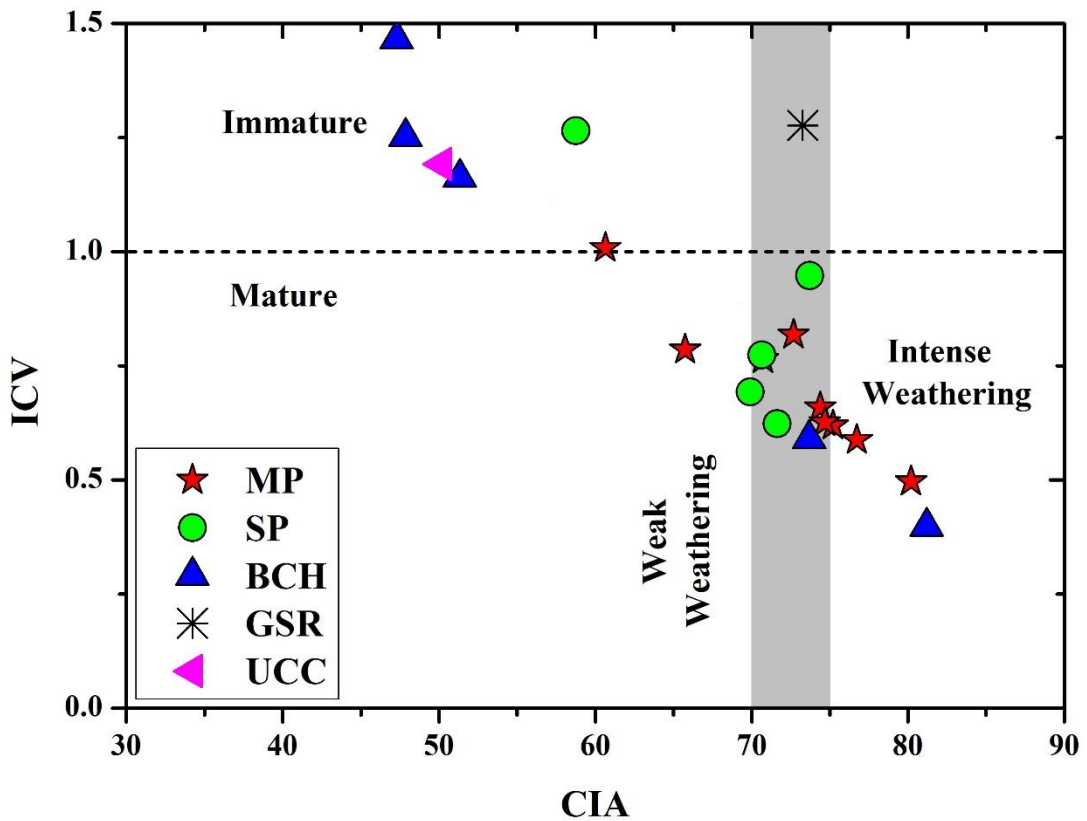
Figure 8.6(C): Binary plot of CIA vs ICV after Long *et. al*., (2012) of Tipam Sandstones.

The extent of weathering behaviour of the sediments can also be represented using the binary plot of Th vs Th/U after McLennan *et. al*., 1993. The value of the ratio of Th/U in the upper crustal rock is between 3.5-4.0 and exceeding the range serve as the weathering trend (McLennan *et. al*., 1993). The Tipam sandstones are showing an average value of Th/U=6.85 which is higher than the value of Th/U in the upper crust and all the plotting falls beyond upper crust region representing moderate to intense weathering.

Higher ratio of Rb/Sr indicate intense weathering of rocks since Sr further leaches more with respect to Rb during the process of diagenesis and weathering. The average value of Rb/Sr of the studied Tipam sandstone is 0.82 which is higher than UCC. The ratios of (Th/U) and (Rb/Sr) indicates moderate nature of weathering of the source rock.
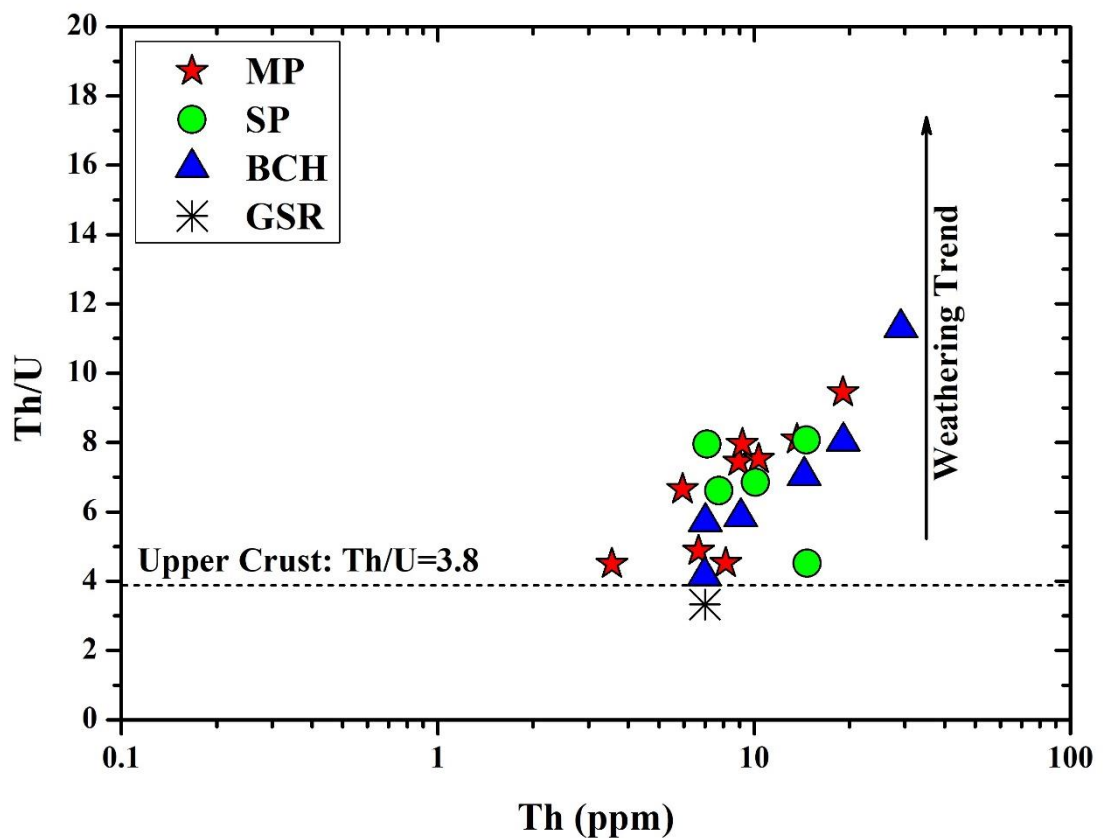
Figure 8.6(D): Th vs Th/U plot after McLennan *et. al*, (1993) of Tipam sandstones.

Based on the studies of various weathering indices employing geochemical data, it is observed that certain major oxides are removed, predominantly CaO which are followed by Na_2O, MgO and K_2O respectively which is also observed by the less

existance of feldspars from thin section study. Certain elemental ratios like Th/U, Rb/Sr etc also show similar interpretation. Hence it can be concluded that before the deposition took place the source of sediments of the studied Tipam sandstones have undergone moderate to intense nature of weathering.

8.6 TECTONIC SETTINGS

During the last few decades many workers such as Bhatia, (1983); (1985); Bhatia and Crook, (1986); Taylor and McLennan, (1985); Roser and Korsch, (1986); McLennan *et. al*., (1990); McLennan and Taylor, (1991) have proposed a number of schemes which is mainly based on the geochemical composition of clastic sediments for recognition of ancient tectonic settings. A commonly used major elemental discrimination plotting which are employed in the present study included viz. (Fe_2O_3+MgO) vs Al_2O_3/SiO_2 (Bhatia, 1983), (Fe_2O_3+MgO) vs K_2O/Na_2O (Bhatia, 1983), and discrimination diagram of immobile trace element have also been used such as La/Sc vs Ti/Zr after Bhatia and Crook, (1986), La-Th-Sc ternary plot after Bhatia and Crook, (1986). The binary plots of discriminant function [DF-1:$(-0.0447xSiO_2)$-$(0.972xTiO_2)$+$(0.008xAl_2O_3)$-$(0.267xFe_2O_3)$+$(0.208xFeO)$-$3.082xMnO)$+$(0.14xMgO)$+$(0.195xCaO)$+$(0.719xNa_2O)$-$(0.032xK_2O)$+$(7.51xP_2O_5)$+0.303 & DF-2:$(-0.421xSiO_2)$+$(1.988xTiO_2)$-$(0.526xAl_2O_3)$-$(0.551xFe_2O_3)$-$(1.61xFeO)$+$(2.72xMnO)$+$(0.881xMgO)$-$(0.907xCaO)$-$(0.177xNa_2O)$-$(1.84xK_2O)$+$(7.244xP_2O_5)$+43.57] after Bhatia., (1983) is also employed in the present study.

For sandstone deposited in continental margin area, Bhatia and Crook, (1986) suggested that the ratio of La/Sc to be 4 such that the samples are plotted near

the La apex in the ternary plot of La-Th-Sc. The average ratio of La/Sc of the studied Tipam sandstones is 4.81 which is almost similar to the La/Sc ratio suggested by Bhatia and Crook, (1986) for samples of continental margins. Plotting of the samples in the ternary plot of La-Th-Sc clustered in the fields of active continental margin (ACM) and continental island arc (CIA) [Figure 8.7(A)]. "Sandstone deposited in active continental margin are showing lower values of Al_2O_3/SiO_2 (0.1-0.2), lower Fe_2O_3+MgO (2-5 %) and higher K_2O/Na_2O ($\approx$1) in which sediments are mostly derived from felsic source such as Granite, Gneiss (Bhatia., 1983)". Tipam sandstones are showing Al_2O_3/SiO_2 (Avg: 0.13), Fe_2O_3+MgO (Avg: 4.63) and K_2O/Na_2O (Avg: 4.32) which are almost similar to the values suggested by Bhatia, (1983). Plotting of the samples in the binary discrimination diagram of (Fe_2O_3+MgO) vs Al_2O_3/SiO_2 (Bhatia, 1983) [Figure 8.7(B)] and (Fe_2O_3+MgO) vs TiO_2 (Bhatia, 1983) [Figure 8.7(C)], majority of the samples fall in active continental margin and few samples clustered near active continental margins and passive continental margins.

Plotting of the samples in bivariant plot of La/Sc vs Ti/Zr (Bhatia and Crook, 1986) shows that majority of the samples of Tipam sandstones clustered in the field of active Continental margins and only a few samples clustered near the ACM field [Figure 8.7(D)]. Moreover, plotting of the studied samples in the binary plot of discrimination function (Bhatia, 1983) also shows that majority of the samples fall in the field of active continental margin with only a few samples in the field of passive margin. Based on the geochemistry together with petrography, it can be inferred that the sediments of the Tipam sandstones falls under active continental margin and recycled orogen setup.
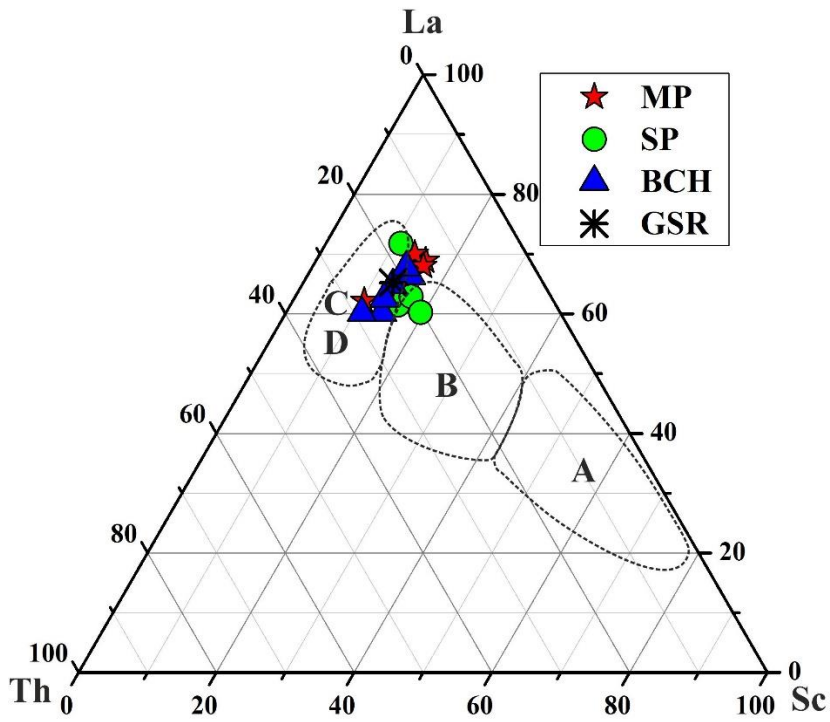
Figure 8.7(A): Ternary plot of La-Th-Sc for tectonic settings (After Bhatia,1983)
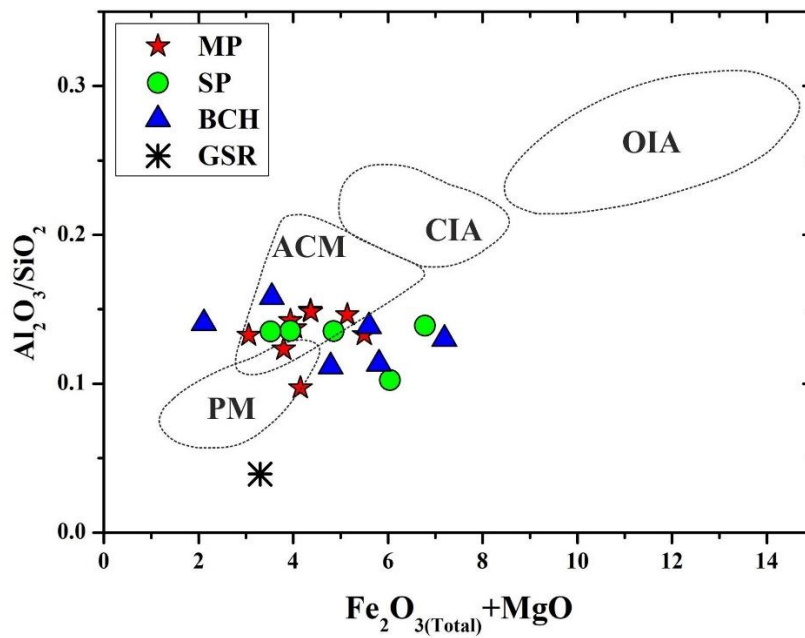
Figure 8.7(B): Discrimination plot of Fe₂O₃+MgO) vs Al₂O₃/SiO₂ (Bhatia,1983)
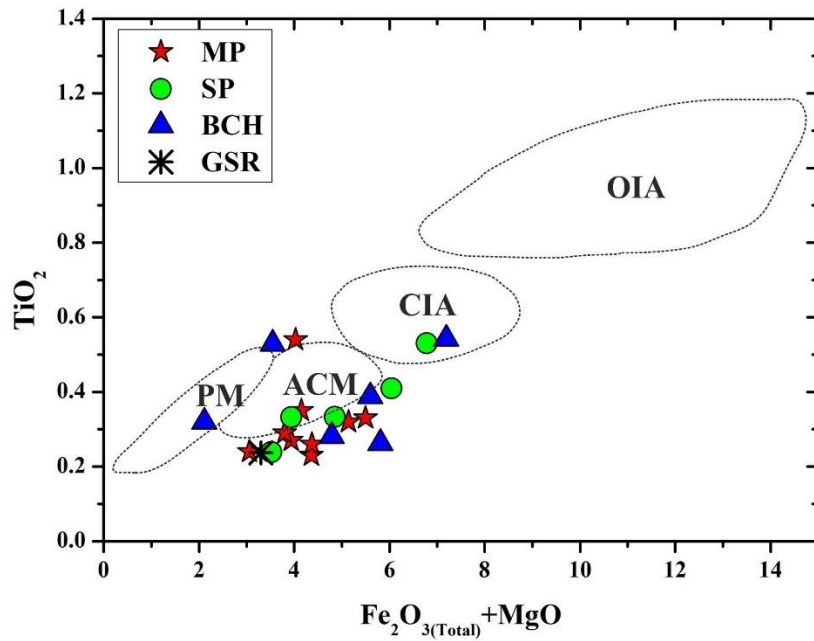
Figure 8.7(C): Discrimination plot of Fe₂O₃+MgO) vs TiO₂ (Bhatia,1983)
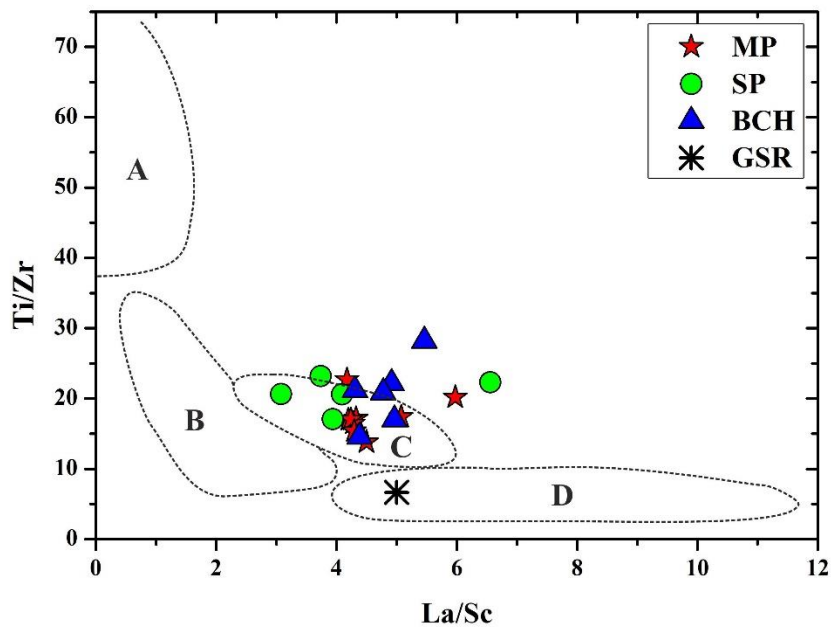
Figure 8.7(D): Bivariant tectonic setting plot using La/Sc Vs Ti/Zr (Bhatia and Crook, 1986).
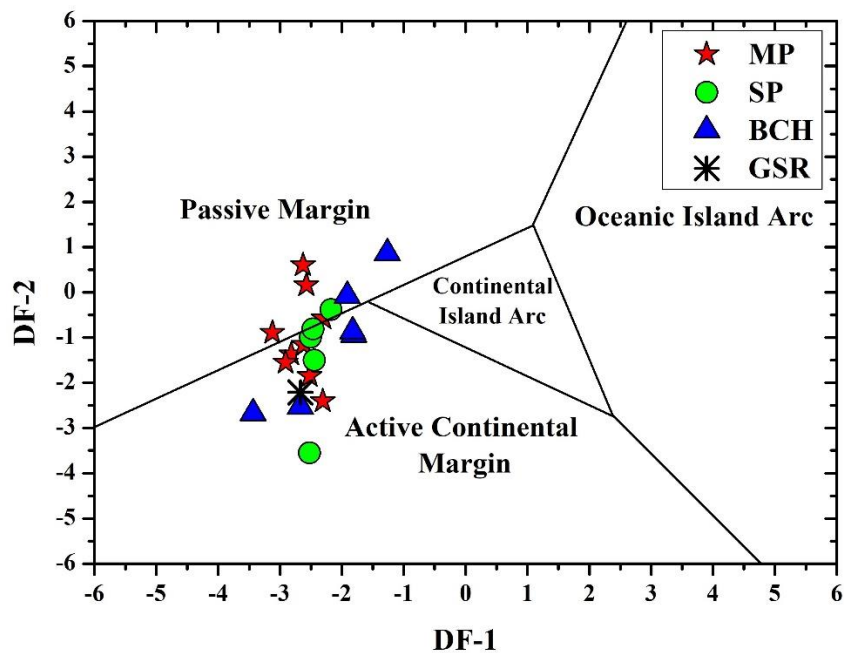
Figure 8.7 (E): Discrimination function plot of DF-1 against DF-2 for tectonic settings of Tipam sandstones after Bhatia, (1983).

8.4 DISCUSSION AND CONCLUSION

Major oxides study reveals the high concentration of SiO_2 (Range: 74.51-82.52 wt % with an average of 79.23%). The concentration of Al_2O_3 varies between 8.02-12.46 wt % with an average of 10.49 wt % which is much lower than the UCC (Rudnick and Gao, 2003, 2005). The low MnO wt % concentration of all the samples reflects low Eu. The low value of Na_2O (Avg: 0.6) can be attributed to a small amount of Na- rich plagioclase; Saeed *et. al.,* (2011) which are also less in the petrographic data (Table 6.1). Positive correlation of as K_2O and P_2O_5A signifies fragmentation of sandstone and clay minerals. The positive correlation of K_2O indicate the enrichment of clay minerals and also indicate the influence of weathering.

The positive correlation and higher concentration of Zr is due to the enrichment of zircon grains which is also supported by the high population of zircon [Average: 8.60; and photomicrograph Plate 7.1 (2a-2f) in heavy mineral analysis]. Negative correlation of Sr with Al_2O_3 and depletion of Cao indicate removal of calcic plagioclase during the process of diagenesis causing less abundance of calcic plagioclase. Positive correlation between Rb and K_2O suggests the presence of K bearing clay minerals such as kaolinite, illite etc.

Plotting of Chondrite normalized average REE of the studied sample represent a relative enrichment of Light Rare Earth elements (LREE: La-Sm); a negative Eu anomaly (Avg: 0.67) and a depleted Heavy Rare Earth Elements (HREE: Gd-Lu). Ratio of $(La/Yb)_N$ (Avg: 10.93) and negative Eu anomalies (Range from 0.48 to 0.79 with an average of 0.67). The overall features suggest that the original source rock is mainly of fractionated felsic source akin to granite and granitoid (Slack and Stevens, 1994).

Using major elemental data, geochemical classification of the studied samples falls at lithic arenites to arkose field. Using the wt % of major oxides CaO, Na_2O and K_2O in ternary plot, majority of the samples falls in andesite field suggesting that the sediments have been sourced from andesitic terrain with intermixing of dacite. Ternary plot after Bracciali *et. al*., (2007) result in the concentration of the samples near the field of felsic [Figure 8.5(B)]. Plotting of the samples in the ternary plot of La-Th-Sc proposed by Jinliang and Xin, (2008) clustered near the granitic field as represented in [Figure 8.5(E)].

The chemical indices of weathering such as Weathering Index of Parker (WIP) after Parker (1970), Chemical Index of Alteration (CIA) after Nesbitt and Young, (1982), Plagioclase Index of Alteration (PIA) after Fedo *et. al.*, (1995), Chemical Index of Weathering (CIW) after Harnois, (1988) and Index of Chemical Variability (ICV) after Cox *et. al.*, (1995) show moderate values of CIA together with negative Eu anomaly representing low to moderate degree of weathering of source rock with some contribution of juvenile sediments from local/near sources with moderate to higher rate of mechanical weathering and short transportation, poor sorting, rapid sedimentation and exhibits less amount of alkali bearing minerals.

Plotting of the samples in various tectonic discrimination function diagram (Fe_2O_3+MgO) vs Al_2O_3/SiO_2 (Bhatia,, 1983), (Fe_2O_3+MgO) vs K_2O/Na_2O (Bhatia, 1983), La/Sc vs Ti/Zr after Bhatia and Crook, (1986), La-Th-Sc ternary plot after Bhatia and Crook, (1986) suggest tectonic settings of active continental margin with few samples falling in Passive continental margin settings.

CHAPTER 9

SUMMARY AND CONCLUSION

The study area is located within Kolasib District of Mizoram, particularly to the north western part of the State. It is covered within the Survey of India Toposheet No 83 D/11 & 83 D/12 and falls within the geographic coordinates of latitudes N24°10'74.0" to N24°20'74.9" and longitudes E92°34'92.4" to E92°35'48.9". Geomorphologically, Mizoram has a hostile terrain characterized by highly undulated, gentle to very steep and rugged topography. Almost all the hill ranges and valleys are narrowly trending in the N-S to NNE-SSW directions. Of the broad stratigraphic succession of Mizoram like Barail, Surma, and Tipam Groups, the study area exposes Tipam Group of rocks, which are best exposed in the north-western part of the State where the present investigation was undertaken.

The lithology of Mizoram sedimentary succession generally includes sandstone, silty-sandstone, siltstone, silty-shale, shale and their admixture of varying proportions along with random pockets of shell-limestone, and intraformational conglomerates. Surma Group of rocks occupies the major portion of the which further subdivided based on the ratio of argillaceous and arenaceous components. Barail Group are found in the northeastern part whereas Tipam Group are found to cover the western part of the state.

The study area is confined to sandstones of Tipam Group exposed around Buhchang, Saihapui and Meidum-Pangbalkawn villages, which is in the western part of Kolasib district, Mizoram. The sandstones in this area are exemplified by its soft

and friable nature because of its low degree of induration and compaction. The sandstones of the study area are associated with alternating bands of shale/mud with varying thickness from one place to another. Parallel beddings, cross-beddings, wave ripples, heterolithic beddings and sole marks like flute caste and load caste are the common Primary sedimentary structures readily observed in the sandstones of the study area. Mud clasts of varied shapes and sizes, and leaching of iron ores are also some of the common sedimentary features found in the sandstones other than the primary sedimentary structures.

Petrography of the Tipam Sandstones reveals that the sandstone varies from sub-lithic arenite to sub-arkose and feldspathic lithic arenite to lithic arkose. Similalrly, the geochemical classification of the investigated sandstone indicated that they are lithic arenite to arkose.

The diversification and content of alkali and alkaline earth elements of terrigenous rocks are greatly affected by the varying degree of weathering in the source area. The chemical indices of weathering employed in the present work are Weathering Index of Parker (WIP) after Parker, (1970); Chemical Index of Alteration (CIA) after Nesbitt and Young, (1982); Plagioclase Index of Alteration (PIA) after Fedo *et. al.*, (1995); Chemical Index of Weathering (CIW) after Harnois, (1988) and Index of Chemical Variability (ICV) after Cox *et. al.*, (1995). The studied sandstones show moderate values of CIA together with negative Eu anomaly which generally represents low to moderate degree of weathering of source rock with some contribution of juvenile sediments from local/near sources with moderate to higher rate of mechanical weathering and short transportation, poor sorting, rapid sedimentation and exhibits less

amount of alkali bearing minerals. Ternary plot of CIA indicates the beginning of chemical weathering and breakdown of plagioclase. The high CIW value of the studied sandstones (Avg: 74.35) indicates moderate to high nature of weathering and the moderate average value of PIA (Range: 38.8 to 90.85, Avg: 71.37) which is higher than UCC (50.22) depict a moderate weathering of plagioclase. The studied Tipam Sandstones are showing high WIP value (Avg: 71.37) and an average of ICV= 0.89 and K_2O/Al_2O_3= 0.16 indicating immense weathered source rocks and immature sediments which may be derived from tectonically active settings. Plotting of Th Vs Th/U [Figure 8.6(D)] represents moderate to intense weathering. Negative correlation of Sr with Al_2O_3 and depletion of Cao indicate removal of calcic plagioclase during the process of diagenesis causing less abundance of calcic plagioclase which is even observed in thin section studies. Positive correlation between Rb and K_2O suggests the presence of K bearing clay minerals such as kaolinite, illite etc. Plotting of petrographical data of the studied samples in QFR diagram for the present study manifest a mixed nature of plutonic and metamorphic origin under humid climatic condition as well as plotting in bivariant plot after Weltje, (1994) and Weathering Index after Grantham and Velbel, (1988) suggest a moderate hill relief under sub-humid climatic conditions.

The analysis and interpretation of monocrystalline and polycrystalline quartz in the form of diamond diagram indicated that the Tipam sandstones are derived from slate and schist of low rank metamorphic rocks. Presence of monocrystalline quartz with wavy extinction [Plate 6.2(J)] suggests a metamorphic source while plutonic source is evident by the presence of non-undulatory monocrystalline quartz and slightly curved inter-crystal boundaries of polycrystalline quartz (>3 crystal unit

161

per grain) [Plate 6.2(I) and Plate 6.6.2(L)]. Granite or pegmatite sources are evident by the presence of perthite [Plate 6.1(G)]. The heavy mineral suite of the present sandstones under study show abundance of both opaque and non-opaque mineral such as zircon, tourmaline, rutile, hornblende, garnet, sillimanite, staurolite, Kyanite, epidote, chlorite and enstatite. The bulk dominance of zircon, tourmaline and rutile along with the dominance of opaque minerals indicate portion of the sediments originate from acid plutonic rock. Presence of few colorless euhedral zircon grains suggests an acidic igneous source with short transportation. Presence of a few perfect euhedral grain of tourmaline may also indicate silicic igneous source with short distance of transportation. According to Heinrich, (1956), presence of epidote along with tourmaline suggests low to medium grade metamorphic source. Based on the observation of heavy mineral suite and ZTR maturity index, it can be concluded that the Tipam sandstone of the study area show moderate maturity and are derived from mixed source where major portion of the sediments were derived from metamorphic source and also from igneous source. However, presence of sub rounded grains of heavies also suggest contribution from reworked sediments. From the geochemical data, the positive correlation and higher concentration of Zr is due to the enrichment of zircon grains which is also supported by the high population of zircon [Average: 8.60; and photomicrograph Plate 7.1 (2a-2f) in heavy mineral analysis]. The relative enrichment of Light Rare Earth elements (LREE: La-Sm); a negative Eu anomaly (Avg: 0.67) and a depleted Heavy Rare Earth Elements (HREE: Gd-Lu) along with high value of ratio of LREE/HREE i.e. $(La/Lu)_N$=(Ranges from 7.27-14.47) suggest that the original source rock is mainly of fractionated felsic source akin to granite and granitoid and show no input from mafic source which was further supported by the

162

enrichment of Zr and negative Eu anomaly. Based on the above plotting and consideration using geochemical data, it can be inferred that the sediments of Tipam sandstones were primarily derived from the uplifted and eroded Himalayan felsic and metamorphic terrain with input from neighboring orogen such as Indo-Burmese Range.

Based on petrographic observation of QFL and Q_mFL_t for various tectonic discriminant diagram it was found that the investigated sandstone falls in recycled orogen with mixed setting. Few Rounded quartz grains stipulate recycled origin while angular grains and present of rock fragments indicate textural immaturity of the rock. Presence of fracturing of quartz grains [Plate 6.2(N)] and kink bend of mica flakes [Plate 6.1(C & E)] indicates the effect of tectonic activity after deposition of sediments. Various discriminant diagrams based on major and trace elements for tectonic settings was also employed in the present study like La-Th-Sc plotting according to Bhatia, (1983); discrimination plot of Fe_2O_3+MgO vs Al_2O_3/SiO_2 (Bhatia,1983); Discrimination plot of Fe_2O_3+MgO vs TiO_2 (Bhatia.,1983); bivariant plot of La/Sc Vs Ti/Zr according to Bhatia and Crook., (1986) and discrimination function plot of DF-1 against DF-2 after Bhatia, (1983) and inferred that the sediments of the studied Tipam sandstones were deposited in an Active Continental Margin setting with slight sediment input from Passive Continental Margin.

To assess the size distribution and depositional environment of a sediments, grain size analysis has been utilized in the present study. From the one function histogram and frequency distribution curves alone, it can be inferred than the sediments were deposited in a mixed environment of marine and fluvial where marine processes are dominating over the river processes. From the Log-probability plot, it

163

can be observed that sorting is generally good in saltation population, whereas sorting is poor to fair in the suspended and rolling populations. Grain size parameters such as Graphic mean, Graphic standard deviation, Graphic skewness and Graphic kurtosis shows that the Tipam sandstones of the study area are medium to fine sand with moderate to moderately well sorted which were deposited in a mixed environment where both marine and fluvial influences are present with high energy fluctuation. Different bivariant scatter plots also suggest mixed environment in the transitional zone where fluvial processes dominate with an influence of marine processes. Calculation of Linear discrimination function of Y_1, Y_2, Y_3 and Y_4 along with the binary plotting depict a fluvial deltaic environment with a shallow agitated marine deposition.

Incorporating all the field, laboratory and result obtained, it can be concluded that the sediments of the Tipam sandstones of the study area were derived mainly from the Himalayan, the Mishmi hills along with the sediment influx from Indo-Burmese orogen which were deposited by the Paleo-Brahmaputra with the influence of marine condition.

REFERRENCES

Alam, M. M. (1991). "Palaeoenvironmental study of the Barail sediments exposed in the northeastern Bangladesh". *Bangladesh J. Sci. Res*. **9(1)**: 25-33.

Amireh B. S., (2014). "Grain size analysis of the Lower Cambrian-Lower Cretaceous clastic sequence of Jordan: Sedimentological and paleo-hydrodynamical implications". *Journal of Asian Earth Sciences*. **97**: 67-88.

Armstrong-Altrin, J.S., (2009). "Provenance of sands from Cazones, Acapulco, and Bahía Kino beaches, México. Rev. Mex". *Ciencias Geol*. **26:** 764–782.

Armstrong-Altrin, J. S., Nagarajan, R., Lee, Y. I., Kasper-Zubillaga, J. J., and Cordoba-Saldana, L. P., (2014). "Geochemistry of sands along the San Nicol′as and San Carlos beaches, Gulf of California, Mexico: Implication for provenance". *Turkish Journal of Earth Science*. **23**: 533–558.

Basu, A., Young, W. S., Suttner, J. L., James, C. W., and Mack, H. G., (1975). "Re – evaluation of the use of Undulatory Extinction and Polycrystallinity in Detrital Quartz for Provenance Interpretation". *Journal of Sedimentary Petrology*. **45**: 873 – 882.

Bharali, B., Borgohain, P., Bezbaruah, D., Vanthangliana, V., Phukan, P. P., and Rakshit, R. (2017). "A geological study on Upper Bhuban Formation in parts of Surma Basin, Aizawl, Mizoram". *Science Vision*. **17(3):** 128-147.

Bhatia, M. R., (1983). "Plate tectonics and geochemical composition of sandstones". *Journal of Geology*. **91**: 611–627.

Bhatia, M.R. (1985). "Rare earth element geochemistry of Australian Paleozoic graywackes and mudrocks: provenance and tectonic control". *Sedimentary Geology*. **45**: 97–113.

Bhatia, M. R. and Crook, K. A. W., (1986). "Trace element characteristics of graywackes and tectonic setting discrimination of sedimenatry basins". *Contributions to Mineralogy and Petrology.* **92**: 181-193.

Blatt, H., (1967). "Original characteristics of clastic quartz grains". *Jour. Sed. Petrol*. **37**: 401-424.

Blatt, H., (1980). "Diagenesis process in sandstones, in P.A. Scholle and P.R. Schluger (eds) Aspect of diagenesis. Soc. Econ". *Paleontologists and Mineralogists. Spec. publication*. **26**: 141-157.

Boggs Sam Jr., (2009). "Petrology of Sedimentary Rocks", Second Edition. 115-116.

Colony, J. R., (1965). "The occurrence of polycrystallinity and undulatory extinction in quartz in sandstone". *Jour. Sed. Petrol*. **35**: 116-135.

Borgohain, P., (2011). "Textural variation of the Tipam reservoir sandstone of Digboi oilfield, Assam". *Indian Journal of Research.* **1(3):** 118-120.

Borgohain, P., (2012). "Grain size distribution of Tipam sandstones in Tipong Pani river section, Assam". *Indian Journal of Research*. **1(4):** 4-6.

Borgohain, P., (2012). "Heavy mineral studies of the subsurface of Tipam Sandstone Formation in parts of Upper Assam basin". *Applied Geology*. **1(12)**: 1-3.

Bracciali, L., Marroni, M., Luca, P., Sergio, R., (2007). "Geochemistry and petrography of Western Tethys Cretaceous sedimentary covers (Corsica and Northern Apennines): From source areas to configuration of margins". *Geol. Soc. Am. Spec. Pap*. **420**: 73–93.

Camiré, G.E., Laflèche, M.R., and Ludden, J.N. (1993). "Archaean metasedimentary rocks from the northwestern Pontiac Subprovince of the Canadian Shield: chemical

characterization, weathering and modeling of the source areas". *Precambrian Research*. **62**: 285–305.

Cheng, Z and Lui, H., (2015). "Digital grain-size analysis based on autocorrelation algorithm". *Sedimentary Geology*. **327**: 21-31.

Chenkual, L., Kataki, T., and Sarma, J. N. (2010). "Heavy Minerals of Tertiary Rocks exposed in Teidukhan Anticline, Kolasib, Mizoram, India". *Sci. Vis* **10(1)**: 8-19.

Chutia, A., and Sarma, N. J., (2013). "A study on geochemical composition and source area weathering of the Tipam sandstones from a few oil fields of Upper Assam Basin, India". *Indian Journal of Applied Research.* **3(8):** 77-79.

Condie, K. C., (1993). "Chemical composition and evolution of upper continental crust: Contrast-ing results from surface samples and shales". *Chemical Geology.* **104**: 1–37.

Cox, R., Lowe, D.R., and Cullers, R.L., (1995). "The influence of sediment recycling and basement composition on evolution of mudrock chemistry in the southwestern United States". *Geochimica et Cosmochimica Acta*. **59**: 2919–2940.

Crook, K. A. W., (1974). "Lithogenesis and geotectonics: The significance of compositional variation in flysch arenites (greywackes): in R.H. Dott., and R.H. Shavar (Eds.) Modern and ancient geosynclinals Sedimentation". *Soc. Econ. Palaeonton. Mineral*. **Spec. Publ. 19**: 304-310.

Cullers, R. L., Barrett, T., Carlson, T. and Robison, B., (1987). "Rare-earth element and mineralogical changes in Holocene soil and stream sediment: a case study in the Wet Mountains, Colorado, U.S.A.". *Chem. Geol.***63**: 275-297.

Cullers, R. L. and Podkovyrov, V. N., (2000). "Geochemistry of the Mesoproterozoic Lakhanda shales in southeastern Yakutia, Russia: Implications for mineralogical and provenance control, and recycling". *Jour. Precambrian Res*. **104**: 77–93.

Dapples, E. C., (1962). "Stages of Diagenesis in the development of sandstone". *Geol.*

Soc. Am. Bull. **73**: 913-933.

Dapples, E. C., (1967). "Diagenesis of sandstone, in G. Larson and G. Chilinar, eds., Diagenesis of sediments. *Amsterdam, Elsivier Pub. Co*. 91-125.

Dapples, E. C., (1979). "Diagenesis of sandstone, in G. Larson and G. Chilinar, eds., DiagemeDevelopments in sedimentology. *Amsterdam, Elsivier Pub. Co*. **25A:** 31-37.

Das, P. K., and Duarah, B. P., (1996). "Heavy mineral suite in the Tura sandstone in and around Dobagiri, East Garo Hills, Meghalaya". *Jour of Paleo. Soc. Of India*. **41**: 83-89.

Das, P. K. and Sarma, Ajanta., (2009). "Petrographic studies of sandstones from Shella formation, Lumshong area, South Jantia Hills, Meghalaya". *Gond Geol. Magz*. **24(2)**

Dickinson, W. R. and Suczek, C., (1979). "Platetectonics and Sandstone Composition". *American Association of Petroleum Geologists Bulletin*. **63**: 2164-2182.

Dickinson, W. R., Bead, L. S., Brakenridge, G. R., Erjavec, J. L., Ferguson, R. C., Inman, K. F., Kenpp, R. A., Lindberg, F. A and Ryberg, P. T., (1983). "Provenance of North American Phanerozoic sandstones in relation to tectonic setting". *Geol Soc Am Bull*. **94:** 222-235.

Dickinson, W. R., (1985). "Interpreting Provenance Relations from Detrital Modes of Sandstones, in Zuffa, G.G., ed". *Provenance of Arenites: Boston, D.Reidel*: 333-361.

Dupre, B., Gaillardet, J., Rousseau, D., and Allegre, C., (1996). "Major and trace elements of river-borne material: theCongo Basin". *Geochim. Cosmochim. Acta.* **60**: 1301-l 321.

Dutta, S. K., and Handique, G. K. (1980). "A study of the Surma-Tipam groups of upper Assam valley, South of Brahmaputra". *Journal of the Paleontological Society of India*. **25:** 42-52.

Evans, P., (1932). "Tertiary succession in Assam". *Trans. Min. Geol. Inst. India*. **27:** 155–260.

Evans, P., (1964)." Tectonic framework of Assam". *J. Geophys. Soc. India*. **5**: 80– 96.

Fedo, C. M., Nesbitt, H. W., and Young, G. M. (1995). "Unraveling the effects of potassium metasomatism in sedimentary rocks and paleosols, with implications for paleoweathering conditions and provenance". *Geology*. **23**: 921-924.

Feng, R., and Kerrich, R. (1990). "Geochemistry of fine-grained clastic sediments in the Archean Abitibi greenstone belt, Canada: implications for provenance and tectonic setting". *Geochimica et Cosmochimica Acta*. **54**: 1061–1081.

Floyd, P.A., Winchester, J.A., Park, R.G., (1989). "Geochemistry and tectonic setting of Lewisian clastic metasediments from the Early Proterozoic Loch Maree Group of Gairloch, NW Scotland". *Precambrian Res*. **45**: 203–214.

Folk R. L., (1954). "The distinction between grain size and mineral composition in sedimentary rock nomenclature". *Jour Geol*. **62**: 344-359.

Folk, R. L., and Ward, W. C. (1957). "Brazos River Bar – A Study on the significance of grain size parameters". *Jour. Sed. Pet*. **27**: 3-26.

Folk, R. L., (1980). "Petrology of Sedimentary Rock". *Hemphill Austin, Tex*. 183p.

Friedman, G. M. (1967). "Dynamic processes and statistical parameters distribution of beach and river sand". *Journal of Sedimentary petrology*. **37**: 327-354.

Friedman, G. M., and Johnson, K. G. (1982). "Exercise in Sedimentology". *John Wiley and Sons, New York*. 24-83.

Ganguly, S., (1983). "Geology and Hydrocarbon prospects of Tripura - Cachar - Mizoram region". *Jour. Petrol. Asia*. **6(IV)**: 105-109.

Ganguly, S. (1975). "Tectonic Evolution of Mizo Hills". *Bull. Geol. Min. Met. Soc. India*. **48**: 28-40.

Ganju, J. L. (1975). "Geology of Mizoram". *Bull. Geol. Min. Met. Soc. India*. **48**: 17-26.

Goldstein, S. J., and Jacobsen, S. B., (1988). "Rare earth elements in river waters. Earth Planet". *Sci. Lett*. **89**: 35-47.

Govind, G., Najman, Y., Copley, A., Millar, I., van der Beek, P., Grujic, D., and Davenport, J. (2018). "Timing and mechanism of the rise of the Shillong Plateau in the Himalayan foreland". *Geology*. **46**: 279-282.

Grantham, J. J., and Velbel, M. A., (1998). "The influence of climate and topography on rock fragment abundance in modern fluvial sands of the southern Blue Ridge Mountains, North Carolina". *Jour. Sedimentary Petrology*. **58**: 219-227.

Harnois, L. (1988). "The CIW index: a new chemical index of weathering". *Sedimentary Geology*. **55**: 319–322.

Hayashi, K.I., Fujisawa, H., Holland, H.D., Ohmoto, H., (1997). "Geochemistry of ~1.9 Ga sedimentary rocks from northeastern Labrador, Canada". *Geochim. Cosmochim. Acta*. **61:** 4115–4137.

Herron, M. M., (1998). "Geochemical classification of terrigenous sand and shales from core or log data". *Sed. Petrol*. **58**: 820-829.

Hole, M. J., Trewin, N. H., Still, J., (1992). "Mobility of the high field strength, rare earth elements and yttrium during late diagenesis". J. Geol. Soc. London. **149:** 689–692.

Holland, H.D., (1978). "The Chemistry of the Atmosphere and Oceans". *New York, Wiley*. 351.

Holtrop, J. F. and Keizer, J., (1970). "Some aspects of the stratigraphy and correlation of the Surma basin wells, East Pakistan". *ESCAFE Miner. Resour. Dev. Ser*. **36:**143–154.

Hossain, Z. M. H., and Roser, B. (2006). "Major and trace elements analysis of Tertiary sedimentary rocks from the Sylhet Basin, Bangladesh". *Geoscience Rept. Shimane Univ*. **25:** 49-59.

Hubert, J. F., (1962). "A ZTR Maturity Index and the dependence of the composition of heavy mineral assemblage with the gross composition od texture of sandstone". *Jour. Sed. Pet.* **32(3)**: 16-23.

Hussain, M. F. and Bharali, B. (2019). "Whole-rock geochemistry of Tertiary sediments of Mizoram foreland basin, NE India: implications for source composition, tectonic setting and sedimentary processes". *Acta Geochim*. https://doi,org/10.1007/s11631-109-00315-3.

Ingersoll, R. V., Bullard, T. F., Ford, R. L., Grimm, J. P., Pickle, J. D., and Sares, S. W., (1984). "The Effect of Grain size on Detrital Modes: A Test of the Gazzi-Dickinson Pointcounting Method". *Journal of Sedimentary Petrology*. **54**: 103–116.

Ingersoll, R. V., and Suczek, C. A. (1979). "Petrology and provenance of Neogene sand from Nicobar and Bengal fans, DSDP sites 211 and 218". *Journal of Sedimentary. Petrology*. **49**: 1217–1228.

Inman, D. L., (1952). "Measures for Describing the Size Distribution of Sediments". *Jour. Sed. Pet.*.**22**: 869-878.

Islam, Aminul. Md., (2010). "Petrography and Provenance of subsurface Neogene sandstones of Bengal Basin, Bangladesh". *Journal Geological Society of India*. **76:** 493-504.

Jason, R. P., and Michael, A. V. (2003). "Chemical weathering indices applied to weathering profiles developed on heterogenous felsic metamorphic parent rocks". *Chemical Geology*. **202** : 397-416.

Jinliang, Z., Xin, Z., (2008). "Composition and Provenance of Sandstones and Siltstones in Paleogene, Huimin Depression, Bohai Bay Basin, Eastern China". *J. China Univ. Geosci*. **19:** 252–270.

Johnsson, M. J., (1993). "The system controlling the composition of clastic sediments, in Johnsson, M. J., and Basu, A., eds., processes controlling the composition of clastic

sediments: Boulder, Colorado". *Geological Society of America, Special Paper*. **284**: 1-19.

Karunakaran, C. (1974). "Geology and Mineral resources of the states of India". *Misc. Publ. Geol. Surv. India*. **30(IV)**: 93-101.

Kroonberg, S. B. (1994)." Effect of provenance, sorting and weathering on the geochemistry of fluvial sands from different tectonic an climatic environments". *Proceedings of the 29th International Geological Congress, Part A*. 69-81.

Krishnamurthy, R. V., Bhattachrya, S. K. and Kusumgar, S., (1986). "Palaeoclimatic changes deduced from 13C/12C and C/N ratios of Karewa lake sediments, India". *Nature*. **323**: 150–52.

Krumbein, W. C., (1938). "Size Frequency Distribution of Sediments". *Jour. Sed. Pet*. **4**: 65-77.

Krumbein, W. C., and Pettijohn, F. J., (1938). "Manual of sedimentary petrography". *Appleton-Century-Crafts Inc, New York*. 549p.

Krynine, P. D., (1984). "The megascopic study and field classification of sedimentary rocks. *Jour-Geol*. **56**: 230-265.

Laird, K. R., Cumming, B. F., Wunsam, S., Rusak, J. A., Oglesby, R. J., Fritz, S. C. and Leavitt, P. R., (2003). "Lake sediments record large-scale shifts in moisture regimes across the northern prairies of North America during the past two millennia". *Proc. Natl. Acad. Sci*. **100**: 2483–2488.

Lahkar, A. D. (2007). "Sedimentological Studies of Tertiary Sediments of Dilli Area, Sibsagar District, Assam". *Unpubl. Ph. D. Thesis of Gauhati University*. 23-42.

Lakhar, A. D., and Das, P. K. (2010). "Size analysis and textural parameters of Tikak Parbat and Tipam sandstones occurring in and around Dilli area, Sivasagar District, Assam. *Jour. Dimoria College*. **8(2)**: 15-30.

Lal, M., Singh, S. K., Sundarajan, V., Shah, L., Das, D., and Saha, T. (1992). "Sedimentological Studies on Bhuban and Bokabil Sub-group and Tipam Sandstone from Rente and Teidukhan Anticline, Mizoram". *Bul.l ONGC*. **29**: 61-68.

Lalmuankimi, C., Tiwari, R. P., Jauhri, A.K. and Ralte, V. Z. (2010). "Foraminifera from the Upper Bhuban formation of Mizoram". *Journal of the Paleontological Society of India.* **55(1):** 71-75.

Lalmuankimi, C., Kumar, S., Laldinpuia and Tiwari, R. P. (2011). "Geochemical study of Upper Bhuban Sandstone in Muthi, Mizoram". *Sic Vision.* **11(1)**

Lalnunmawia, J., and Lalhlimpuii, J., (2014). "Classification and provenance studies of the sandstones exposed along Durtlang road section, Aizawl, Mizoram". *Science Vision*. **14(3)**: 158-167.

Lalnuntluanga, P., Malsawma, J., Lalremruatfela, C., Tiwari, R. P. and Sangode, S. G. (2014). "Correlation of four Magnetographically Constrained Sections of Miocene Bhuban Formation of Surma Basin in Mizoram, India". *Special publication of the Paleontological Society of India.* **5:** 87-100.

Le Maitre, R.W., (1976). "The chemical variability of some common igneous rocks". *J. Petrol*. **17**: 589–598.

Lindholm, R. C. (1987). "A Practical Approach to Sedimentology". *Allen and Unwin*, *London*. 154-176.

M.C. Bridge., (1985). "Diagenetic processes that affect provenance determination in sandstones". *G.G. Zuffa Ed, Provenance of arenites*. 95-114.

McLennan, S. M., (1989). "Rare earth elements in sedimentary rocks: influence of the provenance and sedimentary process". *Geochemistry and Mineralogy of Rare Earth Elements*. **21**: 169-200.

McLennan, S.M., Taylor, S.R., McCulloch, M.T., and Maynard, J.B. (1990). "Geochemical and Nd-Sr isotopic composition of deepsea turbidites: crustal

evolution and plate tectonic associations". *Geochimica et Cosmochimica Acta*. **54**: 2015–2050.

McLennan, S.M, and Taylor, S.R. (1991). "Sedimentary rocks and crustal evolution: tectonic setting and secular trends". *Journal of Geology*. **99**: 1–21.

McLennan, S. M., Hemming, S., Mcdaniel, D. K. and Hanson, G. N., (1993). "Geochemical approaches to sedimentation, provenance and tectonics In Johnsson, M. J. and Basu, A. (Eds), Processes controlling the consumption of clastics sediments". *Geological Society of America, Spec. Paper*. **284**: 21-40.

Mehrotra, R. C., Tiwari, R. P., Srivastava, G. and Shukla, A. (2013). "Further contribution to the Neogene petrified wood forest of Mizoram, India". *Chinese Science Bulletin.* **58 Suppl I:** 104-110.

Middleton, G. V., (1960). "Chemical composition of sandstones". *Geological Society of America. Bulletin.* **71**: 1011-1026.

Moiola, R. J., and Weiser, D. (1968). "Textural Parameters, An Evaluation". *Jour. Sed. Pet*. **38**: 45-53.

Mongelli, G., Critelli, S., Perri, F., Sonnino, M., Perrone, V., (2006). "Sedimentaryrecycling, provenance and paleoweathering from chemistry and mineralogy of Mesozoic continental redbed mudrocks, Peloritani mountains, southern Italy". *Geochem. J*. **40**: 197–209.

Najman, Y., Garzanti, E., (2000). "Reconstructing early Himalayan tectonic evolution and paleogeography from Tertiary foreland basin sedimentary rocks, northern India". *Bull. Geol. Soc. Am*. **112:** 435–449.

Najman, Y., Bickle, M., Fadel, B. M., Carter, A., Garzanti, E., Paul, M., Wijbrans, J., Willett, E., Oliver, G., Parrish, R., Akhter, S. H., Allen, R., Chisty, E., Reisber, L., and Vezzoli, G. (2008). "The Paleogene record of Himalayan erosion: Bengal Basin, Bangladesh". *Earth and Planetary Science Letters.* **273:** 1-14.

Nandy, D. R., Gupta, S. D., Sarkar, K. and Ganguly, A. (1983). "Tectonic Evolution of Tripura - Mizoram Fold Belt., Surma Basin, North East India". *Quart. Jour. Geol. Min. Met. Soc. Ind.*. **35(4)**: 186-194.

Nandy, D.R., (1986). "Tectonics, seismicity and gravity of northeastern India and adjoining areas. Geology of Nagaland Ophiolites". *Geol. Surv. India*, Mem. **119:** 13-17.

Nandy, D.R., (2017). "Geodynamics of northeastern India and the adjoining Region, Revised Edition". *Scientific Book Centre, Guwahati, Assam*. 272.

Nesbitt, H. W., (1979). "Mobility and fractionation of rare earth elements during weathering of a granodiorite". *Nature*. **279**: 206-210.

Nesbit, H. W., and Young, G. M. (1982). "Early Proterozoic climates and plate motions inferred from major element chemistry of lutites". *Nature*. **299**: 715-717.

Ohr, M., Halliday, A. N. and Peacor, D. R., (1994). "Mobility and fractionation of the rare earth elements in argillaceous sediments: implications for dating diagenesis and low-grade metamorphism". *Geochim. Cosmochim. Acta*. **58**: 289-312.

Qiugen, L., Shuwen, L., Baofu, H., Jian, Z., and Zhuyin, C. (2005). "Geochemistry of metasedimentary rocks of the Proterozoic Xingxingxia Complex: Implications for provenance and tectonic setting of the Eastern segment of the Central Tianshan Tectonic zone, North-west China". *Canadian Journal of Earth Sciences*. **42**: 287-306.

Okeyode, I. C., and Jibiri N. N., (2012). "Grain size analysis of the sediments from Ogun River, South Western Nigeria". *Earth Science Research*. **2**: 43-51.

Parker, A., (1970). "An index of weathering for silicate rocks". *Geological Magazine*. **107**: 50 1 -504.

Passega, R. (1957). "Texture and Characteristics of Clastic Deposition". *Bull. Amer. Assoc. Pet. Geol.* **41:** 1957-1984.

Periasamy, V and Venkatashwarlu, M., (2017). "Petrography and Geochemistry of Jurassic Sandstones from the Jhuria Formation of Jara dome, Kachchh Basin, India: Implication for Provenance and Tectonic Setting". *Journal of Earth System Science*. **126(44)**: 1-20.

Pettijohn, F. J. (1957). "Sedimentary Rocks, 3rd edn". *Harper and Row, 1st Edition, New York*. 526.

Pettijohn, F. J., Potter, P. E., and Siever. R. (1972). "Sand and Sandstones". New York, Springer-Verlag. 325.

Pettijohn, F. J., (1975). "Sedimentary rocks, 3rded. Harper and Row, New York". 624-629.

Plank, T. and Langmuir, C. H., (1998). "The Chemical Composition of Subducting Sediments and its consequence for the crust and mantle". *Chemical Geology*. **145**: 325-394.

Rajkonwar, C., Tiwari, R. P., Ralte, V. Z. and Patel, S. J. (2014). "Additional Ichnofossils from Middle Bhuban unit, Bhuban Formation, Surma Group (Lower to middle Miocene), Mizoram and their environmental significance". *Special publication of the Paleontological Society of India.* **5:** 257-271.

Rai, J., Malsawma, J., Lalchhanhima, C., Lalnuntluanga, P.,., Ralte, V. Z. and Tiwari, R. P. (2014). "Nannofossil Biostratigraphy from Bhuban Formation, Mizoram, Northeastern India and its paleoenvironmental interpretations". *Special publication of the Paleontological Society of India.* **5:** 121-134.

Ralte, V. Z., (2012). "Heavy mineral analysis of Tipam sandstone near Buhchang village, Kolasib district, Mizoram, India". *Sci Vis.* **12(1)**: 22-31.

Raman, J. J. M., and Suzuki, S., (2007). "Geochemistry of sandstones from the Miocene Surma Group, Bengal Basin, Bangladesh: Implications for Provenance, tectonic setting and weathering". *Geochemical Journal.* **41:** 415-428.

Raman, J. J. M., McCann, T., Abdullah, R., and Yeasmin, R., (2011). "Sandstone Diagenesis of the noegene Surma group from the Shahbazpur gas field, southern Bengal Basin, Bangladesh". *Austrian Journal of Earth Sciences.* **104(1):** 114-126.

Rintluanga, Pachuau., (1994). "Geology of Mizoram (1st edition)", *New Aizawl Press, Chandmari*, Aizawl. 54.

Roser, B.P., and Korsch, R.J. (1986). "Determination of tectonic setting of sandstone-mudstone suites using SiO2 content and K2O/Na2O ratio". *Journal of Geology*. **94**: 635–650.

Rose, N. L., Boyle, J. F., Du, Y., Yi, C., Dai, X., Appleby, P. G., Bennion, H., Cai, S. and Yu, L., (2004). "Sedimentary evidence for changes in the pollution status of Taihu in the Jiangsu region of eastern China". *Jour. Paleolimnol*. **32**: 41–51.

Roy, K. D., Rahman, Mostafizur Md. and Akther Sarmin., (2006). "Provenance of exposed Tipam sandstoneformation, Surma Basin, Sylhet, Bangladesh." *J.Life Earth Science*. **1(2)**: 35-42.

Rudnick, R. L., and Gao, S., (2003). 3.01 - Composition of the Continental Crust, Treatise on Geochemistry.

Saeed, N. E., Barzi, M. H. and Armstrong-Altrin, J. S. (2011). "Petrography and geochemistry of clastic sedimentary rocks as evidences for provenance of the lower Cambrian Lalun Formation, Posht-e-badam block, Central Iran". *Jour. Of African Earth Sciences.* **61:** 142-159.

Sahoo, M., and Gogoi, K. D. (2009). "Depositional history, processes and mechanism of early Miocene sediments of Upper Assam Basin, India". *Journal Geological Society of India.* **73:** 575-585.

Sahu, B. K. (1964). "Depositional Mechanism for size analyses of clastic sediments". *Jour. Sed. Pet*. **36**: 126-142.

Sarkar, K. and Nandy, D. R. (1977). Structures and Tectonics of Tripura - Mizoram area, India. *Geol. Surv. India. Misc. Publ.* **34**(**1**): 141 - 148.

Sarma, J. N., and Chutia, A., (2013). "Petrography of sub-surface Tipam sandstone formation of a part of Assam basin, India". *Global Research Analysis*. **2(2)**: 112-113.

Sarma, J. N., and Chutia, A,. (2013). "Petrography and heavy mineral analysis of Tipam sandstone exposed on the Tipam hill of Sita Kunda area, Upper Assam, India". *South East Asian Journal of Sedimentary Basin Research.* **1:** 28-34.

Schoenborn, W.A., Fedo, C.M., (2011). "Provenance and paleoweathering reconstruction of the Neoproterozoic Johnnie Formation, southeastern California". *Chem. Geol*. **285**: 231–255.

Seiver, R., 1979. Plate tectonic controls on diagenesis. *Journal of Geology*, **87**: 127-155.

Taylor, S. R., and McLennan, S. M., (1985). "The Continental Crust; Its Composition and Evolution". *London, Blackwell.* 312.

Sengupta, S., (1966). "Geological and geophysical studies in the western part of Bengal Basin, India". *Am. Assoc. Pet. Geol. Bull*. **50:** 1001-1017.

Sengupta, S., (1994). "Textbook on Sedimentology". *Oxford Publication, New Delhi*. 314-319.

Sengupta, S. M. (2007). Introduction to Sedimentology, 2nd Edition, *CBS Publisher and Distributor, New Delhi*. 61-82.

Shepard, F. P., and Young, R. (1961). "Distinguished Between Beach and Dune Sands". *Jour. Sed. Pet.* **31**: 196-214.

Shrivastava, B. P., Ramachandran, K. K. and Chaturvedi, J. G. (1979). "Stratigraphy of Eastern Mizo Hills". *Bull. ONGC*. **16(2)**: 87-94.

Sincavage, R. S., Paola, C. and Goodbred, S. L., (2019). "Coupling Mass Extraction and Downstream Fining with Fluvial Favies changes across the Sylhet Basin of the Ganges-Brahmaputra-Meghna Delta". *JGR Earth* Surface. **10.1029**: 1-14.

Singh, Y. R., Sijagurumayum, U. and Guruaribam, V. (2011). "Paleoecology of the Upper Bhuban and Tipam sediments of Mizoram, India- Palinological evidence". *Himalayan Geology*. **32(1):** 57-62.

Slack, J.F., and Stevens, P.J. (1994). "Clastic metasediments of the Early Proterozoic Broken Hill Group, New South Wales, Australia: geochemistry, provenance, and metallogenic significance". *Geochimica et Cosmochimica Acta.* **58**: 3633–3652.

Suttner, L. J., Basu, A. and Mack, G., (1981). "Climate and the origin of quartz". *Jour. Sed. Pet*. **51**: 1235-1244.

Suttner, L. J., and Dutta, P. K., (1986). "Alluvial sandstone composition and paleoclimate framework mineralogy". *Jour. Sed. Pet*. **56**: 329-345.

Tiwari, R. P. and Mehrotra, R. C. (2000). "Study of fossil wood from the Tipam Group (Neogene) of Mizoram, India". *Tertiary Research*. **20(1-4):** 85-94.

Tortosa, A., Palomares, M. and Arribas, J., (1991). "Quartz grain types in Holocene deposits from the Spanish Central System: some problems in provenance analysis; In: Developments in Sedimentary Provenance Studies (eds) A C Morton, S P Todd and P D W Haughton". *Geol. Society of. London, Spec. Publ.* **57:** 47–54.

Uddin, A and Lundberg, N., (1998). "Unroofing history of the eastern Himalaya and the Indo-Burma Ranges: Heavy-mineral study of Cenozoic sediments from the Bengal Basin, Bangladesh". *Journal f Sedimentary research*. **68**: 465-472.

Uddin, A., and Lundberg, N. (2003) "Miocene sedimentation and Subsidence during Continent-Continent Collision, Bengal Basin, Bangladesh". *Sedimentary Geology.* **164:** 131-146.

Uddin, Ashraf., Kumar, Pranav., Sarma, N. Jogen., and Akhter, H. Sayed (2007). "Heavy minerals constrain on the provenance of Cenozoic sediments from the foreland basins of Assam and Bangladesh: Erosional history of the eastern Himalayas and the Indo-Burma ranges". *Developments in sedimentology*. **58**: 823-847.

Uddin, Ashraf., and Lundberg, Neil., (2008). "Unroofing history of the eastern Himalaya and the Indo-Burman Ranges: Heavy-mineral study of Cenozoic sediments from the Bengal Basin, Bangladesh". *Journal of Sedimentary Research*. **68(3)**: 465-472.

Vereshchagin, O. S., Khudoley, A. K., Ershova, V. B., Prokoviep, A. V., and Schneider, G. V., (2018). "Provenance of Jurassic-Cretaceous siliciclastic rocks from the Norther Siberian Craton: an integrated heavy mineral study". *Journal of Geoscience*. **63**: 199-213.

Visher, G. S. (1969). "Grain Size Distribution and Depositional Processes". *Jour. Sed. Pet.* **39:** 1074-1106.

Weljte, G. J., (1994). Provenance and dispersal of sand-sized sediments: recognition of dispersal pattern and sources of sand-sized sediments by means of inverse modelling techniques. *Geol. Ultraiectina.*

Wilde, P., Hunt, M. S. Q., and Erdtmann, B. D. (1995). "The Whole-rock Cerium anomaly: a potential indicator of eustatic sea-level changes in shales of the anoxic facies". *Sedimentary Geology*. **101**: 43-53.

Xeujing, X., Mingcai, Y., Lianzhong, L., and Huijun, S. (2007). "Usuable values for Chinese Standard Referrence Samples of Stream Sediments, Soils, and Rocks: GSD 9-12, GSS 1-8 and GSR 1-6". *Geostandards and Geoanalytical Research*. **9(2)**: 277-280.

BRIEF BIO-DATA OF THE CANDIDATE

NAME : C. ZORAMTHARA

FATHER'S NAME : LALNGILNEIA

MOTHER'S NAME : LALSANGZUALI

DATE OF BIRTH : 19.01.1987

NATIONALITY : INDIAN

TRIBE : SCHEDULE TRIBE

PERMANENT ADDRESS : TUIKUAL SOUTH, KAISARA ROAD

AIZAWL, MIZORAM-796001

EMAIL : olivin7@gmail.com

NUMBER OF PUBLICATION : 1 (ONE)

APPENDICES

PARTICULARS OF THE CANDIDATE

NAME OF THE CANDIDATE : C. ZORAMTHARA

DEGREE : Ph.D.

DEPARTMENT : DEPARTMENT OF GEOLOGY

TITLE OF RESEARCH : SEDIMENTOLOGICAL STUDIES ON TIPAM ROCKS OF KOLASIB DISTRICT, MIZORAM

DATE OF ADMISSION : 09.08.2011

APPROVAL OF RESEARCH PROPOSAL

1. B.O.S : 14.05.2012

2. SCHOOL BOARD : 15.05.2012

Ph.D. REGISTRATION : MZU / Ph.D / 436 of 15.05.2012
NO. & DATE

EXTENSION (IF ANY) : 2 YEARS

ANY AWARD/ FELLOWSHIP : NET (JRF), UGC JULY, 2011

HEAD
Department of Geology